1-1-1982

Determination of the immediate source areas and probable sediment transport pathways of New Jersey beach sands.

Tom Scot Schroeder

DETERMINATION OF THE IMMEDIATE SOURCE AREAS AND PROBABLE SEDIMENT TRANSPORT PATHWAYS OF NEW JERSEY BEACH SANDS

by

Tom Scot Schroeder

A Thesis

Presented to the Graduate Committee

of Lehigh University

in Candidacy for the Degree of

Master of Science

in

Geological Sciences

Lehigh University

1982

CERTIFICATE OF APPROVAL

This thesis is accepted and approved in partial fulfillment of the requirements for the degree of Master of Science.

MAY 1, 1982
(date)

Professor in Charge

Chairman of Department

ACKNOWLEDGEMENTS

This study was supported by The National Oceanic and Atmospheric Administration, Office of Sea Grant, Department of Commerce, under grant number NA-79AA-0063 to the New Jersey Marine Sciences Consortium, and by Sigma Xi, The Scientific Research Society.

The writer is particularly indebted to Professor Bobb Carson for his constant guidance in the field, in the laboratory, and during the writing of this work.

Special thanks are due Professor James Parks for his computer programs and his help in statistical analyses, and to Professor J.D. Ryan for his assistance in the petrographic aspects of this paper.

The writer sincerely appreciates the aid of his fellow geologists at Lehigh, especially that of Peter Sudano in the sample collection.

Finally, particular gratitude is due my wife, Monica, for her support and encouragement, and my father, who started me in the right direction.

TABLE OF CONTENTS

	Page
CERTIFICATE OF APPROVAL	ii
ACKNOWLEDGEMENTS	iii
LIST OF TABLES	vii
LIST OF FIGURES	viii
ABSTRACT	1
INTRODUCTION	2
Purpose	2
Previous Work	2
Sampling	9
THE GEOLOGY OF THE NEW JERSEY COASTAL REGION	12
Coastal Plain	12
Shore Zone	17
Continental Shelf	18
SEDIMENTATION IN THE COASTAL ZONE	20
Fluvial Transport	20
Longshore Currents	21
Sand Transport on the Continental Shelf	22
STATISTICAL ASSESSMENT OF PREVIOUS WORK	24
Results	24
Discussion	44

		Page
FIELD AND LABORATORY ANALYSES OF NEW JERSEY BEACH SANDS		58
	Size Analysis	58
	Results	58
	Discussion	60
	Mineralogy	61
	Results	61
	Discussion	61
	X-ray Analysis	62
FIELD AND LABORATORY ANALYSES OF POSSIBLE SOURCE SANDS		67
	Description of Source Sands	67
	Mineralogy of Source Sands	68
	Results	68
	Discussion	73
CORRELATION OF BEACH AND SOURCE SANDS		74
	Zone 3	74
	Zone 1	76
	Zone 2	78
	Reevaluation of Shelf Sand Textures	79
GENESIS OF THE BEACH SANDS		80
CONCLUSIONS		83
REFERENCES		85
APPENDIX I.	Beach, Shelf, and River Sample Locations and Descriptions.	92
APPENDIX II.	Heavy Mineral Data of McMaster (1954). Values are number percentages except for magnetite, which is weight percent. x denotes trace (0.5% or less) amount.	98

		Page
APPENDIX III.	Methods.	108
APPENDIX IV.	Preliminary Varimax Rotated Factor Measures Resulting from R-mode Factor Analysis of Data Obtained by McMaster (1954).	112
APPENDIX V.	Varimax Rotated Factor Loading Matrices Resulting from R-mode Factor Analysis of Data Obtained by McMaster (1954).	115
APPENDIX VI.	Final R-mode Factor Measures Resulting from Factor Analysis on Data Presented by McMaster (1954).	117
APPENDIX VII.	Oblique Projection Matrices Resulting from Q-mode Factor Analysis on Four Variables Obtained by McMaster (1954) (glauconite, hornblende, tourmaline, and black opaques).	120
APPENDIX VIII.	Size Analysis Results. All values have been converted to millimeters.	123
APPENDIX IX.	Point Count Results. Values are number percentages.	124
APPENDIX X.	Textures of Shelf and River Samples.	129
APPENDIX XI.	Oblique Projection Matrices Resulting from Q-mode Factor Analysis on Point Count Data.	132
VITA		137

LIST OF TABLES

Table		Page
1	Correlation Coefficients for the Number Percentages of Glauconite, Hornblende, Tourmaline, and Black Opaques (McMaster, 1954) in New Jersey Beach Sands.	43
2	X-ray Diffraction Peak Positions and Relative Intensities for the Black Opaque Minerals in Sample B11, and Corresponding Powder Diffraction File Data (Berry, 1967).	64
3	X-ray Diffraction Peak Positions and Relative Intensities for Heavy Minerals (magnetically separated) of Sample B23, and Powder Diffraction File Data for Hornblende (Berry, 1967).	66

LIST OF FIGURES

Figure(s)		Page(s)
1	Sample locations and beach zones of McMaster (1954).	5
2	Sample locations.	10
3	Geomorphic coastal plain provinces in New Jersey (Wolfe, 1977).	13
4	Generalized geology of New Jersey (Markewicz, 1969).	14
5	Post-Miocene geology of New Jersey (Markewicz, 1969; Wolfe, 1977; Owens and Minard, 1979).	15
6	Plots of cumulative percent total variance versus R-mode factors for the heavy mineralogy of the New Jersey beach sands (McMaster, 1954).	26
7-9	Plots of varimax rotated R-mode factor measures versus sample locations (distance from north, i.e. south from Sandy Hook) resulting from analysis of data of McMaster (1954).	28-30
10-12	Cluster diagrams resulting from Q-mode cluster analysis on factor measures obtained from R-mode analysis of data of McMaster (1954). The resulting zonations are indicated.	33-35
13	Beach zones determined by Q-mode cluster analysis on factor measures resulting from R-mode analysis on data of McMaster (1954).	37
14-16	Plots of oblique projection Q-mode factor loadings versus sample locations (distance from north, i.e. south from Sandy Hook) resulting from analysis of data of McMaster (1954).	39-41
17	Hypothetical sediment transport directions for the New Jersey coast (Swift, 1975).	47
18-23	Plots of mineralogical data of McMaster (1954) for New Jersey beach sands. Percentages are relative to other heavy minerals (s.g. greater than 2.85 Mg/m^3). Sample locations are distances from north (i.e. south from Sandy Hook). Curves were fitted by a computer program using a polynomial regression (Shi, 1978). The zones resulting from statistical analysis of McMaster's (1954) data are indicated.	51-56

LIST OF FIGURES (cont'd)

Figure		Page
24	Size analysis results plotted against sample locations. Sample locations are shown in figure 2.	59
25	Glauconite abundance in shelf samples. Percentages are relative to other minerals counted (hornblende, tourmaline, and black opaques). Sample locations are distances south from Sandy Hook.	69
26	Hornblende abundance in shelf samples. Percentages are relative to other minerals counted (glauconite, tourmaline, and black opaques). Sample locations are distances south from Sandy Hook.	70
27	Tourmaline abundance in shelf samples. Percentages are relative to other minerals counted (glauconite, hornblende, and black opaques). Sample locations are distances south from Sandy Hook.	71
28	Black opaques abundance in shelf samples. Percentages are relative to other minerals counted (glauconite, hornblende, and tourmaline). Sample locations are distances south from Sandy Hook.	72
29	Mineralogical zones for beach, shelf, and river samples.	75
30	River channels on the New Jersey coastal plain and continental shelf (Swift, 1980).	81

ABSTRACT

The heavy mineralogy of the New Jersey beach sands shows abrupt along-the-coast changes resulting in three mineralogical zones; zone 1 (Brigantine Inlet to Cape May Inlet); zone 2 (Barnegat Inlet to Brigantine Inlet and Cape May Inlet to, and including, the Delaware Bay shore); and zone 3 (Sandy Hook to Barnegat Inlet). Factor analysis results indicate that zone 1 sands are relatively rich in hornblende and hypersthene, zone 2 sands contain a relatively high percentage of black opaque minerals and tourmaline, and zone 3 sands are characterized by relatively large quantities of glauconite and collophane. The immediate source for the sand of zone 3 beaches, and the beaches of Cape May and the Delaware Bay shore is the coastal formations (Cohansey, Kirkwood, Cape May) which are subject to wave attack. South of Barnegat Inlet to Cape May Inlet the beaches are separated from the mainland by a lagoon complex. These barrier beaches are supplied exclusively with sand from the continental shelf, as indicated by analysis of the adjacent shelf sands. The abrupt change in mineralogy at Brigantine Inlet is apparently due to different sources of sand on the shelf rather than selective sorting by longshore transport. These two distinct shelf sand sources reflect Pleistocene fluvial deposits on the New Jersey coastal plain/continental shelf.

INTRODUCTION

Purpose

This study seeks to determine the immediate source areas and sediment transport pathways of the New Jersey beach sands. Knowledge of the provenance and dispersal patterns of the beach sands is fundamental to understanding the problem of beach preservation. It is critical that beach management programs reinforce rather than impede natural processes.

Possible immediate source areas for the New Jersey beach sands are rivers (Hudson, Raritan, Mullica, Great Egg Harbor, and Delaware), coastal headlands (Kirkwood, Cohansey, and Cape May Formations), and the continental shelf (including Pleistocene sediments underlying the beaches as well as modern shelf sediments). As Swift (1970) explains,

> "Pleistocene sediments are commonly exposed at the foot of many ocean beaches, and major storms frequently cut through the beach prism to generate more sediments from the underlying Pleistocene (deposits)."

Previous Work

The heavy mineralogy of New Jersey beach sands has been studied by several investigators, and a large amount of data is available in the literature. However, the data has not been analyzed by multivariate statistical techniques.

Factors controlling the deposition of heavy minerals have been extensively studied by Rittenhouse (1943), and his findings form the basis for many subsequent studies.

MacCarthy (1931) examined the texture of beach sands from Montauk, New York, to Georgetown, South Carolina, and noted that New Jersey beach sands become finer both north and south of Manasquan, New Jersey, suggesting a littoral current divergence point (nodal point) in this area. He also observed that sands become coarser in the vicinity of inlets, especially approaching Delaware Bay, due to the convergence of littoral and tidal currents during both ebb and flood tides. MacCarthy concluded that sands of each coastal segment (i.e. portions of the beach separated by inlets or estuaries) form a unit, and transportation of large amounts of sand does not occur from unit to unit. Estuaries, in particular, make good barriers to longshore transport.

Colony (1932) performed the first detailed mineralogical study of the New Jersey beach sands. He studied the Atlantic coast sands of Long Island and New Jersey, noted changes in mineralogy along the coast, and concluded that the New Jersey beach sands are not related to those of Long Island because of differing mineral compositions. The New Jersey sands have a mineralogy similar to the New Jersey coastal plain sediments, and hence this is their inferred source, while the sands of Long Island beaches are of Wisconsinan glacial origin. Colony also states that the New Jersey beach sands are from a source "twice removed" because they are reworked detrital matter

from coastal plain sediments which were ultimately derived from the Appalachian region.

The most complete mineralogical and textural study of New Jersey beach sands to date is that of McMaster (1954). He collected 140 beach sand samples at one mile intervals from Sandy Hook to Reeds Beach, New Jersey, and presented a plethora of size and petrologic data. McMaster found four areas with dissimilar mineral compositions along the coast (figure 1): (1) Sandy Hook to Shark River - the "glauconite zone" consists of medium sand which has a heavy mineral fraction (specific gravity greater than 2.85 Mg/m^3) with 2 - 37 percent (by number) glauconite, and a light mineral fraction with 7 - 16 percent (by number) glauconite; (2) Shark River to Little Egg Inlet - a "black opaque zone," which consists of medium and coarse sand, including less than 1 percent (by weight) heavy minerals, of which greater than 50 percent (by number) are black opaque minerals. This zone has a greater relative abundance of staurolite and zircon, and the light mineral fraction includes less than 4 percent (by number) feldspar; (3) Little Egg Inlet to Cape May - the "hornblende zone" is comprised of fine sand of which greater than 2 percent (by weight) are heavy minerals. There is a predominance of hornblende in the heavy mineral fraction, as well as significant amounts of epidote and hypersthene. Feldspar makes up 13 - 22 percent (by number) of the light mineral fraction; (4) Cape May to Reeds beach - a second "black opaque zone" which has mineral composition and texture similar

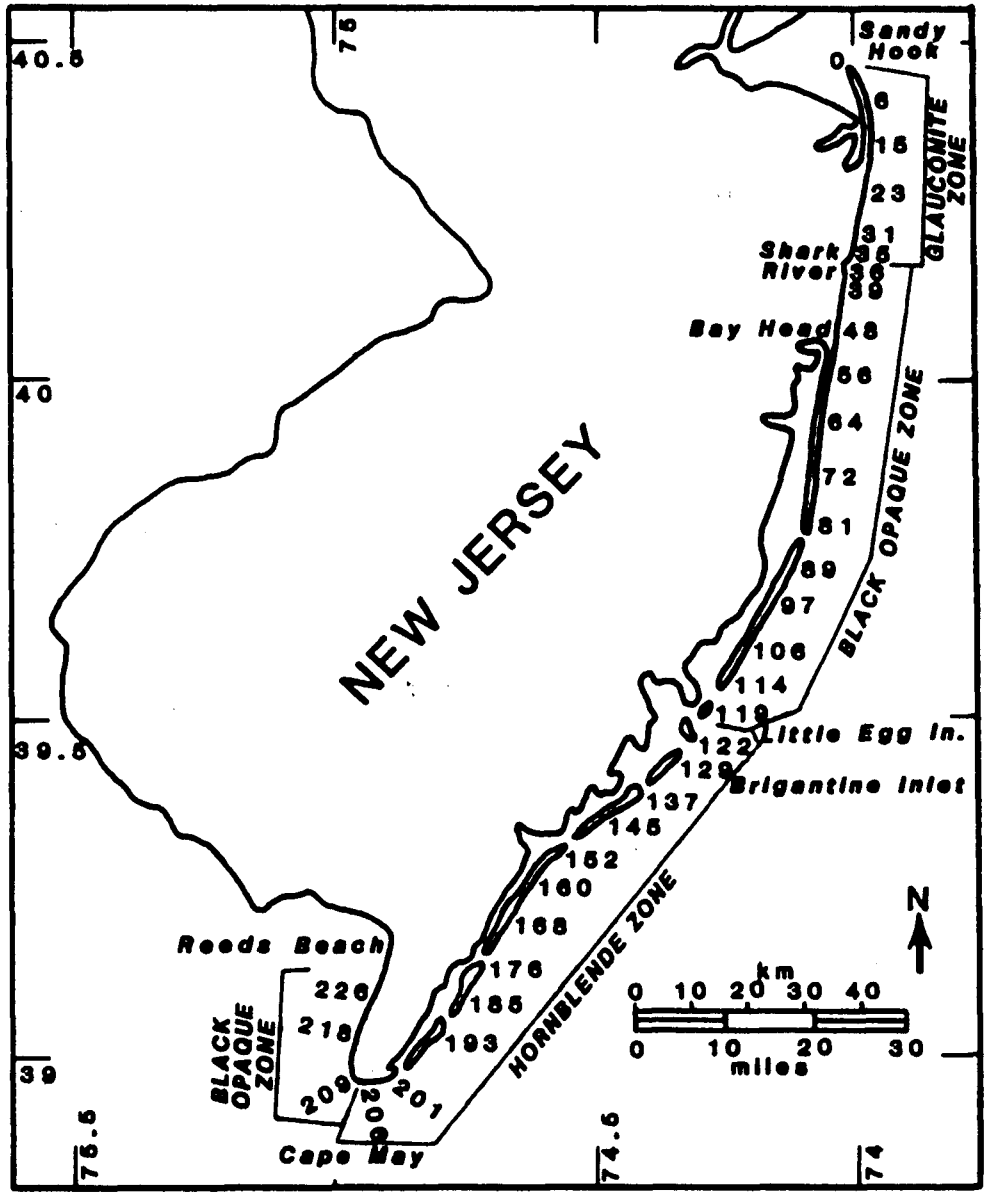

Figure 1. Sample locations and beach zones of McMaster (1954).

to the area from Shark River to Little Egg Inlet. The detailed mineralogy of the black opaque minerals was not determined by McMaster.

From his data, McMaster assigns source areas to each of the four zones. In the glauconite zone, headlands south of Sandy Hook are subject to wave attack, and hence the Tertiary, Quaternary, and Recent formations of the mainland are inferred to contain the immediate source material for the beaches. This conclusion is supported by the fact that the beach sand mineralogy is comparible to that of the mainland formations. Tertiary formations from Asbury Park to Monmouth contain abundant glauconite and hence supply the greatest volume of sediment. McMaster explains that in the glauconite zone, sediment is transported predominantly toward the north by littoral currents, but storms from the north succeed in transporting glauconite in large amounts as far south as Shark River.

Conditions similar to those of the glauconite zone exist south of Shark River to Bay Head (northern black opaque zone) where the Cape May Formation (Pleistocene) crops out adjacent to and landward of the beaches. The beach sand mineralogy in this zone is similar to the mineralogy of the Cape May Formation, and McMaster concludes that this coastal plain formation is the immediate source for the beach sands.

In the southern black opaque zone (Cape May to Reeds Beach) the Cape May Formation crops out along the Delaware Bay shore and also represents the immediate source material for the beaches of this area.

The immediate source of beach sand is not easily defined from Bay Head to Cape May (northern black opaque zone and hornblende zone) because the beaches are separated from the mainland by lagoons. McMaster concludes that the only immediate source for these beach sands must be the sediments of the continental shelf. He supports this conclusion with mineralogical data which shows that the inner shelf sediments and beach sands have similar composition. The continental shelf sediments in this area, according to McMaster, are either Cape May material, glacially derived sediment deposited after the Cape May Formation material, or a mixture of these two deposits. The beach sands of the black opaque zone are mineralogically similar to the Cape May material. McMaster concluded that hornblende zone beach sands, due to their mineralogy and texture, are composed essentially of fine grained glacial sands.

The sediments are apparently transported southward from Bay Head to Cape May, yet McMaster found a fairly abrupt change in mineralogy at Little Egg Inlet, which he attributed to selective sorting. McMaster concludes that both medium and fine sand are transported in the northern area but only the coarser sediments are deposited, yielding the mineralogy of the black opaque zone from Bay Head to Little Egg Inlet. The fine, glacially-derived sands are transported and deposited south of Little Egg Inlet because this is a relatively low energy environment (due to a more gradual offshore slope), and this selective deposition, he maintains, produced the mineralogy of the hornblende zone.

Additional mineralogical data were obtained by Biederman (1958). He studied beach and dune sands of Stone Harbor and the Barnegat Bay areas, and found that the average quartz content in the beach sands was 94.9 percent near Barnegat Bay and only 71.1 percent at Stone Harbor. He also noted that the beach profile was less steep at Stone Harbor than near Barnegat Bay (3 degrees beach slope against a 9 degree slope), but Biederman's study did not deal with the reasons for these differences.

Sherif, et al (1973) used x-ray diffraction to identify heavy minerals of New Jersey beach sands, and the results agreed with those of McMaster (1954).

Cataldo (1980) studied coastal sediment transport from Little Egg Inlet to Cape May, and concluded on the basis of textural and mineralogical data that the continental shelf is an important source of beach sand in this area.

New Jersey coastal plain deposits have been studied by MacClintock and Richards (1936), Markewicz (1969), Owens and Sohl (1969), and Owens and Minard (1979). The formations along the Atlantic coast of New Jersey have been examined by McMaster (1954), and their compositions are outlined in his paper.

Sediments of the central Atlantic continental shelf have been examined by Alexander (1934), Shepard and Cohee (1936), Stetson (1938, 1939, 1949), Uchupi (1963), Donahue, et al (1966), Hubert and Neal (1967), Uchupi (1968), Stanley (1969), Friedman and Sanders

(1970), Milliman (1972), Milliman, et al (1972), Swift, et al (1972), and Frank and Friedman (1973).

Hydrographic conditions existing on the continental shelf off New Jersey have been studied by Bumpus (1965, 1969), McClennen (1973, 1973a), Smith and Lawrence (1975), and Butman, et al (1976).

The most obvious topographic features of the New Jersey continental shelf are the ridges and swales. They have been examined by Duane, et al (1971), McKinney, et al (1974), Stahl and Koczan (1974), Stubblefield, et al (1975), and Stubblefield and Swift (1976).

Pleistocene drainage patterns have been inferred from the presence of buried river valleys on the shelf by Veatch and Smith (1939), Ewing, et al (1963), Kelling, et al (1975), Twitchell, et al (1977), Knebel (1979), Swift, et al (1980), and Kelley (1981).

Sampling

In August of 1979 twenty-eight beach sand samples were taken at 8 kilometer intervals from Sandy Hook to Reeds Beach, New Jersey (figure 2). Sample locations and beach descriptions are given in Appendix I. At each location 3 subsamples were taken from the high tide line. Heavy minerals are most concentrated at this part of the beach because the velocity of the water returning on the ebb is less than that on the flood tide, and therefore lighter minerals of a given size are removed (Rasmussen, 1941). The subsamples were spaced about 80 meters apart. Composite samples were made by combining equal

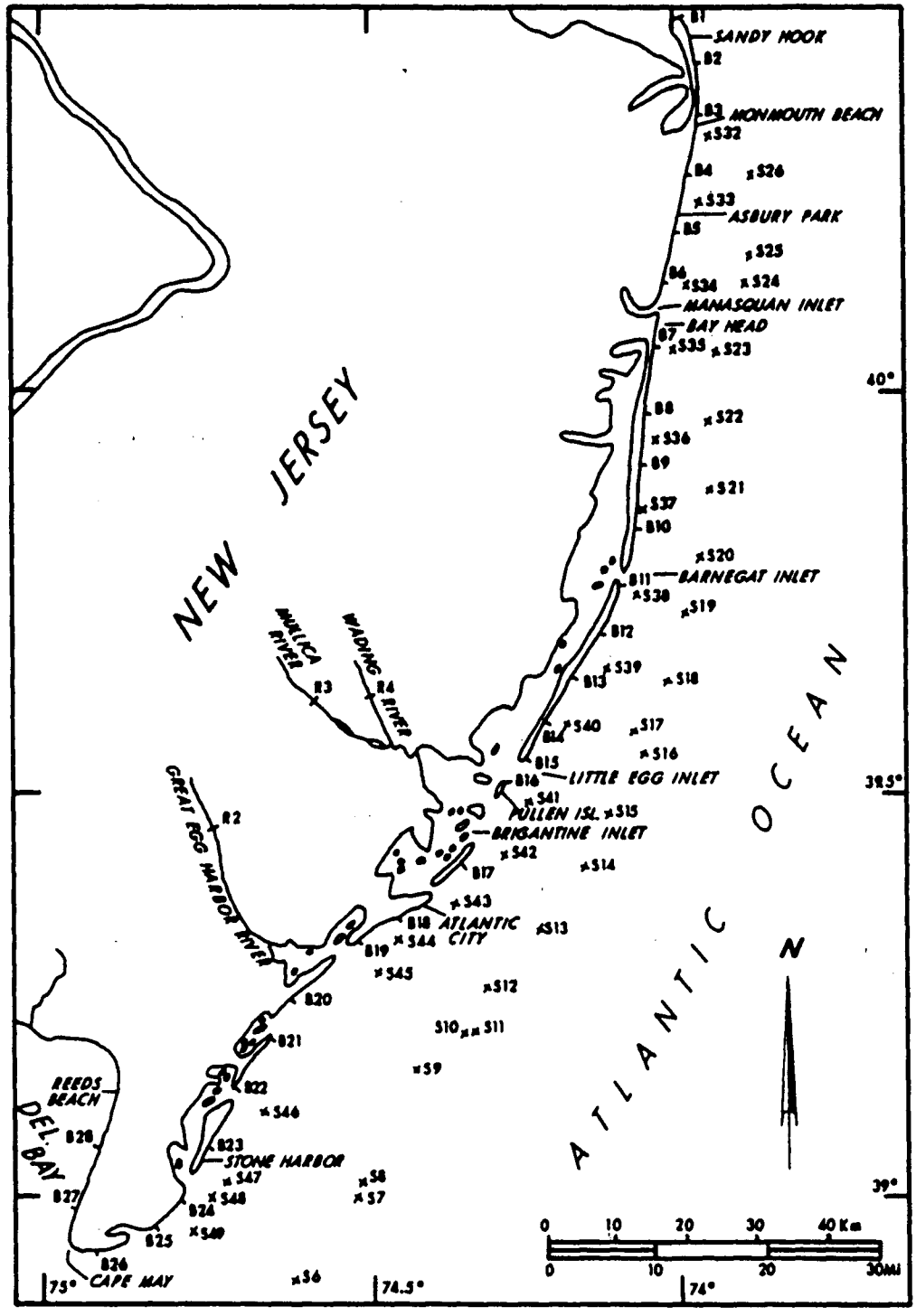

Figure 2. Sample locations.

parts by weight of each subsample. This was done to reduce the sampling error, which is a function of the homogeneity of the sediment, the location of the sample, and the manner in which sampling was done (Krumbein, 1934). A flat shovel was used to scrape off less than one centimeter of surface sediment to insure that each sample contained few sedimentation units (Macpherson and Lewis, 1978).

Continental shelf sediments were obtained in May and June, 1980. Locations (figure 2) were chosen along two shore-parallel traverses on the shelf; one at a depth of about 9 meters and a second at 18 meters. The depth varied greatly within traverses; however by this sampling design, mineralogical changes parallel to the coast could be determined, and comparisons could also be made between the two distances from shore.

Loran-A was used to locate the shelf sample positions. The samples were taken with a Smith-MacIntyre grab, and were subsequently sealed in plastic bags. The color of the sediments was determined with the aid of a Rock Color Chart (Geological Society of America, 1970) based on the Munsell system. Sample descriptions are tabulated in Appendix I.

In June 1980 three samples were taken from three rivers: the Great Egg Harbor River, the Mullica River, and the Wading River (figure 2). A VanVeen grab sampler was utilized from bridges along major roads. Descriptions of these samples are given in Appendix I.

THE GEOLOGY OF THE NEW JERSEY COASTAL REGION

Coastal Plain

The coastal plain is the largest geomorphic province of New Jersey and includes all of New Jersey southeast of the Piedmont province (figure 3). The coastal plain consists of southeast dipping unconsolidated clays, marls, silts, and sands of late-Cretaceous and Tertiary age. Three subprovinces are recognized; an outer lowland, an inner lowland, and a central upland (Wolfe, 1977).

The geologic history of the coastal plain formations (figures 4 and 5) is one of alternating periods of submergence and emergence of the land mass. During the post-Eocene emergence there was extensive erosion of the ultimate source areas for the New Jersey beach sands: the Piedmont lowlands, New Jersey highlands, and Valley and Ridge provinces (figure 3) (Wolfe, 1977).

During middle-Miocene time, seas transgressed over large parts of southern New Jersey. Clay, silt, and sand were deposited as the Kirkwood Formation (figure 4). Overlying the Kirkwood is the Cohansey Formation (Miocene), which was deposited during another marine transgression following a brief period of emergence after Kirkwood deposition. The Cohansey Formation consists of clay, sand, and gravel.

The Beacon Hill gravel is of Pliocene age and represents the remnants of stream deposits (figure 5) (Wolfe, 1977).

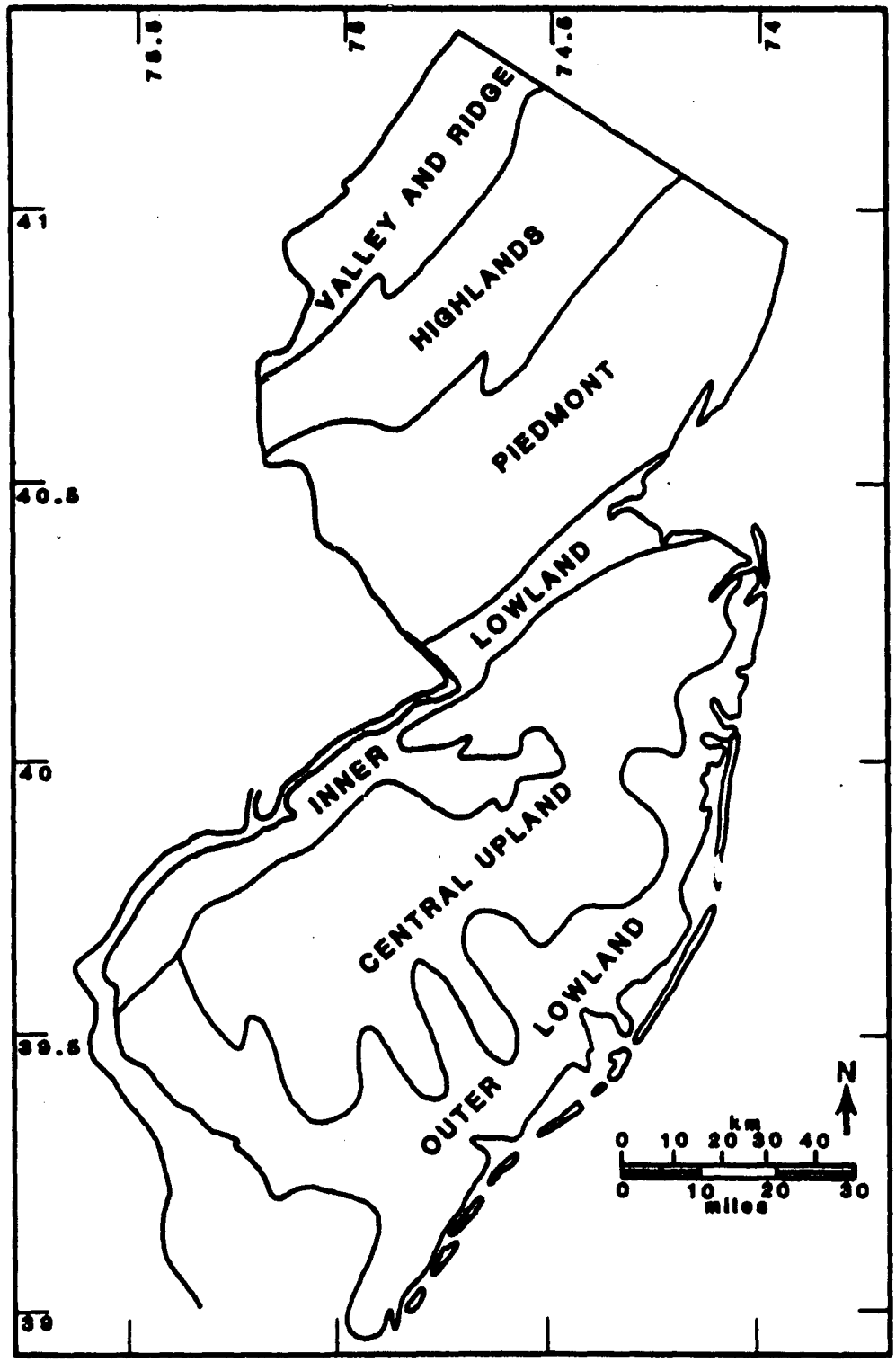

Figure 3. Geomorphic coastal plain provinces in New Jersey (Wolfe, 1977).

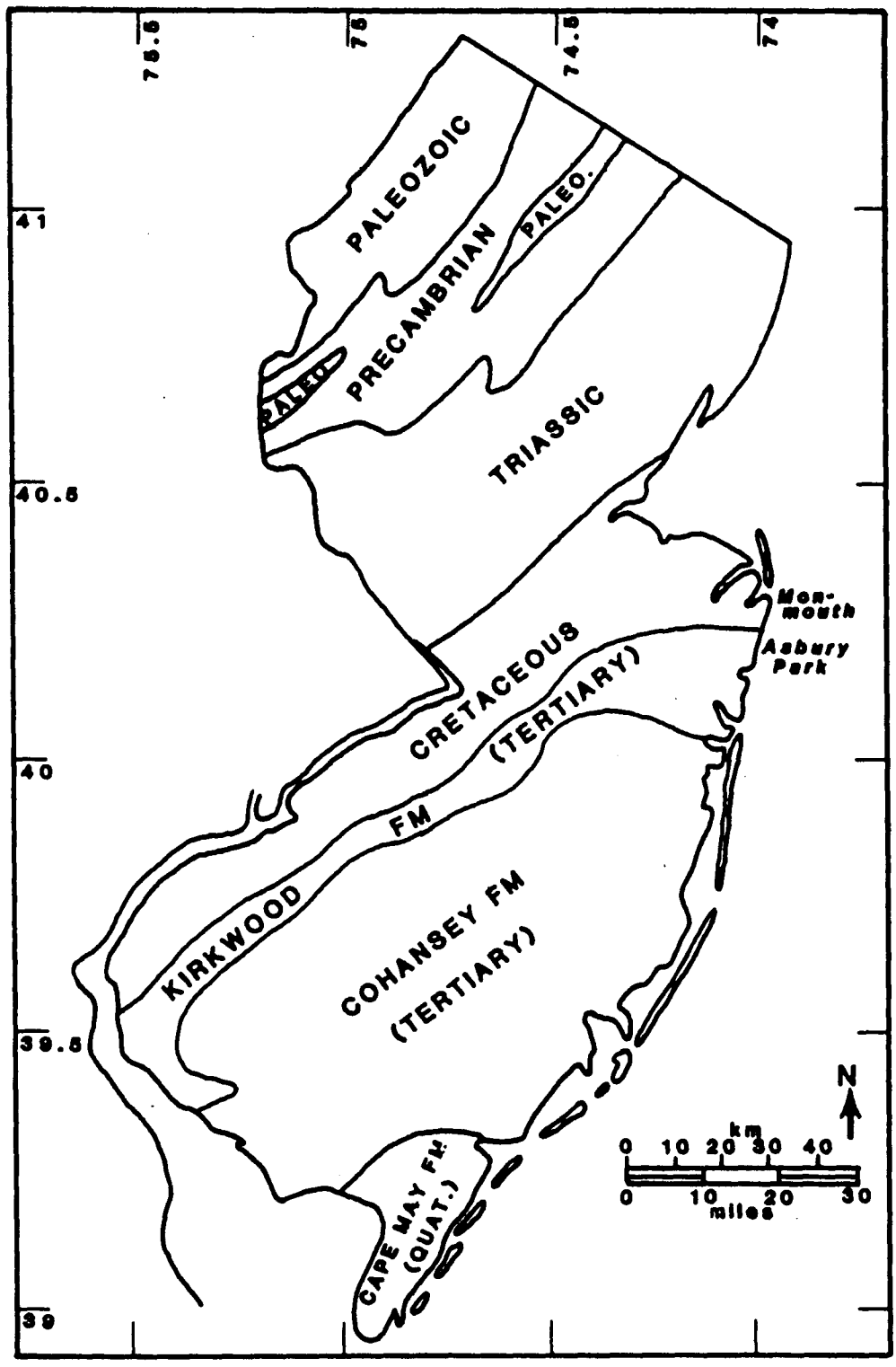

Figure 4. Generalized geology of New Jersey (Markewicz, 1969).

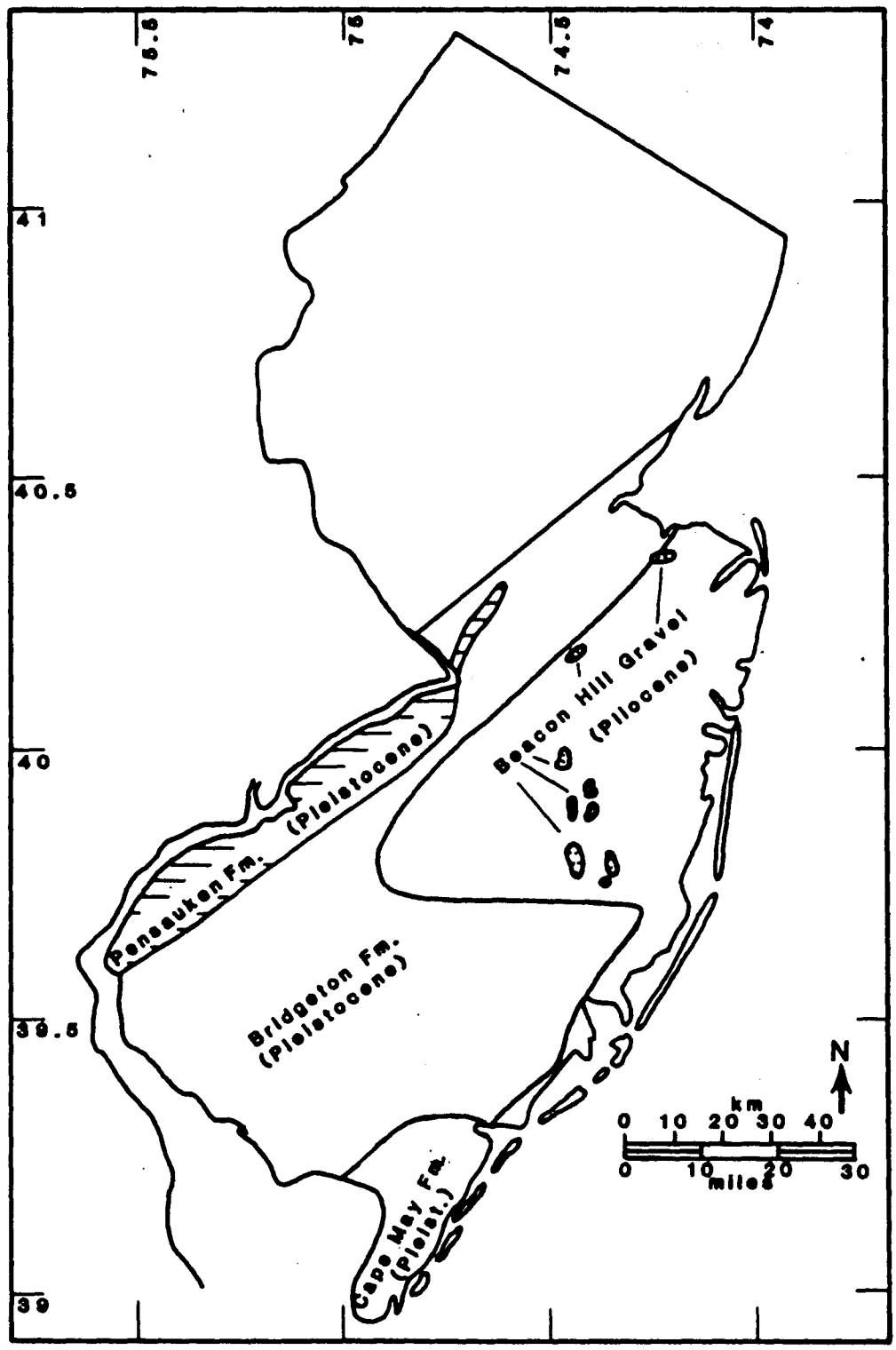

Figure 5. Post-Miocene geology of New Jersey (Markewicz, 1969; Wolfe, 1977; Owens and Minard, 1979).

Three Pleistocene glacial stages are recognized in New Jersey; Kansan, Illinoisan, and Wisconsinan. Each is preceeded by an interglacial stage; Aftonian, Yarmouth, and Sangamon, respectively (Wolfe, 1977).

The Bridgeton Formation was deposited during the Aftonian interglacial stage and part of the Kansan glacial stage (figure 5). As sea level rose during Aftonian time, the Beacon Hill, Cohansey, Kirkwood, and older formations were eroded and redeposited along the coast by fluvial and shallow marine processes as sand and gravel lenses. Large boulders indicate that ice rafting contributed to the Bridgeton Formation during Kansan time, but a dominantly fluvial origin is indicated because of horizontal gravel beds, cross stratification in coarse beds, and lenses of gravel (Wolfe, 1977). Owens and Minard (1979) conclude that the Bridgeton was deposited in a river channel which migrated from the central upland (figure 3) in a southward direction producing the flat southeast sloping surface in southern New Jersey. They indicate that an ancestral Hudson River is responsible for the channel.

The Pensauken Formation (figure 5) was deposited during the Yarmouth interglacial stage and part of the Illinoisan glacial stage. It is similar to the Bridgeton Formation in composition and fills some post-Bridgeton valleys (Wolfe, 1977). Owens and Minard (1979) state that the Pensauken and Bridgeton Formations formed in a similar manner, but the Pensauken channel migration occurred on the Delmarva Peninsula of Delaware. The ancestral Hudson is again believed to be the river involved.

During the Sangamon interglacial stage the Cape May Formation (figures 4 and 5) was deposited as sand and gravel lenses at the coast, and along present streams and rivers as bordering terraces, natural levees, and overbank deposits. The presence of marine fossils within portions of the formation, and its occurrence as river border deposits indicates a paralic origin. The Cape May Formation is different from the Bridgeton and Pensauken Formations in composition as it lacks weathered chert and feldspar, and soft Triassic rock fragments (Wolfe, 1977).

The last glacial advance was the Wisconsinan glacial stage (75,000-18,000 years B.P.) when northern areas of New Jersey were buried by glacial ice. This advance caused a lowering of sea level, and therefore stream erosion in southern New Jersey. During the Holocene transgression (18,000-7,000 years B.P.) fluvial sediments were redeposited as a sand blanket covering the present continental shelf.

Shore Zone

In general, the coastline of New Jersey follows a pattern that is also seen on the Long Island, Delaware, and Virginia-North Carolina coasts. That pattern consists of an asymmetric coastal unit; the northern end has a north-trending spit, to the southwest there is a stretch of mainland beach followed by a south trending spit, and finally a barrier island chain (Swift, 1975). Hayden and Dolan (1979) call this repetitious motif an "ensemble region."

They also note an along-the-coast asymmetry where there is a "transition between barriers generally (partially) attached to the mainland and free standing spits and barriers."

Various shore forms define the New Jersey coast (figure 2). From Sandy Hook in the north to Monmouth Beach there is a northward trending spit indicating littoral sand transport in a northward direction. From Monmouth Beach to Bay Head the mainland is separated from the ocean by a series of narrow mainland beaches. South of Bay Head to Cape May there is a barrier island chain which is separated from the mainland by lagoons. At Cape May and along Delaware Bay the mainland lies adjacent to the ocean and bay (McMaster, 1954).

During the Holocene transgression the coastline retreated landward. This displacement resulted in the erosion of headlands and may have been accompanied by a landward migration of barriers maintaining their elevation relative to rising sea level.

Continental Shelf

The New Jersey continental shelf is a moderately smooth, seaward sloping surface with sand ridges, channels, and terraces (Uchupi, 1968). Most of the shelf sediments are relict (Emery, 1968) in that they are (at least partially) unrelated to the present depositional regime. These relict sediments are coastal plain deposits that were submerged during the Holocene transgression. When sea level was 80 meters lower than at present, essentially all river sediment was

deposited directly into submarine canyons which cut the shelf edge. But as sea level rose above this point, river sediments were deposited at the river mouths, and longshore currents were able to redistribute the sediment as nearshore deposits (McClennen, 1973).

The most prominant feature on the New Jersey shelf is the ridge and trough topography. The origin of the ridges is apparently related to barrier beach and lagoon formation during the Holocene transgression, and landward migration of the barriers (McClennen, 1973). This transgression was responsible for the deposition of the offshore sand sheet (Swift, et al, 1972). The sea level rise was not uniform, and during times of relative standstill, barriers may have been built up forming ridges in the offshore sand sheet. Periods of relatively rapid sea level rise resulted in thin segments of the sand sheet.

McKinney, et al (1974) found that there are three orders of ridge and trough topography present off New Jersey. The first order features are ridges up to 14 meters high, two to six kilometers apart, which trend northeast-southwest. Superimposed on these features is a second order of ridges that are two to five meters high, 0.5 to 1.5 kilometers apart, trending northeast-southwest. A third order consists of large scale current lineations of low relief (up to 1.5 meters), trending east-northeast by west-southwest, and lying ten to twenty-five meters apart. The first and second order features apparently formed during the Holocene transgression, but the second order was formed in slightly deeper water. The third order lineations are thought to be a response to "helical-flow structure within the flow field of a major storm" (McKinney, et al, 1974).

SEDIMENTATION IN THE COASTAL ZONE

Fluvial Transport

Rivers were responsible for supplying large quantities of sediment to the continental shelf during lower stands of sea level, but their role as an immediate source of modern beach sand in New Jersey is probably not important (Meade, 1969; Milliman, et al, 1972; Neiheisel, 1973). The Holocene transgression resulted in the drowning of river systems in New Jersey, and the formation of estaries at the river mouths (Emery, 1971).

Neiheisel (1973) studied the Delaware Bay estuary and found a landward transport of sediment in agreement with Meade (1969). Milliman, et al (1972) found that little terrigenous sediment escapes modern estuaries of the eastern United States during normal runoff, but large quantities can escape during storms and floods. They base this conclusion on examination of satellite photographs which show sediment plumes escaping estuaries during large storms. Tropical storm Agnes (June 1972) caused the Susquehanna River to discharge more sediment into the upper-Chesepeake Bay than had been discharged over the past several decades (Schubel, 1974). The sediments apparently did not reach the ocean, but were instead trapped by the Chesepeake Bay estuary, as evidenced by a lack of suspended solids in the southern bay.

Longshore Currents

Coast parallel transport occurs due to longshore currents (littoral drift). These currents are due to oblique wave approach and longshore variation in wave height (Komar, 1976). In New Jersey the littoral drift is thought to diverge in the Manasquan region (figure 2; Duane, et al, 1971). North of Manasquan the littoral drift is generally northward, and south of Manasquan the drift is dominantly southward.

Krauser and Coch (1978) studied Brigantine Inlet, New Jersey (figure 2) and found the inlet to be sediment starved in that it received only a small amount of relatively fine sediment by longshore drift. This sediment is then reworked by ebb and flow tidal currents to form an ebb delta and a flood delta. The bottom topography of New Jersey lagoons suggests that they are largely floored by tidal deltas (Fischer, 1961). The deltas are actively growing as long as the inlet supplies sediment. As the inlet position changes with time, so do the positions of the deltas.

It is possible that little sediment transfer is occurring across inlets in New Jersey. Much of the longshore-transported sand is apparently utilized in accreting the down-current end of the barriers, and the sand that does reach inlets may be reworked in forming tidal deltas, rather than being transported across the inlet.

Sand Transport on the Continental Shelf

Three active sediment transport mechanisms on the continental shelf are waves, currents, and bioturbation. The significance of waves and currents depends on the nature, frequency, and velocities produced by each, but also is influenced by the intensity of bioturbation (McClennen, 1973). As water depth increases, the effect of waves on the bottom sediments decreases exponentially. Beyond a certain depth (about nine meters in this area) called the wave base, particles are not stirred up by "normal oscillatory wave induced water motion" (Dietz, 1963). Storms can cause waves strong enough to affect sediments at greater depths, however. McClennen (1973) found that wind waves are sufficient to erode sediments eight percent of the time at a depth of thirty meters off New Jersey.

Currents on the New Jersey shelf reflect semidiurnal rotary tides, and wind driven flow (McClennen, 1973). Tides cause a cyclic motion of particles with little net transport, but wind induced currents superimposed on the cyclic motion cause a net southwesterly drift.

Bumpus (1965) used sea-bed drifters and found that drift along the bottom on the continental shelf is variable depending on the wind regime. Offshore drift dominates seaward of a line that is one-half to three-quarters the distance between the shore and the ninety meter contour. This is about a 35 to 45 meter

depth off New Jersey. Onshore drift dominates landward of this line.

Winter storms are important in moving large quantities of sediment that would not be transported under normal conditions. Butman, et al (1976) observed significant movement of surficial sand during winter storms that was primarily alongshore, either southwest or northeast. Near-bottom flow during these storms was 30 to 44 centimeters per second. During normal conditions near-bottom flow was 10 to 15 centimeters per second and dominated by semidiurnal tides. Swift (1970) states,

> "...recent studies of the middle Atlantic shelf indicate that the shelf relict (deposited at a lower stand of sea level) sand blanket is indeed a sufficiently active sediment domain to be a potential source of sediment for the nearshore modern (deposited when sea level was at or near present position) sand prism."

STATISTICAL ASSESSMENT OF PREVIOUS WORK

McMaster (1954) examined 140 beach sand samples from the high tide line taken at one mile intervals along the entire coast of New Jersey (figure 1). Size analysis for all samples, and petrographic analysis for about every fifth sample are presented. The heavy mineral data is shown in Appendix II. McMaster presented heavy mineral data for six size intervals. Three of these size fractions, .297 to .210 mm (1.75-2.25ø), .210 to .149 mm (2.25-2.75ø), and .149 to .105 mm (2.75-3.25ø), are present in significant amounts in most samples. For the present study, separate multivariate analyses were run on each size fraction.

McMaster (1954) based his beach zonations on the abundances of three heavy mineral groups: glauconite, hornblende, and black opaques. The validity of these indicators can be tested statistically with multivariate techniques. R-mode factor analysis of McMaster's (1954) data was used to determine the lowest number of minerals needed to define the beach zones sufficiently for this study.

Results

The first objective in R-mode factor analysis (Davis, 1973; Klovan, 1975) is to determine the number of factors that are significant, or that describe the samples sufficiently so that

a comprehensive geologic interpretation is possible. For initial analysis the computer program (Parks, 1970) was set to yield ten factors. The percent of total variance accounted for by each factor is included in the output, and plots of total percent variance versus factor numbers were constructed (figure 6) to evaluate the significance of the factors generated. These plots show that the break points (point on graph where increase in total percent variance declines) are at three factors for the 1.75 to 2.25 phi fraction, three factors for the 2.25 to 2.75 phi fraction, and two factors for the 2.75 to 3.25 phi fraction.

The varimax rotated factor measures resulting from the R-mode analysis are shown in Appendix IV. Plots of varimax rotated factor measures against sample locations were made to see which factors were geologically meaningful, and these plots are shown in figures 7 through 9. Each of the three factors selected from the 1.75 to 2.25 phi fraction (figure 7) shows a distribution different from the other two indicating that each is a unique contributor to the mineralogy of beach sands along the coast. Three factors were also selected from the 2.25 to 2.75 phi fraction, but they all show similar distributions along the coast (figure 8). Only the first factor can be considered important in contributing to the mineralogical zonations of the New Jersey beaches. The 2.75 to 3.25 phi fraction yields results similar to that of the 2.25 to 2.75 phi fraction in that only one factor appears to provide unique information.

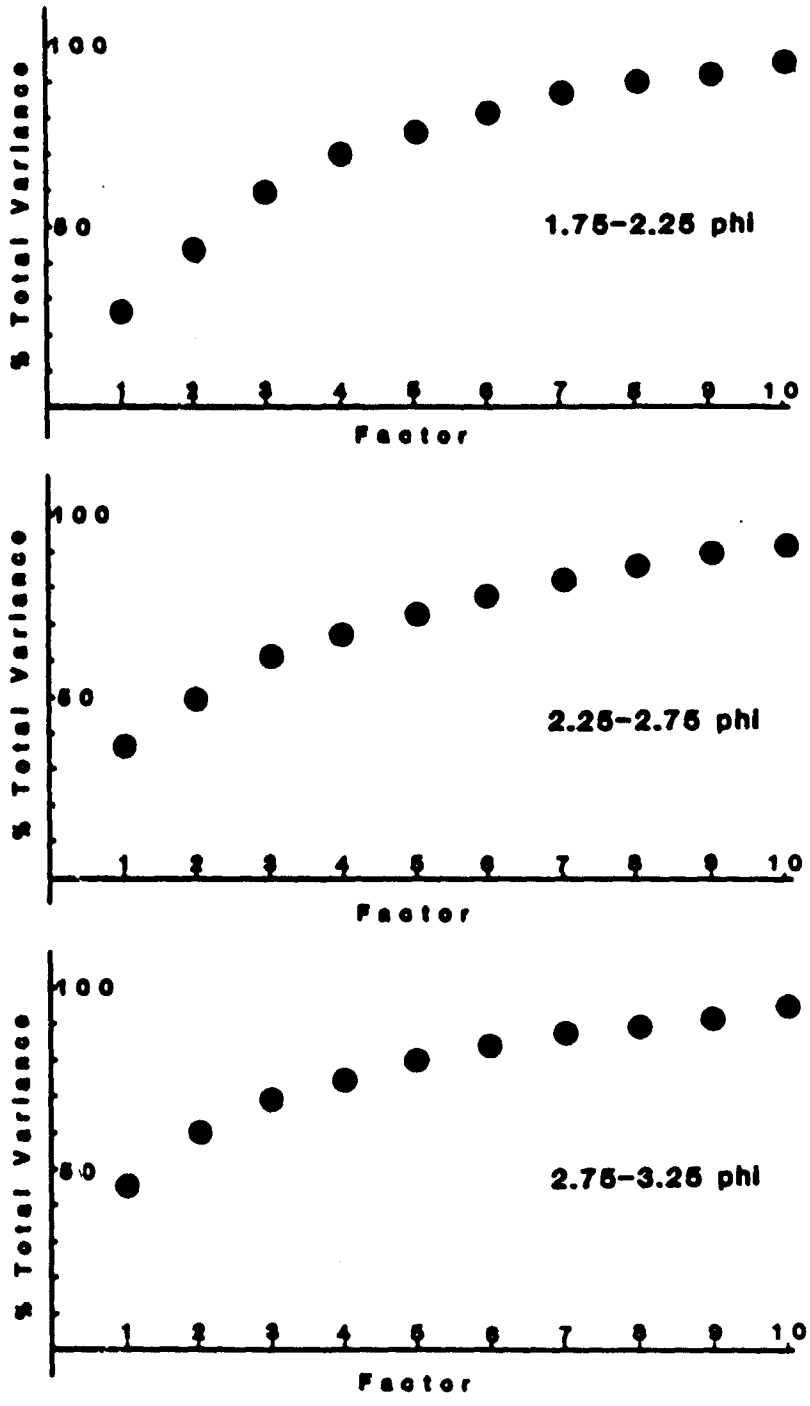

Figure 6. Plots of cumulative percent total variance versus R-mode factors for the heavy mineralogy of the New Jersey beach sands (McMaster, 1954).

Figures 7-9. Plots of varimax rotated R-mode factor measures versus sample locations (distance from north, i.e. south from Sandy Hook) resulting from analysis of data of McMaster (1954).

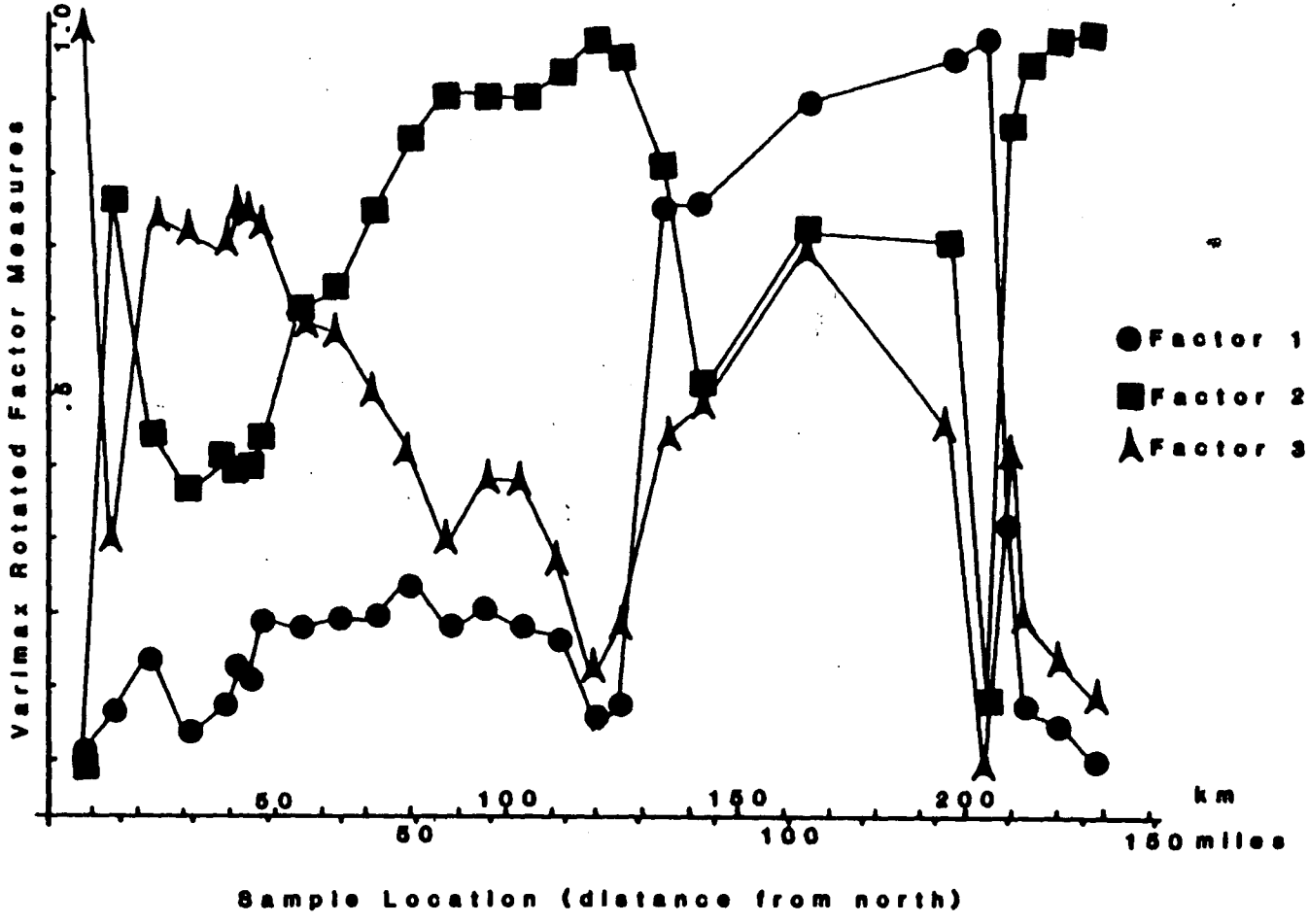

Figure 7. 1.75-2.25 phi fraction

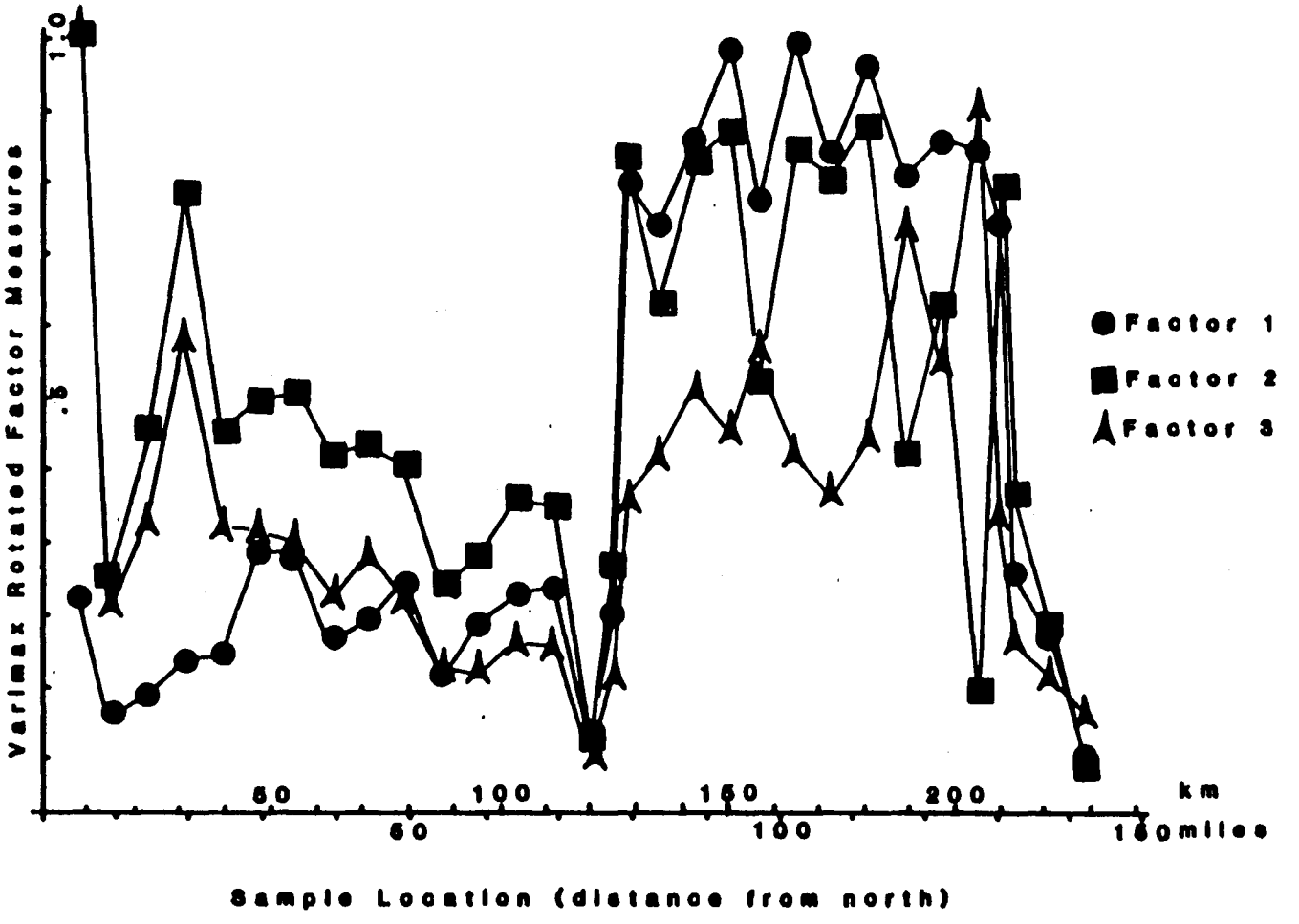

Figure 8. 2.25-2.75 phi fraction

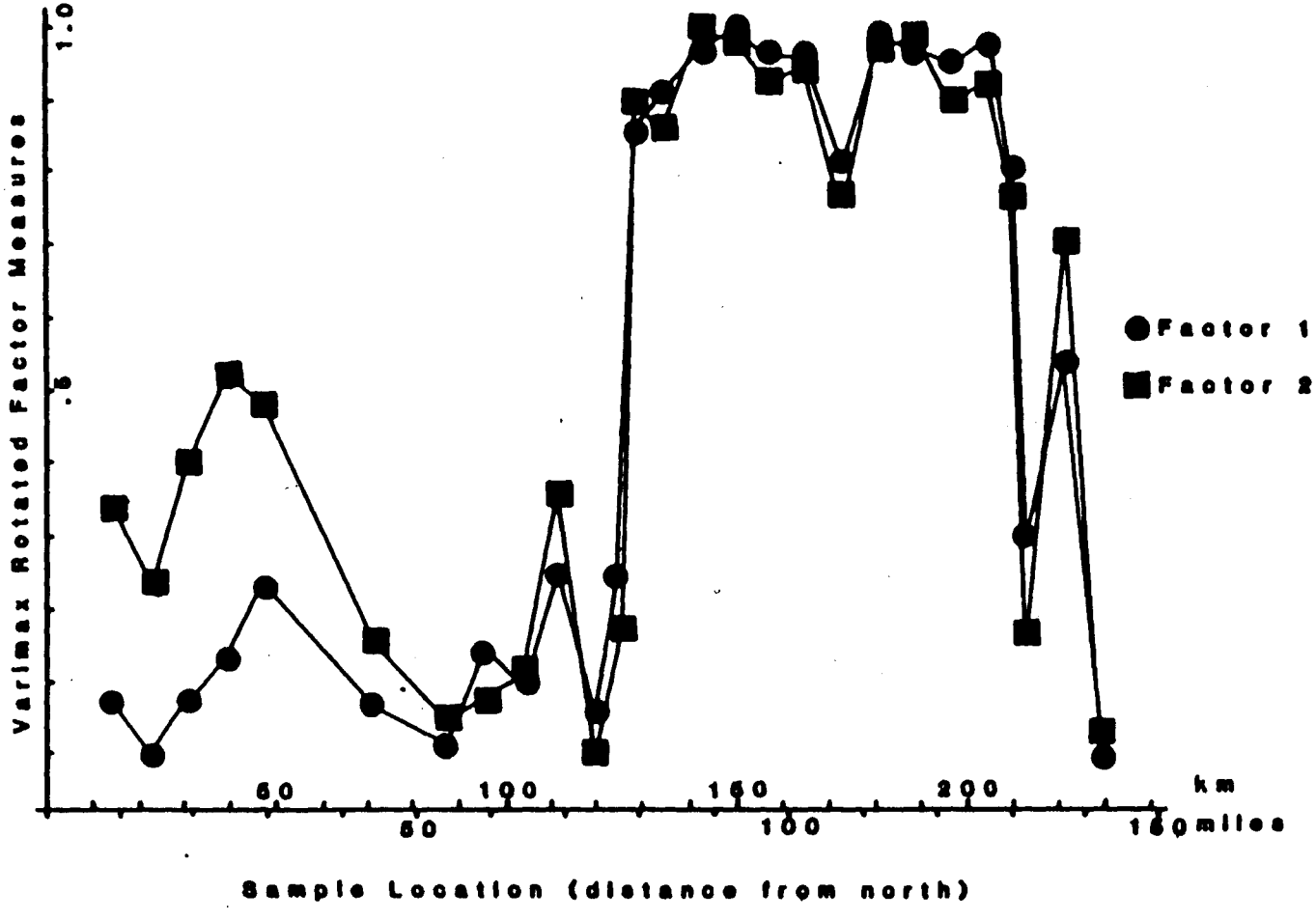

Figure 9. 2.75-3.25 phi fraction

After important factors are identified they must be analyzed to see what variables (minerals) dominate the factors (mineral assemblages). This is determined by R-mode factor analysis. The resulting factor loadings are presented in Appendix V. A high positive loading indicates that the mineral species is diagnostic of the mineral assemblage, and a high negative loading means the mineral species is relatively low in abundance. Factor 1 displays high loadings for hornblende (.926-.972) and hypersthene (.793-.895) in all size fractions examined. Factor 2 has high loading on tourmaline (.723) with lesser loading on black opaques (.388). The black opaques show a high negative loading in the other two factors (1 and 3). Glauconite (.656) and collophane (.611) display high loadings in factor 3. In summary, the factors are dominated by the following minerals:

Factor 1 (all sizes) - hornblende, hypersthene
Factor 2 (1.75 to 2.25 phi fraction) - tourmaline, black opaques
Factor 3 (1.75 to 2.25 phi fraction) - glauconite, collophane

To test McMaster's (1954) mineralogical zones (figure 1), cluster analysis (Parks, 1966; 1970) was done on the factor measures resulting from an R-mode analysis (using 3 factors for the 1.75-2.25Ø fraction, and 1 factor for the 2.25-2.75Ø and 2.75-3.25Ø fractions). The factor measures used in the cluster analysis are shown in Appendix VI. Cluster analysis results are represented by cluster diagrams (figures 10-12), and the resulting groupings (zones) are shown on the diagrams. A map of these zones defined

Figures 10-12. Cluster diagrams resulting from Q-mode cluster analysis on factor measures obtained from R-mode analysis of data of McMaster (1954). The resulting zonations are indicated.

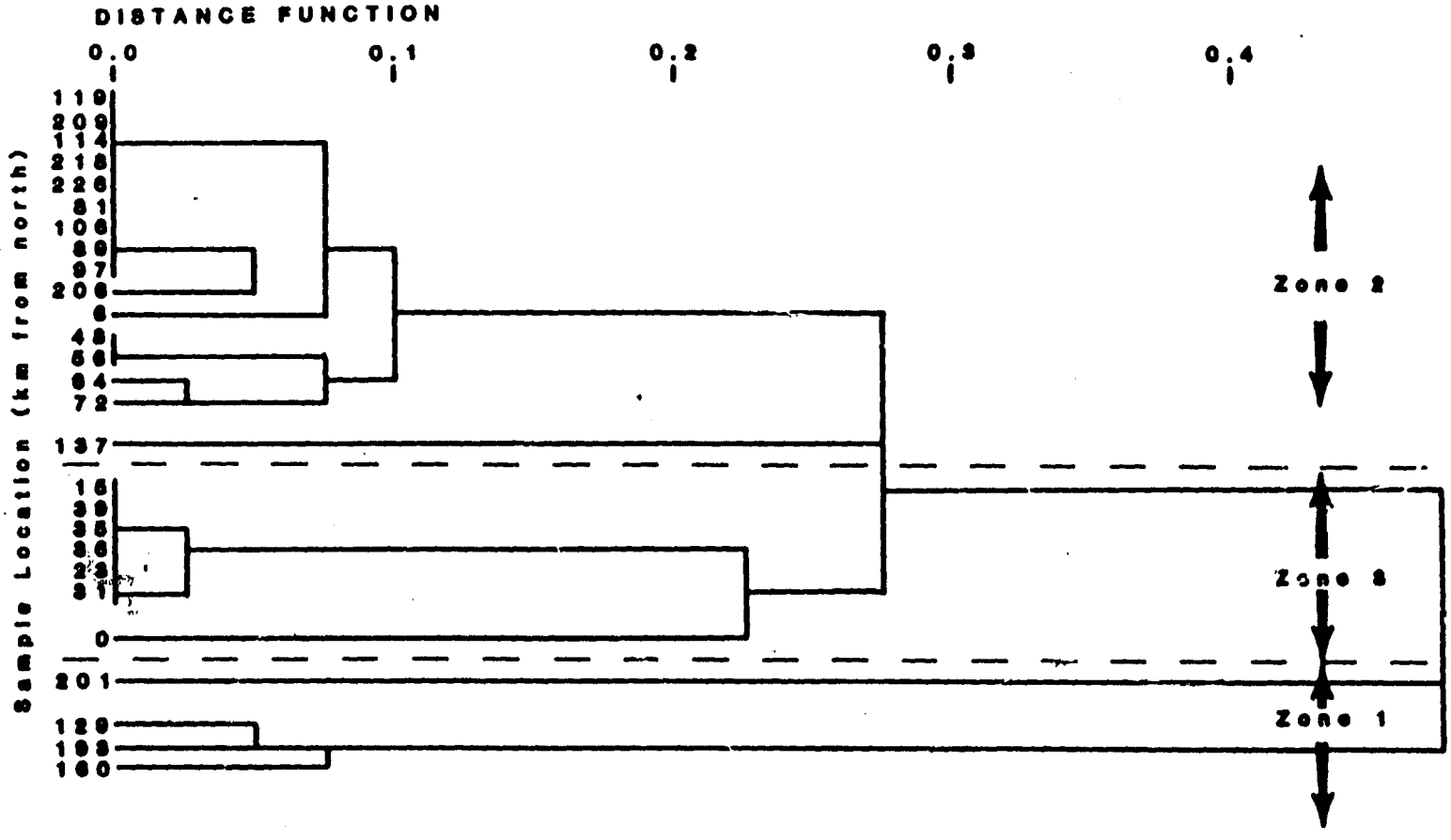

Figure 10. 1.75-2.25 phi fraction

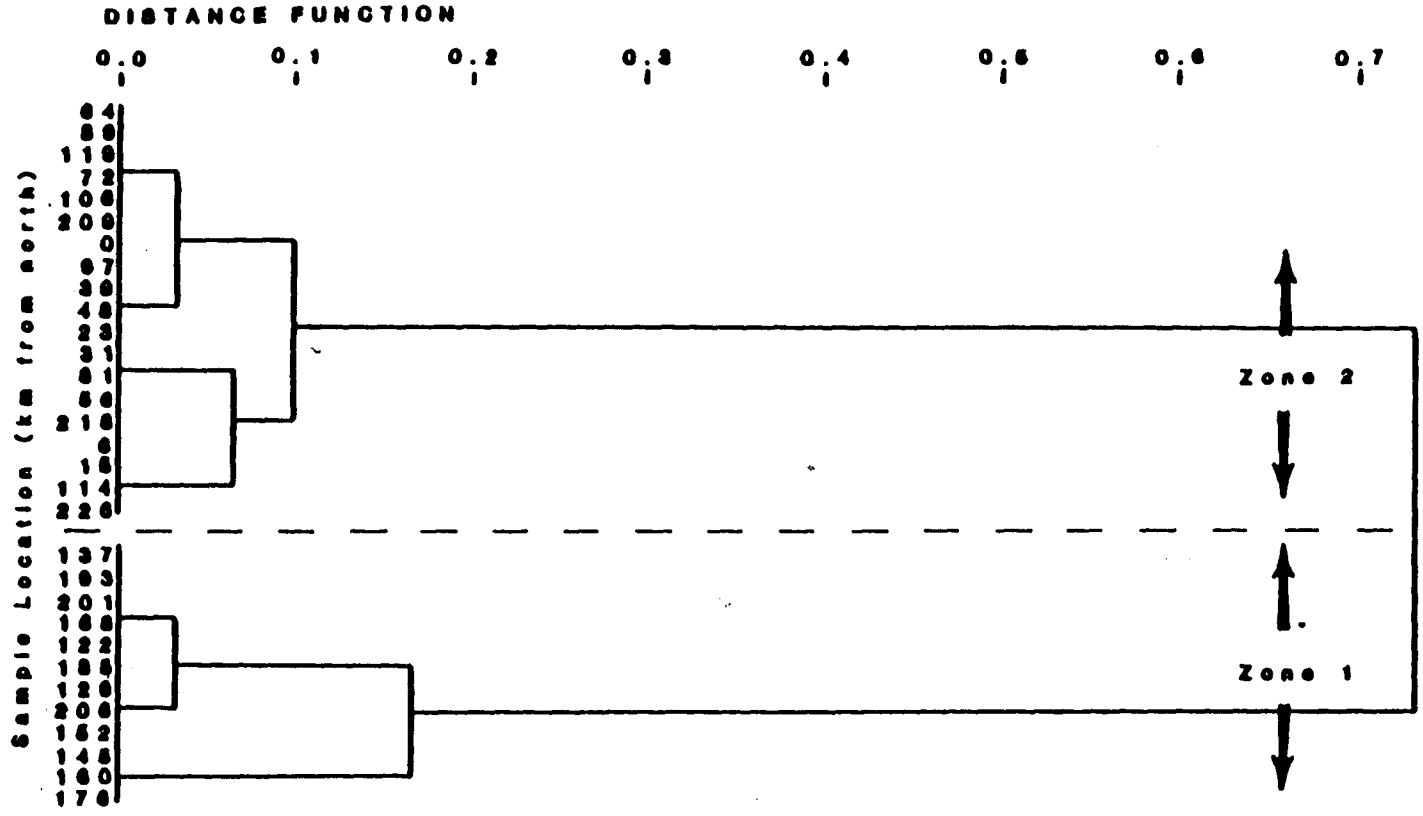

Figure 11. 2.25-2.75 phi fraction

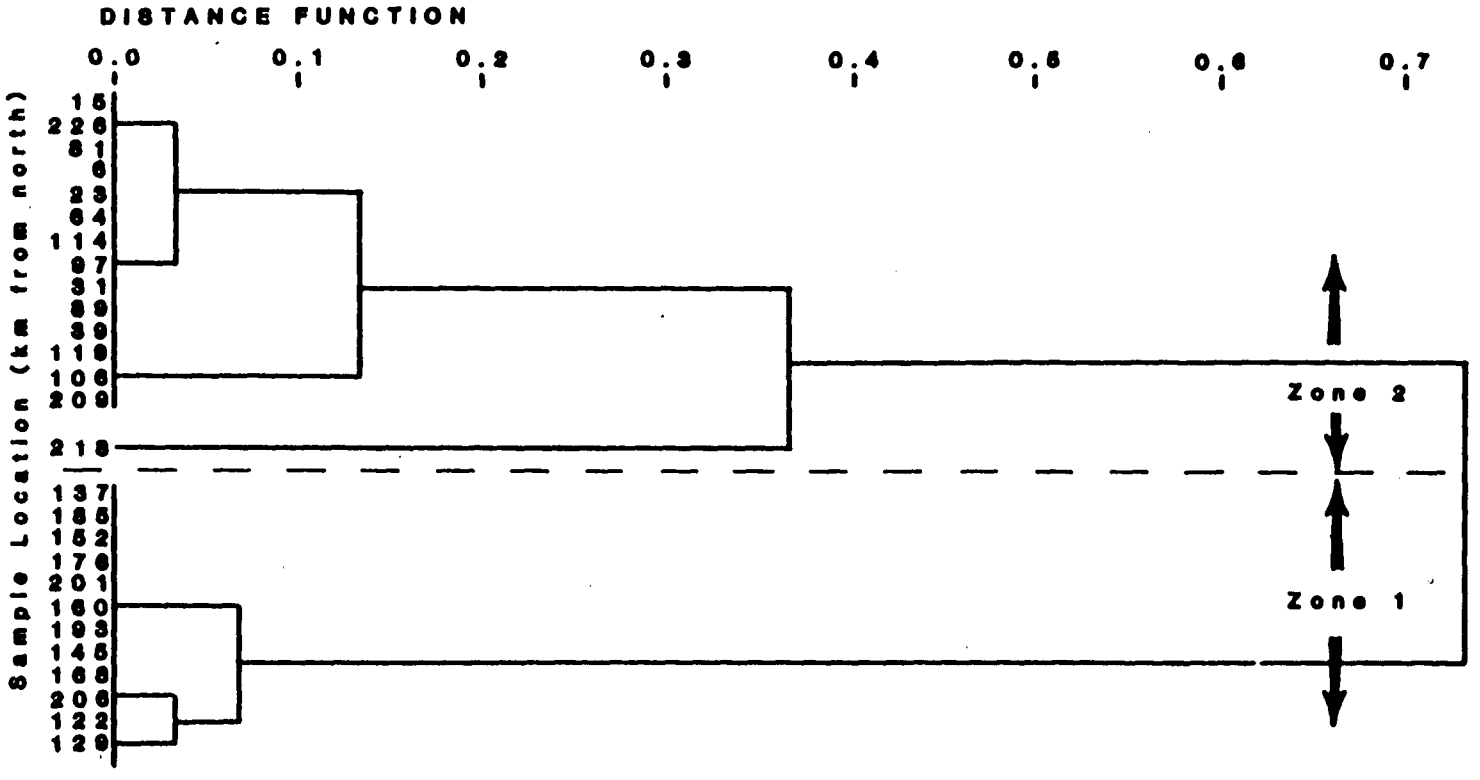

Figure 12. 2.75-3.25 phi fraction

by Q-mode cluster analysis based on mineral data is shown in figure 13. Cluster diagrams for the three size fractions (figures 10-12) show similar patterns, with the 2.25 to 2.75 phi and 2.75 to 3.25 phi fractions yielding identical sample groupings. The 1.75 to 2.25 phi fraction shows slightly different results because of the presence of three factors rather than one, as in the two finer fractions. The most important difference is the additional cluster of samples 0 through 39, which is indicated only in the coarsest fraction because these northern samples are coarser (McMaster, 1954). Although this zone was observed only in the 1.75 to 2.25 phi fraction, it represents a portion of the coast which is defined by a unique mineralogy.

To understand the sediment transport pathways associated with the beach zones, Q-mode factor analysis was used (Manson and Imbrie, 1964). The resulting oblique projections are shown in Appendix VII. Graphs of the projections are presented in figures 14 through 16. Caution should be exercised when interpreting the projection plots. Oblique projections are factor loadings which have been (1) varimax rotated to make the values cluster around zero and one, and (2) obliquely rotated so that end member samples fall directly on their respective axes at a value of plus one. Quantification of the real contribution of each end member (source area) to each sample was not attempted, but generalizations on the degree of mixing between zones can be made. It is apparent from the oblique projections that little mixing occurs at the boundaries of beach zone 1 (km 120, km 208) as

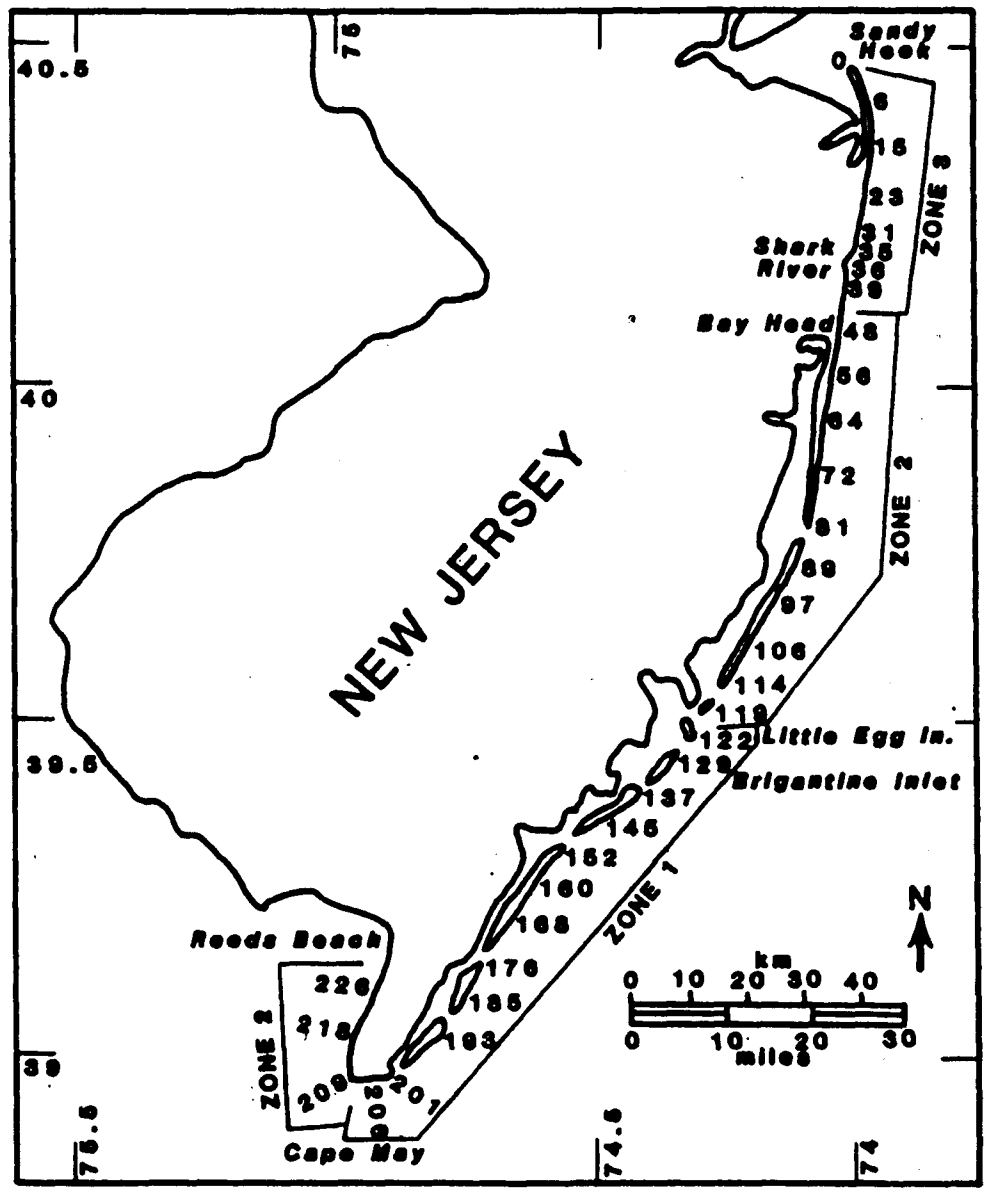

Figure 13. Beach zones determined by Q-mode cluster analysis on factor measures resulting from R-mode analysis on data of McMaster (1954).

Figures 14-16. Plots of oblique projection Q-mode factor loadings versus sample locations (distance from north, i.e. south from Sandy Hook) resulting from analysis of data of McMaster (1954).

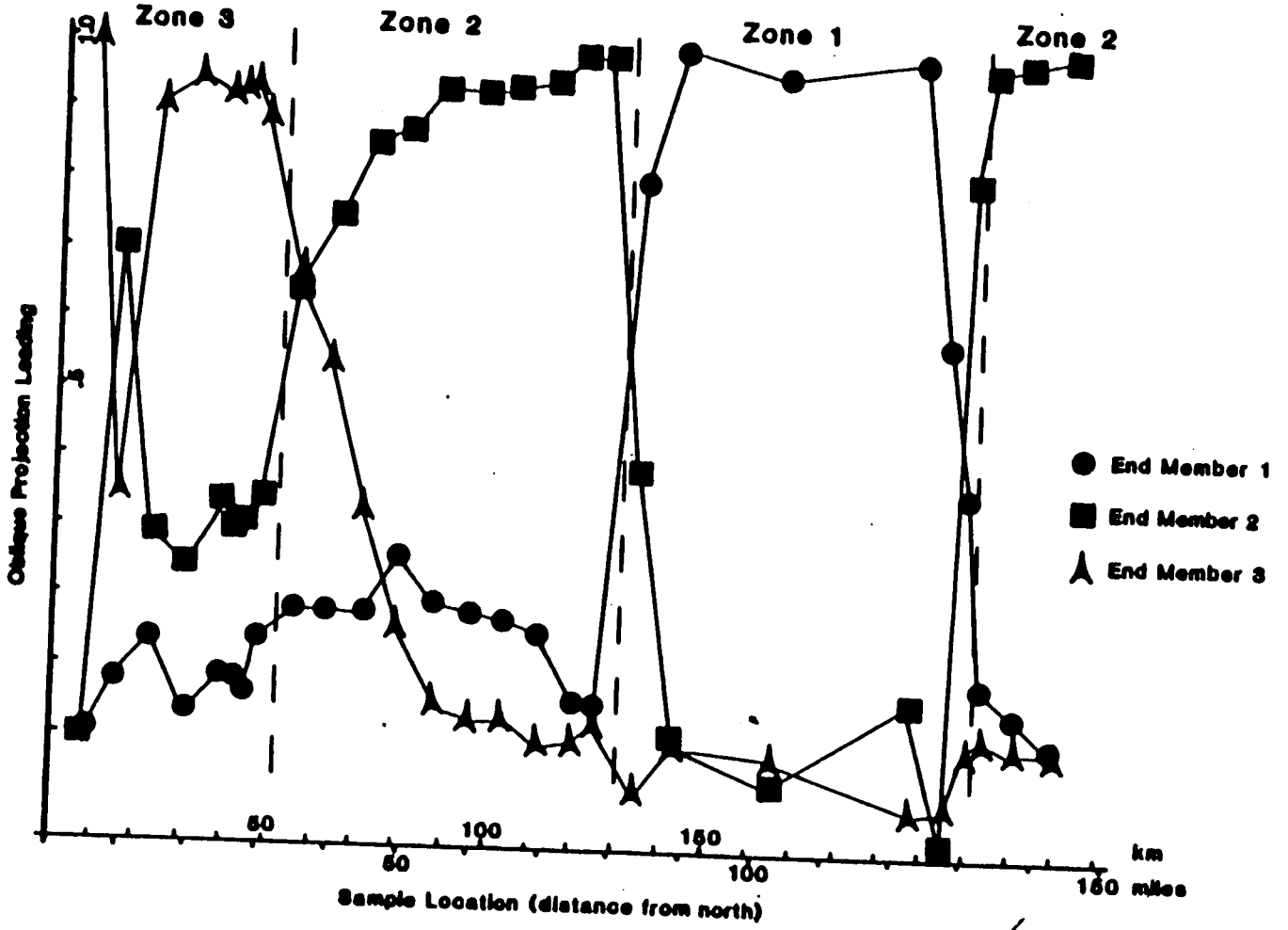

Figure 14. 1.75-2.25 phi fraction

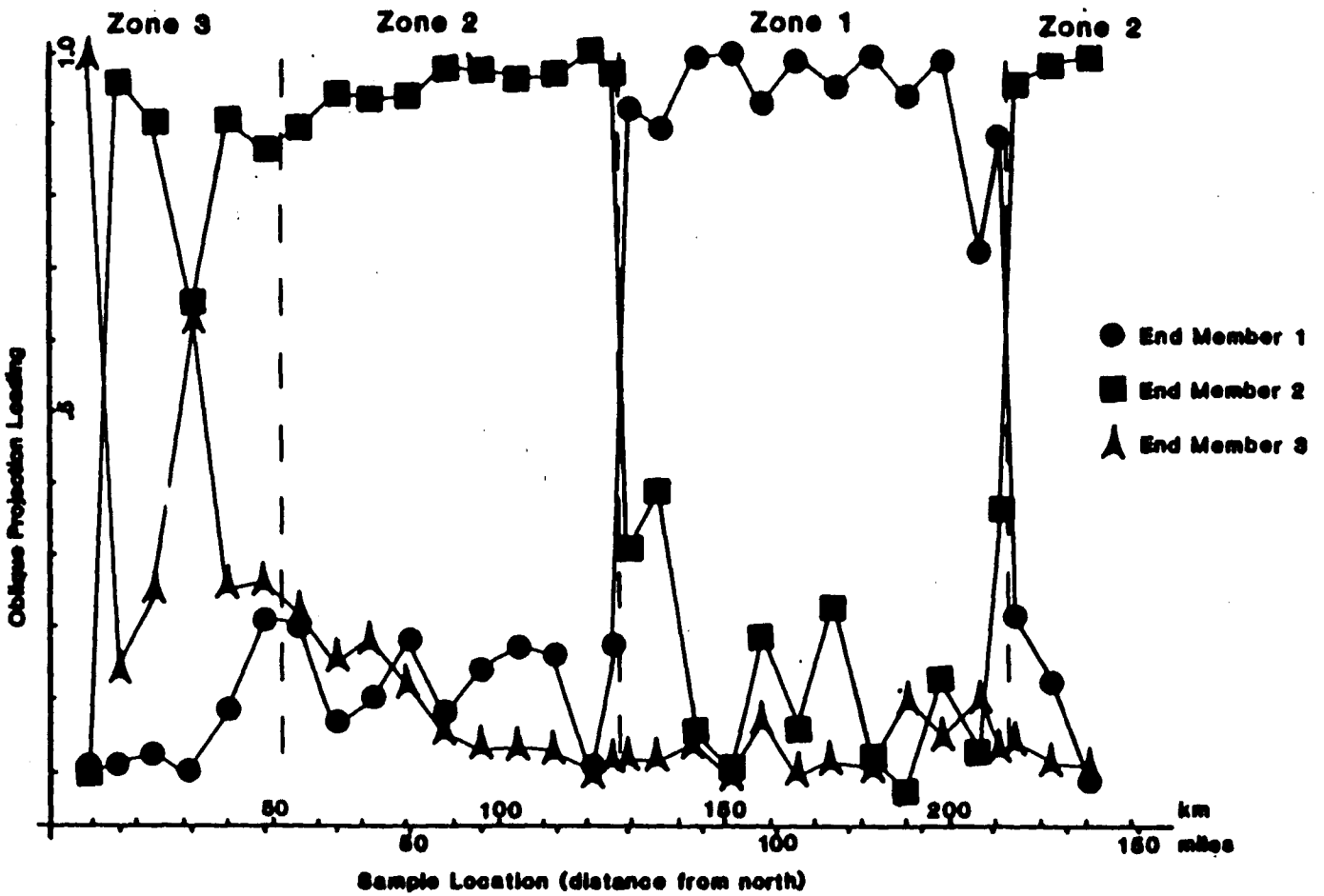

Figure 15. 2.25-2.75 phi fraction

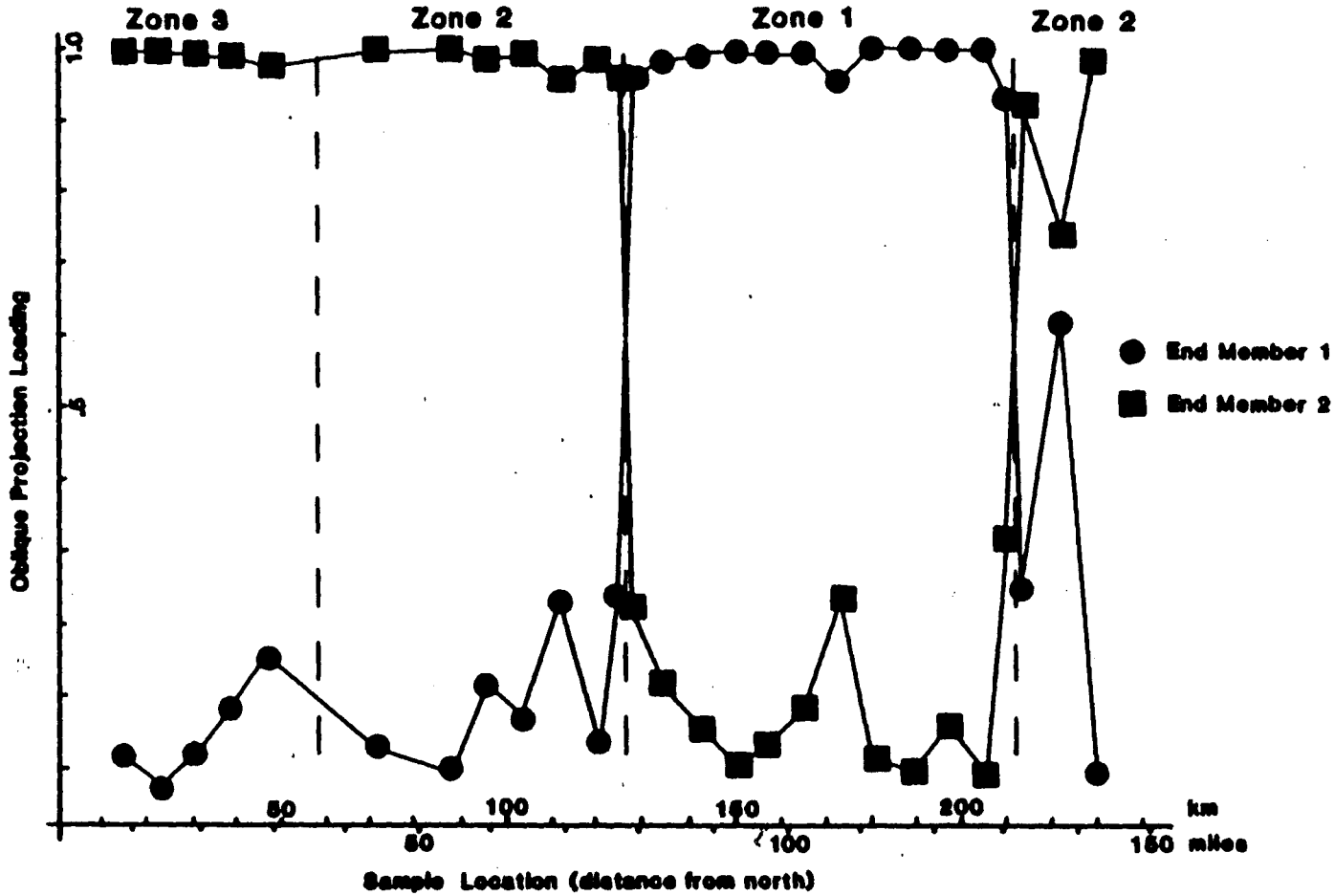

Figure 19. 2.75–3.25 phi fraction

indicated by the abrupt change of the values at both boundaries (figures 14-16). The oblique projection loadings for beach zone 2 show abrupt variation at the southern boundary (km 120), but a more gradual change north of Manasquan Inlet (figure 2; km 46). Here it appears that zone 2 sand is contributing to the beaches of zone 3 in all size fractions.

If the two most important minerals from each of the three factors are used in Q-mode factor analysis, the resulting zones are the same as if all minerals are considered. These 6 minerals, as defined by R-mode factor analysis, are hornblende, hyperthsene, black opaques, tourmaline, glauconite, and collophane. The correlation coefficients between these six minerals (table 1) show that hornblende and hypersthene have a reasonably high correlation (r greater than 0.70). Hypersthene can therefore be eliminated without losing much information. Collophane can also be eliminated because of its low percentages in the finer sizes (less than 1%), and its scarcity in even the 1.75 to 2.25 phi fraction (less than 2%; Appendix II). Tourmaline and black opaques should both be included because even though they are both diagnostic of the zone 2 sands, they have a low correlation with each other (-.07 to .26). Therefore, Q-mode analysis was run on McMaster's (1954) data using only four minerals (hornblende, glauconite, tourmaline, and black opaques). The resulting reordered oblique projection loadings (Appendix VII) reveal the same beach zonations as those found when using all variables. The only change is that sample 201 is moved from zone 1 to zone 2 in the 1.75 to 2.25

TABLE 1. Correlation Coefficients for the Number Percentages of Glauconite, Hornblende, Tourmaline, and Black Opaques (McMaster, 1954) in New Jersey Beach Sands.

1.75-2.25 ∅:	Collo-phane	Glauc-onite	Horn-blende	Hyper-sthene	Tour-maline	Black Opaques
Collophane	1.00					
Glauconite	.33	1.00				
Hornblende	-.13	-.36	1.00			
Hypersthene	-.18	-.41	.72	1.00		
Tourmaline	-.01	-.12	-.05	-.26	1.00	
Black Opaques	-.19	-.57	-.29	-.15	.26	1.00
2.25-2.75 ∅:						
Glauconite		1.00				
Hornblende		-.35	1.00			
Hypersthene		-.27	.78	1.00		
Tourmaline		.15	-.10	-.05	1.00	
Black Opaques		-.09	-.78	-.64	.02	1.00
2.75-3.25 ∅						
Glauconite		1.00				
Hornblende		-.48	1.00			
Hypersthene		-.36	.89	1.00		
Tourmaline		.31	.03	.13	1.00	
Black Opaques		.47	-.99	-.90	-.07	1.00

phi fraction. This is considered to represent a very small loss of information resulting from a great simplification of the heavy mineral data.

Discussion

It was anticipated that more than one factor would result from these analyses, and the total percent variance accounted for by the factors would come to over 90 percent, but this was not the case due to the complexity of the data. The beach sand mineralogy is a composite of contributions from many possible immediate sources which include coastal formations, different areas of the continental shelf, and a few large rivers. A contribution from coastal formations may result in one primary factor and many other subordinate factors (factors obtained in the R-mode analysis which are not significant) due to the variable mineralogy of these formations along the coast. The same can be said for the continental shelf. In effect the problem is not one of unique point sources but of broad sources that apparently extend along much of the coast.

The three mineralogical zones defined by this study (figure 13) coincide with the previously described hornblende, black opaque, and glauconite zones of McMaster (1954; figure 1) with only one difference. McMaster extends the glauconite zone as far south as Shark River (sample 35), but the cluster analysis results indicate that the zone actually extends 4 kilometers farther south to Manasquan Inlet (sample 39).

The distribution of R-mode factor measures along the coast (figures 7-9) shows that factor 1 has the highest factor measures in the "hornblende zone" (McMaster, 1954) (samples 122-206), factor 2 is highest in the "black opaque zone" (samples 48-119, 209-226), and factor 3 shows the highest values in the "glauconite zone" (samples 0-39). Therefore there are three mineralogical zones defined by the factor/cluster analysis on McMaster's (1954) mineralogical data. Zone 1 extends from Little Egg Inlet to Cape May and is characterized by relatively large quantities of hornblende and hypersthene. Zone 2 (sands containing relatively high amounts of black opaques and tourmaline) is discontinuous and runs from Manasquan Inlet to Little Egg Inlet in the north, and from Cape May to Reeds Beach (Delaware Bay) in the south. Zone 3 starts at the northern tip of Sandy Hook and extends to Manasquan Inlet, and contains relatively large amounts of glauconite and collophane.

The Q-mode factor analysis results (figures 14-16) suggest that Little Egg Inlet (figure 2) acts as a barrier to sand traveling with the littoral drift. This is in agreement with McCarthy's (1931) findings that the sand of each coastal segment acts as a unit, and beach sediment is not significantly transported from unit to unit.

Based on the preceding analysis of McMaster's (1954) data, hypotheses can be formed concerning the immediate source areas for the New Jersey beach sands. The zone 3 sand is coarse glauconitic sand, and its source is probably correctly identified by McMaster (1954). Since Tertiary formations are exposed to ocean wave attack

from Asbury Park to Monmouth (figure 4), and because these formations have glauconite as an abundant constituent, these formations appear to be the immediate source for zone 3 beach sand. Figure 17 shows the hypothetical sediment transport directions for the New Jersey coast (Swift, 1975). The zone 3 material is carried north from the outcrops to Sandy Hook. Large northerly storms, however, have carried large quantities of zone 3 sand as far south as Manasquan Inlet.

From Cape May to Reeds Beach (figure 13) zone 2 material blankets the Delaware Bay beaches. McMaster (1954) is again probably correct in assuming that these Delaware Bay shore sediments, which are characterized by black opaques and tourmaline, are supplied by the Cape May Formation which crops out along the entire beach zone, and has a mineral composition comparable to the zone 2 material (McMaster, 1954).

From Manasquan Inlet to Cape May (zones 1 and 2, figures 2 and 13), coastal outcrops can no longer be the immediate source for the beach sands because the beaches here are separated from the mainland by a lagoon complex. Littoral drift is apparently not sufficient to supply sand from the north, as evidenced by the lack of glauconite in these sands. The only immediate sources remaining are the continental shelf and rivers.

At Little Egg Inlet (km 118) there is a discontinuity in both sand texture and mineralogy (McMaster, 1954). This is the boundary of zones 1 and 2. New Jersey beaches north of Little Egg Inlet consist of medium and fine sand with a heavy mineral fraction which is rich in black

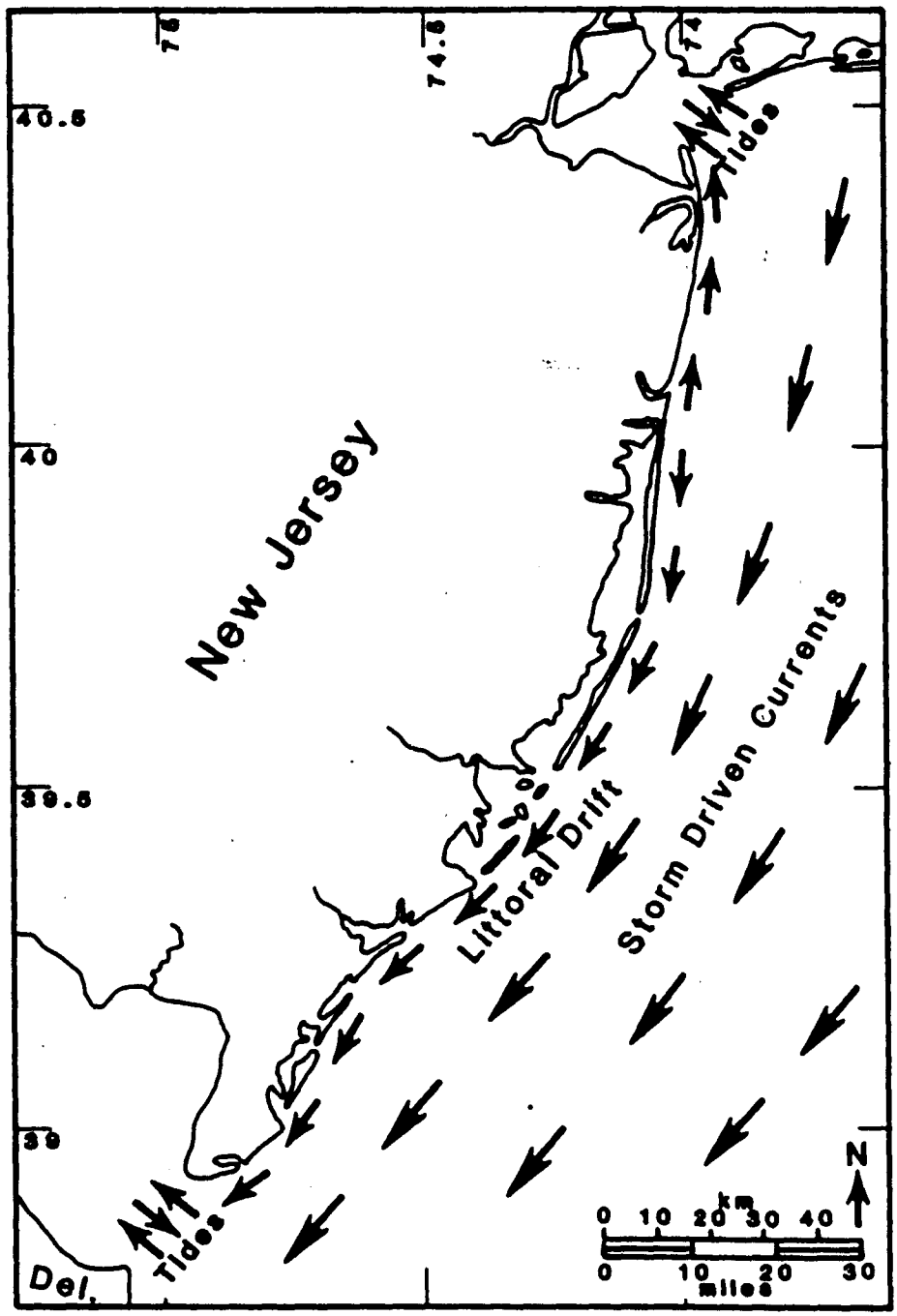

Figure 17. Hypothetical sediment transport directions for the New Jersey coast (Swift, 1975).

opaques. Beaches to the south of the inlet are made up exclusively of fine sands with a hornblende-rich heavy mineral fraction. McMaster (1954) explains this drastic change in sand properties by stating:

> "The gradual offshore slope of the ocean bottom may be responsible for the fine sand beaches south of Little Egg Inlet."

This implies that a sorting mechanism is responsible for the discontinuity in beach sand properties. Sorting can be due to differences in sand size and/or density. Cataldo (1980) concluded on the basis of apparent density data that the effect of hydraulic sorting along the south coast of New Jersey (km 129-206) is overshadowed by the effects of onshore/offshore sediment transport, and transgression. McMaster does not elaborate on the proposed mechanism, and his selective sorting hypothesis should be considered along with the possibility of different sources for sediments north and south of Little Egg Inlet.

Sorting by particle size assumes that only coarse material is deposited on the relatively steep beach face slopes north of Little Egg Inlet, and the finer material is carried south by littoral drift until the offshore slope becomes small enough to affect wave dissipation and deposition. While this process may be valid, for it to explain the differing mineralogies of zone 1 and zone 2, mineralogical variations should not be noted within a single size class. It is clear that the median size abruptly decreases south of Little Egg Inlet (McMaster, 1954), but the beach sand mineralogy changes within all size classes, and this change cannot be explained by size sorting.

To check for the significance of sorting by density along the coast of New Jersey, plots of the abundance of various minerals of different densities are shown in figures 18 through 23. Black opaques in general have a specific gravity greater than 4.1 Mg/m^3 (Hurlbut, 1971). Hornblende (s.g.=3.2 Mg/m^3) and tourmaline (s.g.=3.0-3.25 Mg/m^3) have lower specific gravities. If density sorting is the mechanism which forms the zone boundary at Little Egg Inlet (km 118), tourmaline and hornblende should show similar distributions. However tourmaline (figure 22) has a distribution more similar to that exhibited by black opaque minerals (figure 23) (i.e. increased abundance north of Little Egg Inlet). Hornblende, in contrast, is more abundant south of the inlet (figure 20; km 118). Therefore, sorting by density cannot explain the discontinuity in sand properties at Little Egg Inlet. It may, however, be operating to some degree along the coast.

By comparing the distributions of minerals of different specific gravities within a single size fraction, the role of sorting by particle density along the coast can be evaluated. In zone 3, glauconite (figure 19) and collophane (figure 18) are the most diagnostic minerals. Collophane has a higher specific gravity (s.g.= 3.15-3.20 Mg/m^3) than glauconite (s.g. greater than 2.3 Mg/m^3; Hurlbut, 1971), and since the dominant current direction is north for this zone, glauconite should show a greater abundance north of collophane's distribution. In all three sizes this is the case.

Figures 18-23. Plots of mineralogical data of McMaster (1954) for New Jersey beach sands. Percentages are relative to other heavy minerals (s.g. greater than 2.85 Mg/m^3). Sample locations are distances from north (i.e. south from Sandy Hook). Curves were fitted by a computer program using a polynomial regression (Sill, 1978). The zones resulting from statistical analysis of McMaster's (1954) data are indicated.

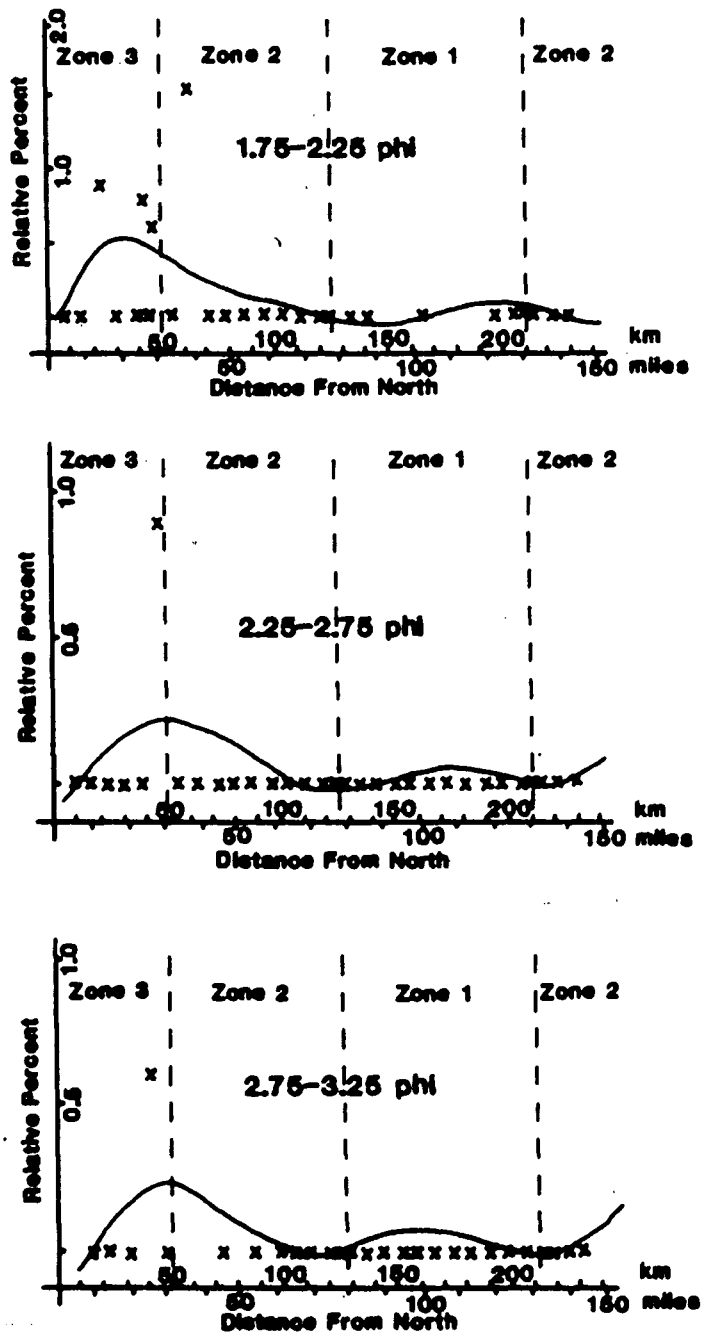

Figure 18. Collophane (s.g.=3.15-3.20Mg/m^3).

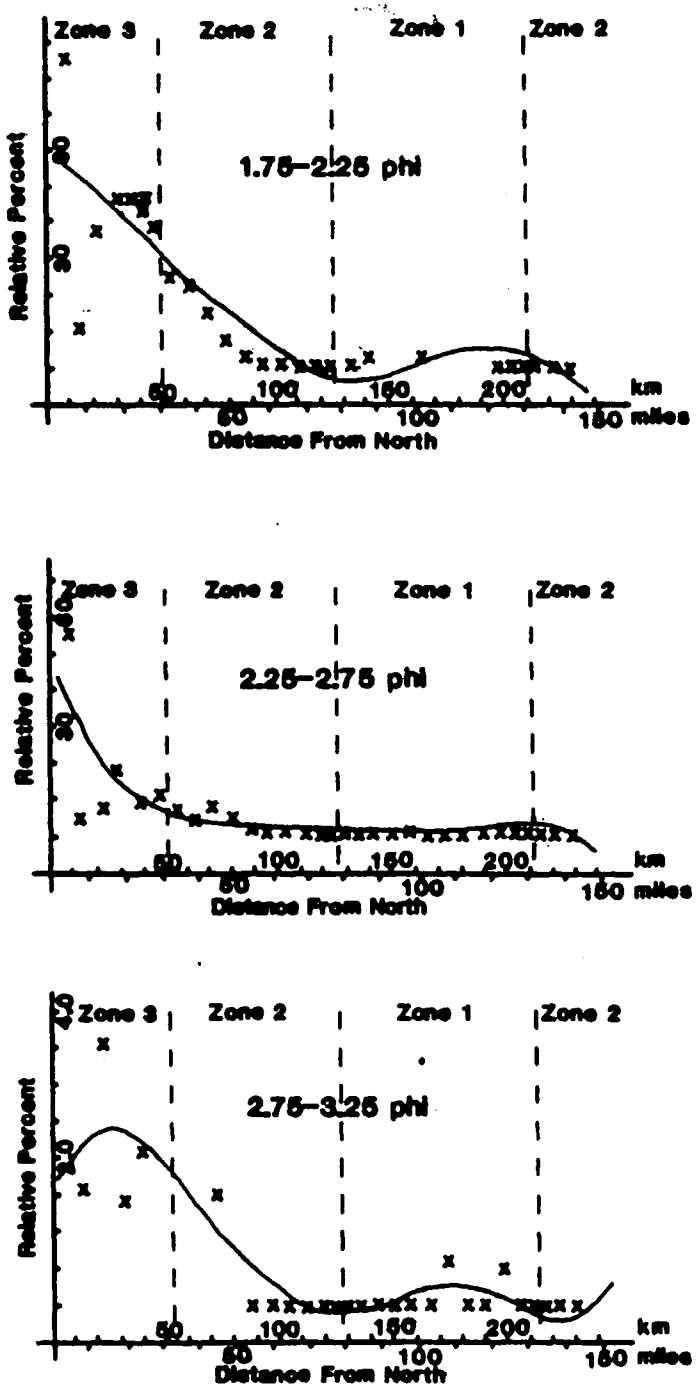

Figure 19. Glauconite (s.g. greater than 2.3Mg/m^3).

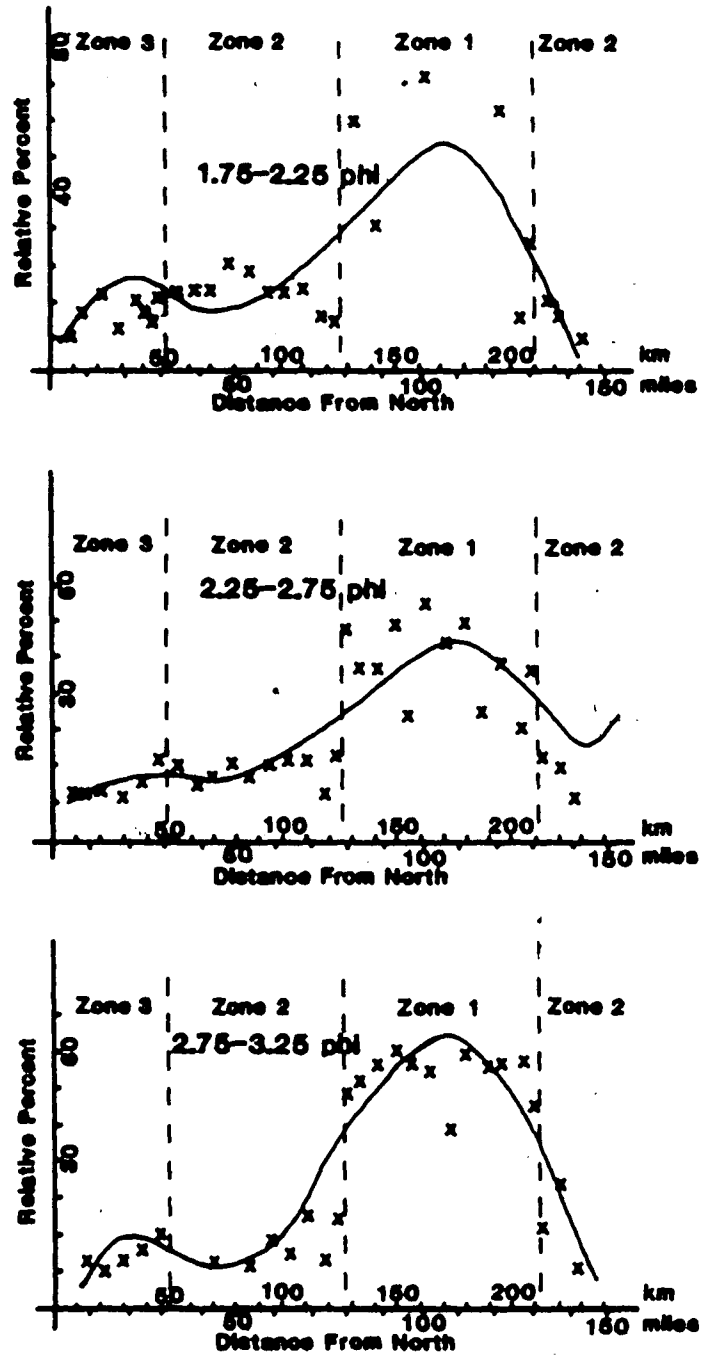

Figure 20. Hornblende (s.g.=3.2Mg/m^3).

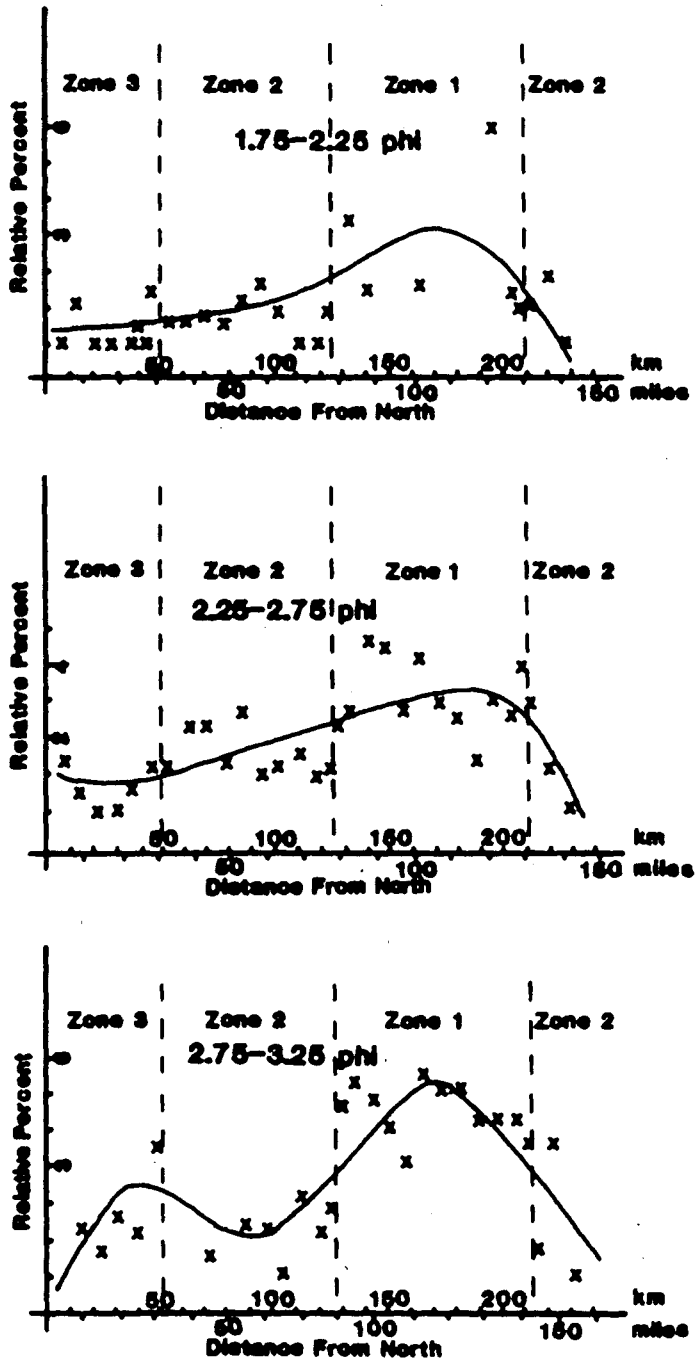

Figure 21. Hypersthene (s.g.=3.4-3.5Mg/m^3).

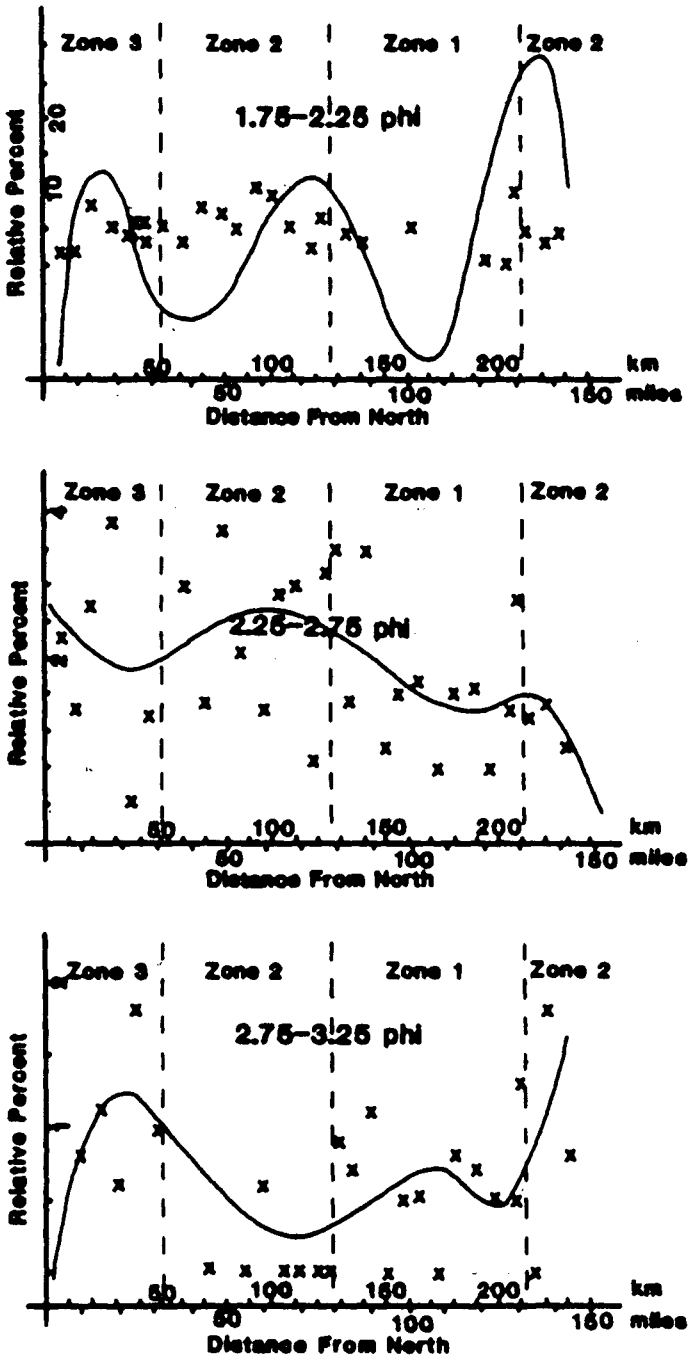

Figure 22. Tourmaline (s.g.=3.0-3.25Mg/m^3).

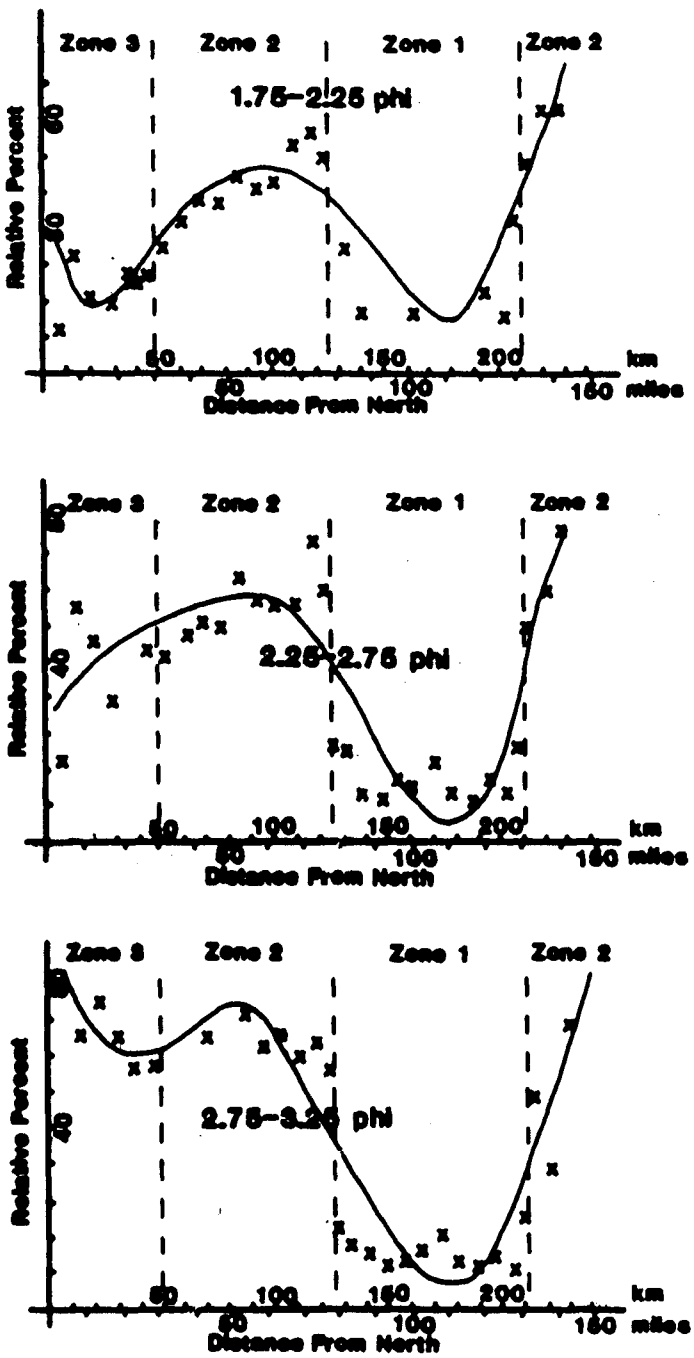

Figure 23. Black opaques (e.g. greater than 4.1Mg/m^3).

As zone 3 sands are transported to the north the denser mineral (collophane) is deposited first, and the less dense mineral (glauconite) dominates further north. A similar pattern can be seen in zone 2 where the dominant current direction is south. The less dense (s.g. = 3.0 - 3.25 Mg/m^3; Hurlbut, 1971) tourmaline (figure 22) is deposited in greatest amounts to the south of the denser (s.g. greater than 4.1 Mg/m^3) black opaques (figure 23). This pattern is unclear in the 2.75 to 3.25 phi fraction because of the lack of tourmaline in this size class.

In zone 1, hornblende (figure 20) and hypersthene (figure 21) are the characteristic heavy minerals. The peak abundances for these two minerals are located in the same place, as might be expected since they have similar specific gravities (hornblende s.g. = 3.2 Mg/m^3, hypersthene s.g. = 3.4 - 3.5 Mg/m^3; Hurlbut, 1971).

It is clear that sorting by particle density is occurring within beach zones. But it is not an important mechanism for determining the zonations because it does not operate between beach zones. As a result, zonations appear to be entirely due to source area variations, and different potential source areas for zones 1 and 2 must be found to explain their occurrence.

FIELD AND LABORATORY ANALYSES OF NEW JERSEY BEACH SANDS

Beach sand samples were obtained to: (1) check mineral identifications and abundances of McMaster (1954), and (2) identify the minerals in the category McMaster called "black opaques." Laboratory methods used to analyze the samples are presented in Appendix III.

Size Analysis

Results

The results of the size analysis are presented in Appendix VIII, and graphically presented in figure 24. The median, Trask sorting, and Trask skewness were calculated with the aid of a computer program (Creager, et al, 1962). McMaster (1954) calculated these size parameters for his sand samples, so they form the basis for comparison.

The median sand sizes for samples B1 through B7 (zone 3) show no well defined trends (figure 24) as there is a large variation between adjacent samples. From Manasquan Inlet to Little Egg Inlet (northern zone 2) the sands show a steady decrease in median size (figure 24). In zone 1 (Little Egg Inlet to Cape May, samples B16-B26, figure 24) the sand is the finest of all the beaches in New Jersey, and there is no decrease in median size (figure 24). On the Delaware Bay shore (southern

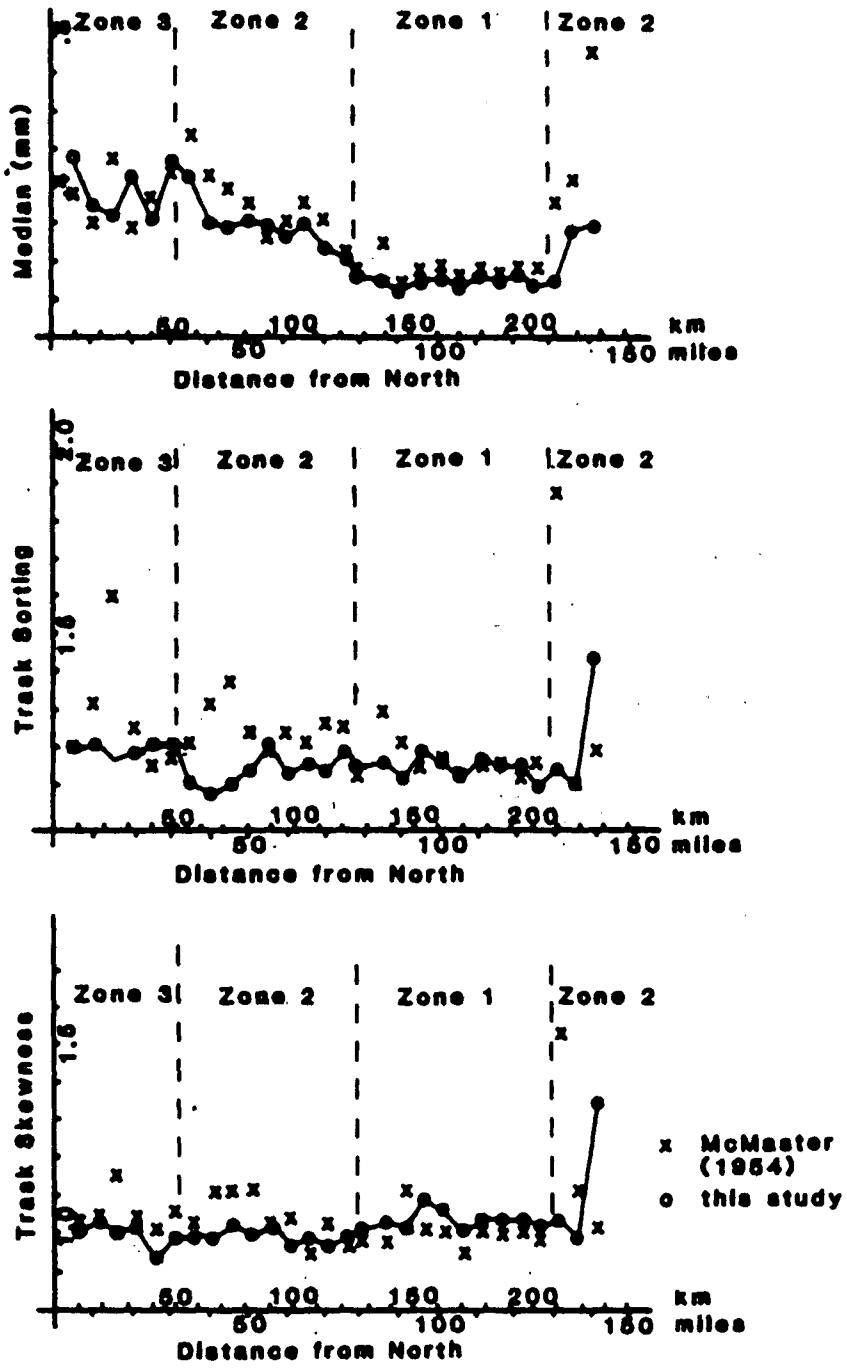

Figure 24. Size analysis results plotted against sample locations. Sample locations are shown in figure 2.

zone 2, samples B27-B28, figure 24) the sands are coarser than in zone 1.

The Trask sorting and Trask skewness results show no obvious trends (figure 24), but the sorting values for this study are generally lower (by about 0.1 units) than McMaster's (1954) values, indicating that either sorting has improved since that study or the analyses are not wholly comparable. Agreement with McMaster's (1954) results was found for median size and Trask skewness, as indicated by the graphs (figure 24).

Discussion

The large variation in median sand size in zone 3 (Sandy Hook to Manasquan Inlet, figure 24) suggests that shoreline configuration, beach-face slope, wave and current strength, and perhaps other local factors control the local grain size (McMaster, 1954).

In northern zone 2 (Manasquan Inlet to Little Egg Inlet, figure 24) there is a southerly increase in fineness which is linear. This is in agreement with MacCarthy's (1931) findings, and implies that: (1) sand is being transported by littoral currents with a dominant southward direction, and (2) sand is transported across major inlets (Manasquan, Barnegat) in this zone.

The constancy of sand size in zone 1 (Little Egg Inlet to Cape May, figure 24) suggests that there is no continuous transport, and associated sorting, of sand along this zone. This constancy of size may be due to the barrier system being cut by frequent inlets,

which retards the transport of sand between adjacent islands.

The distinct change in sand size at Little Egg Inlet (km 118; figure 24) implies a change in immediate source areas for zones 1 and 2, since (as discussed previously) selective sorting is not a viable mechanism.

Only two samples were analyzed on the Delaware Bay shore (southern zone 2), so no conclusions can be drawn concerning the direction and extent of sediment transport.

Mineralogy

Results

The results of the mineralogical analysis of the beach sand samples are presented in Appendix IX. For some samples, a size fraction could not be analyzed because it was nearly absent from the sample. The data indicate that of the heavy minerals counted (black opaques, glauconite, hornblende, and tourmaline), glauconite dominates samples B1, B3, B6, and B10 (54-88% of the 1.75-2.25Ø fraction), black opaques dominate samples B8, B12, B14, B16, B27, and B28 (48-96% of the 2.25-2.75Ø fraction), and hornblende is the most abundant mineral in samples B18, B21, B23, and B25 (68-78% of the 2.75-3.25Ø fraction).

Discussion

No real comparison with McMaster's (1954) data is possible because a heavy liquid with a lower specific gravity (2.78 Mg/m^3 vs 2.85 Mg/m^3) was used in this study, and therefore more glauconite

was counted. However, the basic mineralogic trends should be the same as those observed by McMaster. That is, hornblende should be dominant in zone 1 (samples B16, B18, B21, B23, and B25), glauconite should be most abundant in the 1.75 to 2.25 phi and 2.25 to 2.75 phi fractions of zone 3 (samples B1, B3, and B6), and black opaques should dominate zone 2 (samples B8, B10, B12, B14, B27, and B28). In general this was the case. But sample B16 (figure 2; boundary between zones 1 and 2) contains more black opaques (about 70%) than hornblende (about 15%; Appendix IX) in all but the finest fraction (2.75 to 3.25 phi). In addition, glauconite shows an abundance in samples B8 and B10 (northern zone 2) as well as B1, B3, and B6 (zone 3). These differences may indicate a change in the beach zone boundaries since McMaster's (1954) work. Zone 3 appears to extend farther south today than Manasquan Inlet (figure 2), and zone 1 presently may extend as far south as Brigantine Inlet (figure 2).

X-ray Analysis

The actual minerals constituting the "black opaques" were not determined by McMaster (1954). X-ray diffraction of one sample was undertaken to identify the black opaque mineralogy. No attempt was made to quantitatively determine the mineral abundances. For the analysis, sample B11 was chosen because it falls near the center of the "black opaque zone" of McMaster (1954). X-ray diffraction methods are outlined in Appendix III.

Initially, a trace amount (less than 0.5%) of magnetite was removed with a hand magnet The results of the x-ray diffraction are presented in table 2, and they indicate that the minerals present are hornblende, rutile, pseudorutile, ilmenite, and galena. Hornblende appeared as a black opaque in the reflected light of the binocular microscope when the black opaques were physically separated from sample B11, but it is not a constituent of the black opaque grains identified in transmitted light.

The presence of ilmenite, rutile, and pseudorutile is compatible with Meglio's (1979) findings that the Tertiary Kirkwood and Cohansey Formations (figure 4), which form the surface of the coastal plain over a wider area than any other formations, contain black opaque grains which are predominantly pseudorutile, with less and variable amounts of rutile, and minor amounts of ilmenite. The Cape May Formation (figure 4) is also believed to contain commercial amounts of ilmenite (Meglio, 1979).

The possibility that the mineral identified as hornblende has been incorrectly labeled by previous authors (Colony, 1932; McMaster, 1954; Biederman, 1958) was investigated because past x-ray work on samples from Stone Harbor, N.J. (zone 1) has not exhibited good hornblende x-ray diffraction peaks (Carson, personal communication).

TABLE 2. X-ray Diffraction Peak Positions and Relative Intensities for the Black Opaque Minerals in Sample B11, and Corresponding Powder Diffraction File Data (Berry, 1967).

d-spacing observed (Å)	observed relative intensity*	Powder Diffraction File Data**									
		Galena		Hornblende		Ilmenite		Pseudorutile		Rutile	
		dÅ	I/I_o	dÅ	I/I_o	dÅ	I/I_o	dÅ	I/I_o	dÅ	I/I_o
8.36	100			8.40	100						
3.90	15							8.85	40		
3.47	25	3.43	84								
3.27	20			3.26	20						
3.25	30									3.25	100
3.12	60			3.10	70						
2.95	20	2.97	100								
2.81	20			2.79	12						
2.75	20					2.74	100				
2.71	20			2.70	20						
2.55	15					2.54	85				
2.49	20							2.49	60	2.49	50
2.23	25							2.19	50	2.19	25
		2.10	57								
1.86	5					1.86	85				
		1.79	35								
1.72	5					1.72	100				
1.69	35							1.69	100	1.69	60
1.50	5					1.50	85				
1.45	5					1.47	85				

* relative to all observed black opaque peak heights

** d-spacings and intensities relative to other heights for the mineral

Sample B23 was used in the analysis because McMaster's (1954) findings indicate that it should contain large amounts (greater than 30%) of hornblende in the heavy mineral fraction. To further concentrate the hornblende, magnetic separations were done on the bulk heavy mineral fraction (methods outlined in Appendix III). All of hornblende's most intense peaks were clearly revealed (table 3). Therefore, it is clear that the dominant heavy mineral in the beaches of southern New Jersey is indeed hornblende.

TABLE 3. X-ray Diffraction Peak Positions and Relative Intensities for Heavy Minerals (magnetically separated) of Sample B23, and Powder Diffraction File Data for Hornblende (Berry, 1967).

d-spacing observed (Å)	observed relative intensity (I/I_o)	Powder Diffraction File Data Hornblende	
		dÅ	I/I_o
8.42	94	8.40	100
3.26	27	3.26	20
3.11	100	3.10	70
2.80	26	2.79	12
2.70	24	2.70	20

FIELD AND LABORATORY ANALYSES OF POSSIBLE SOURCE SANDS

Potential immediate sources for New Jersey beach sands are mainland formations, the continental shelf, and local rivers. The mainland formations have been examined (McMaster, 1954; Wolfe, 1977; Owens and Minard, 1979), and their contribution to the beach sands north of Bay Head (zone 3; figure 13) has been demonstrated (McMaster, 1954). Coastal formations also supply the beach sand for the Delaware Bay shore beaches (McMaster, 1954).

The immediate source of the beach sands from Bay Head to Cape May (zones 1 and 2; figure 13) cannot be the coastal formations because these beaches are separated from the mainland by lagoons. In the middle of this coastal area there is an apparent change in sources at Little Egg Inlet (the boundary of beach zones 1 and 2; figure 13). Zone 1 material is rich in hornblende, which is of uncertain origin (i.e. adjacent coastal formations show no comparable mineralogy; McMaster, 1954). Coastal formations have, in fact, mineralogies compatible with the zone 2 sands, being relatively rich in black opaques (McMaster, 1954).

Description of Source Sands

Shelf and river sample descriptions are presented in Appendices I and X. The results indicate that the shelf sand textures are variable (very fine to very coarse grained), as are the river sample

textures (sandy mud to coarse sand). The color is also variable and appears to be dependant on the texture. Coarse sands are yellowish (Munsell code 10YR), and muddy sands are greenish (Munsell code 5Y) and darker. The organic constituents of the shelf samples reflect the position on the ridges and swales from which the sample was taken (McKinney, et al, 1974). Sand dollars indicate proximity to a ridge crest, and crabs or large shells indicate a trough location. Shell fragments are ubiquitous to the New Jersey shelf.

Mineralogy of Source Sands

Methods used to obtain the heavy mineralogy of the source sands are outlined in Appendix III.

Results

The results of the microscopic analysis are listed in Appendix IX. The data is plotted against distance along the coast in figures 25 through 28.

The distribution of heavy minerals in the New Jersey inner-continental shelf sediments is similar to the distribution on the beaches. Glauconite (figure 25) is most abundant near Sandy Hook (km 2), and is nearly absent in shelf sediments south of Barnegat Inlet (km 84). Black opaques (figure 28) are an abundant (19-94%) constituent of shelf sands along the entire coast, but they seem to be most abundant (greater than 50%) in areas seaward of zone

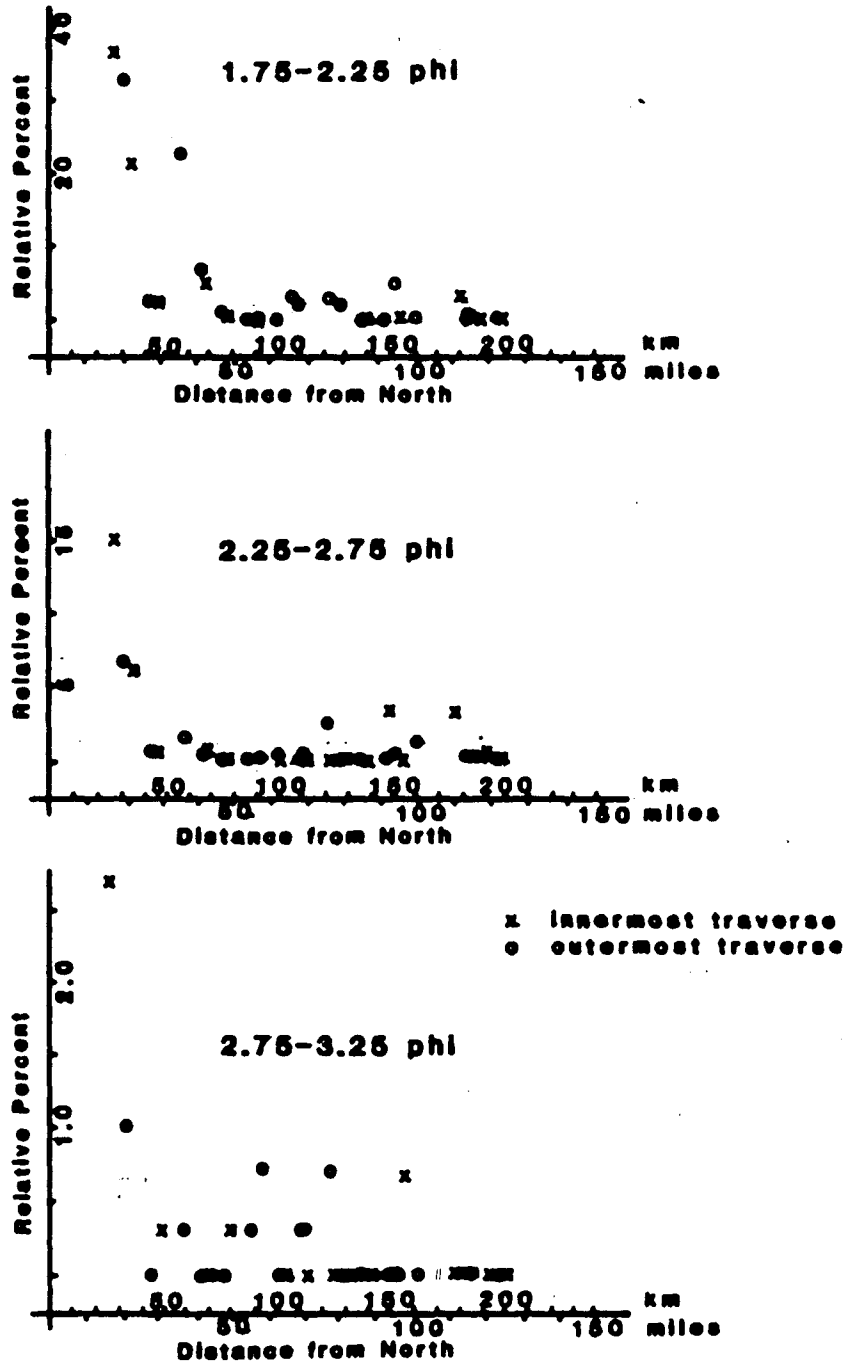

Figure 25. Glauconite abundance in shelf samples. Percentages are relative to other minerals counted (hornblende, tourmaline, and black opaques). Sample locations are distances south from Sandy Hook.

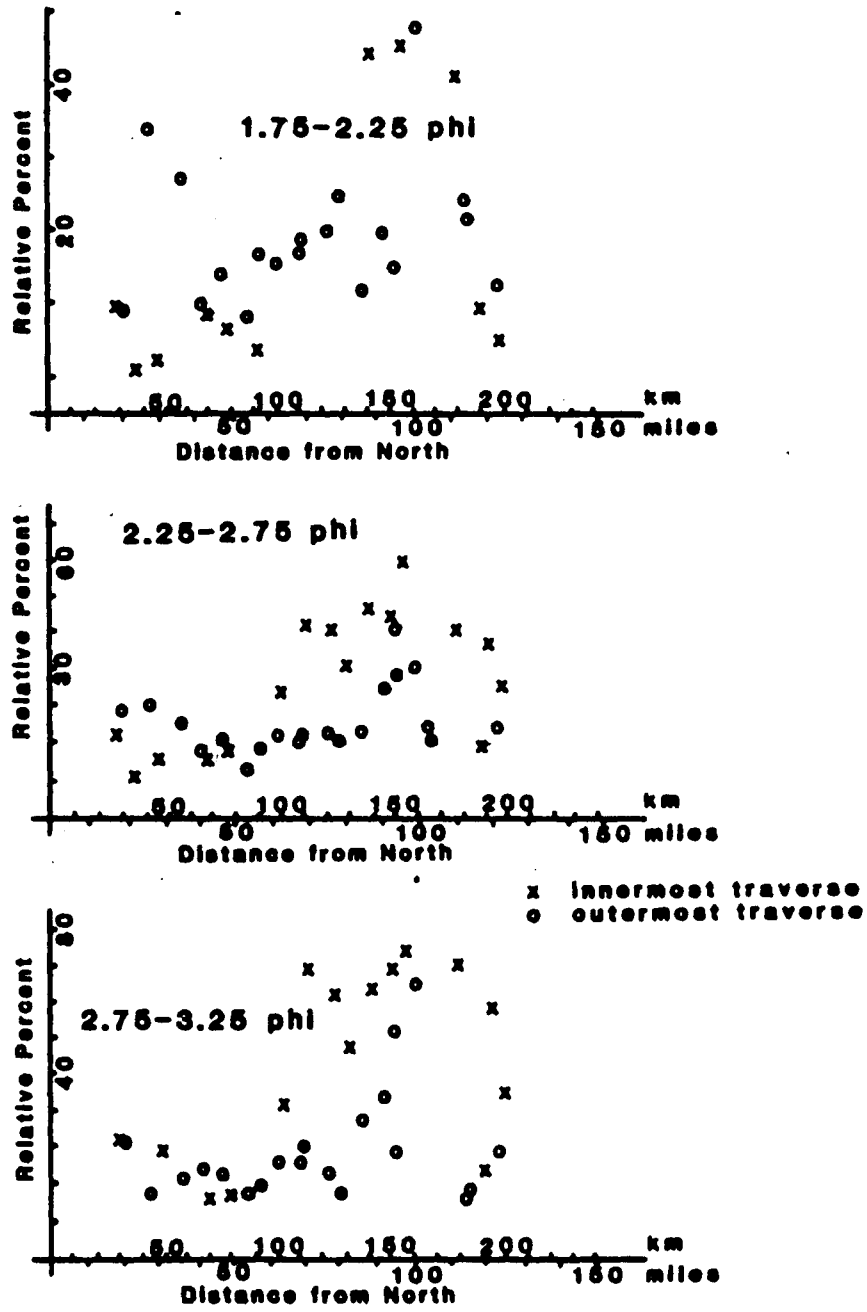

Figure 26. Hornblende abundance in shelf samples. Percentages are relative to other minerals counted (glauconite, tourmaline, and black opaques). Sample locations are distance south from Sandy Hook.

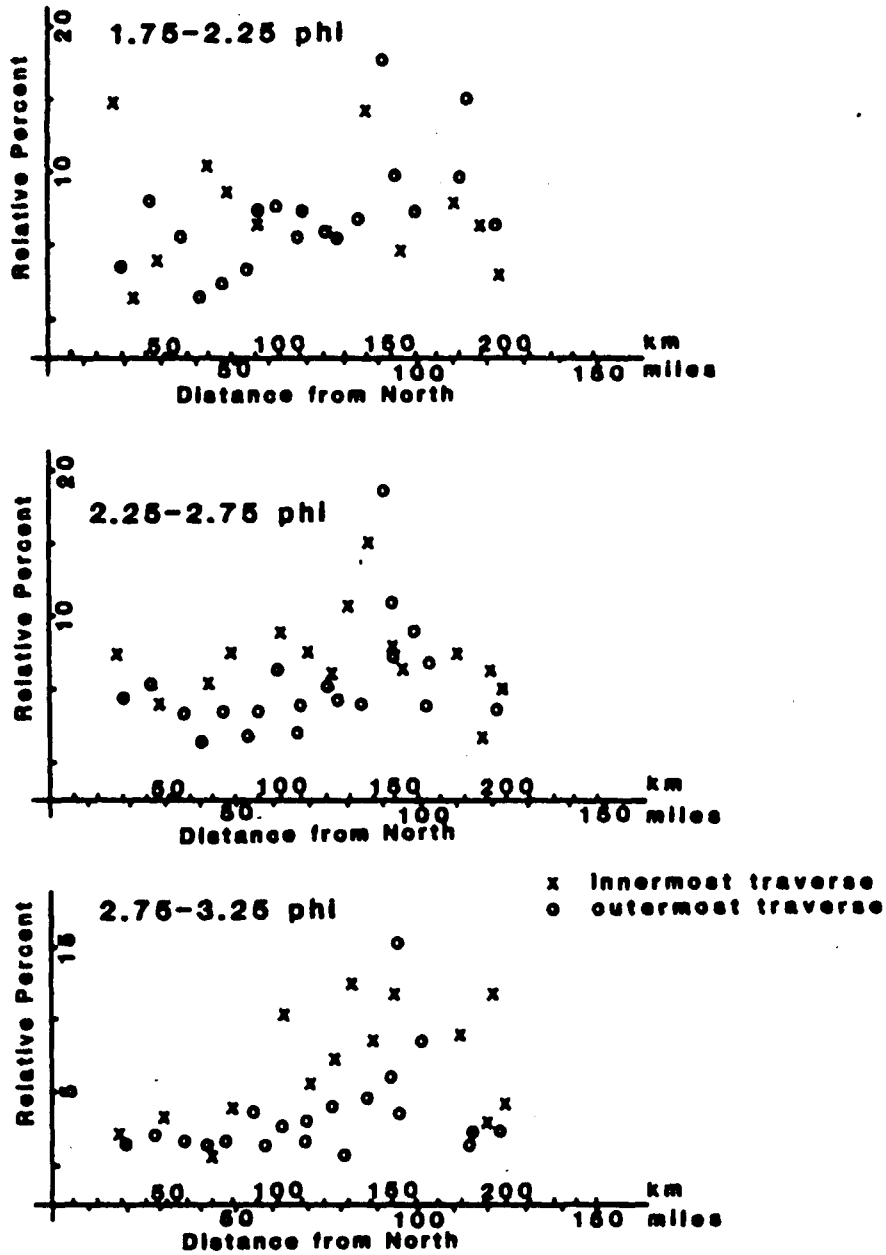

Figure 27. Tourmaline abundance in shelf samples. Percentages are relative to other minerals counted (glauconite, hornblende, and black opaques). Sample locations are distances south from Sandy Hook.

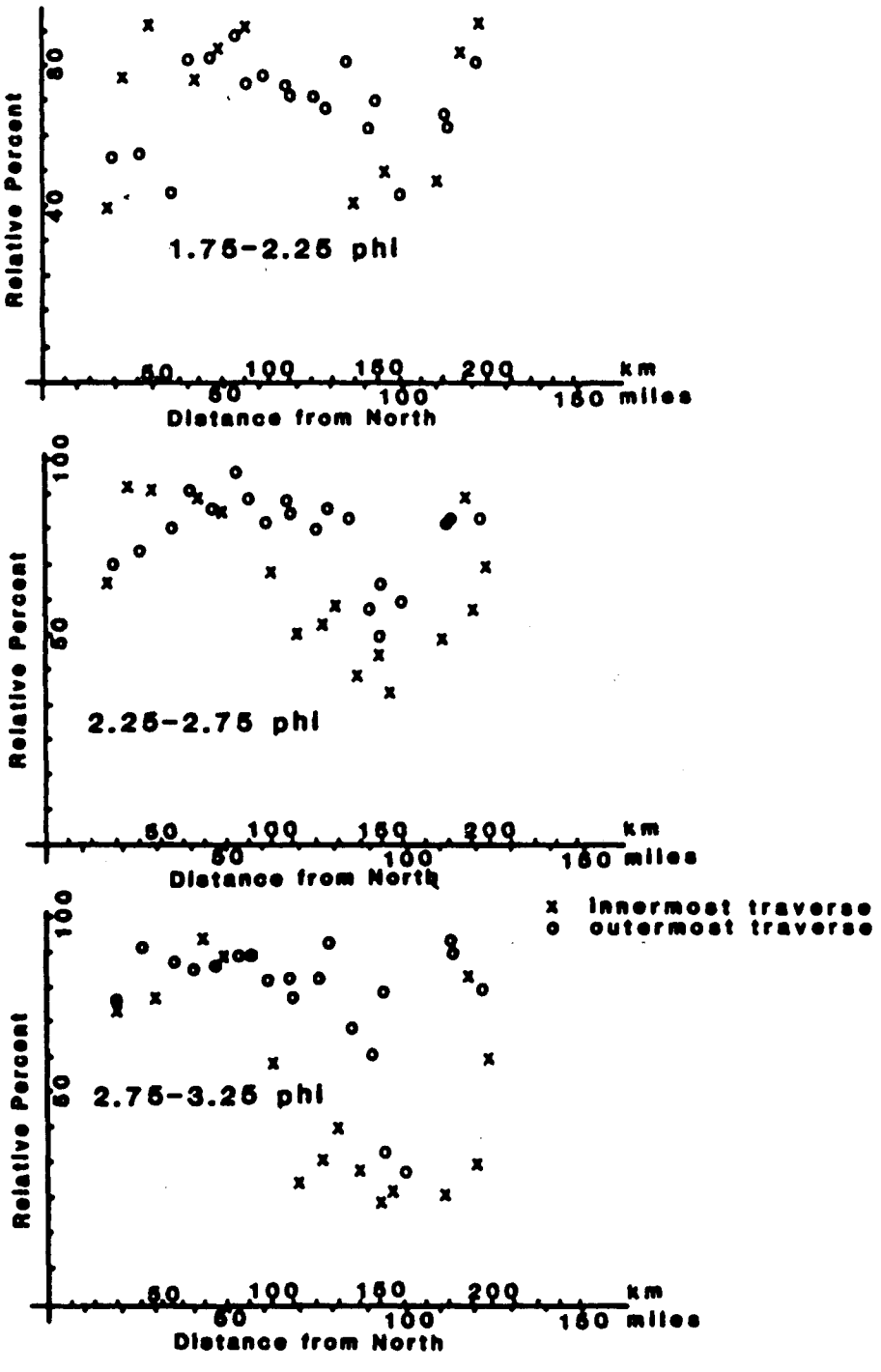

Figure 28. Black opaques abundance in shelf samples. Percentages are relative to other minerals counted (glauconite, hornblende, and tourmaline). Sample locations are distances south from Sandy Hook.

2 beaches (km 51-117). Hornblende (figure 26) is much more abundant (greater than 30%) seaward of zone 1 beaches (km 122-208) than elsewhere (less than 20%).

The river samples are dominated (greater than 97%) by black opaques, and show little hornblende (less than 0.5%), glauconite (0.0%), and tourmaline (less than 2.5%).

Discussion

The mineralogical results indicate that the shelf sands, in general, reflect the mineralogy of the adjacent beach sands. Because of the lack of hornblende in the river samples, it is apparent that rivers are not supplying hornblende-rich sand to zone 1 beaches.

CORRELATION OF BEACH AND SOURCE SANDS

Point count data for beach, shelf, and river sands was submitted to Q-mode factor analysis so that beach zones could be correlated with potential source areas. The resulting oblique projection matrices are shown in Appendix XI. These results are summarized in figure 29. A sample was placed in a zone according to the highest projection loading (Appendix XI) of that sample.

Zone 3

The glauconite-rich beach sand zone does not derive its sand from the continental shelf. No shelf samples are grouped with the beach samples in this zone, but there is a relatively large amount of glauconite (greater than 20% of the 1.75-2.25Ø fraction) in the shelf sands near Sandy Hook (figure 2). These results indicate that shore formations have supplied some material to the shelf, but the shelf sands cannot be the major contributor to the zone 3 beaches.

Beach zone 3 extends from Sandy Hook (km 2) to Barnegat Inlet (km 76). This is 41 kilometers farther south than the boundary drawn by McMaster (1954). Much more (17-54% in the 1.75-2.25Ø and 2.25-2.75Ø fractions) glauconite was found in the beach sands from Manasquan Inlet (km 51) to Barnegat Inlet (km 76) in this study (partly because of the use of a lower specific gravity heavy liquid in this study), which may indicate a change in sources for beaches in this area since 1954. Sand is being supplied dominantly by

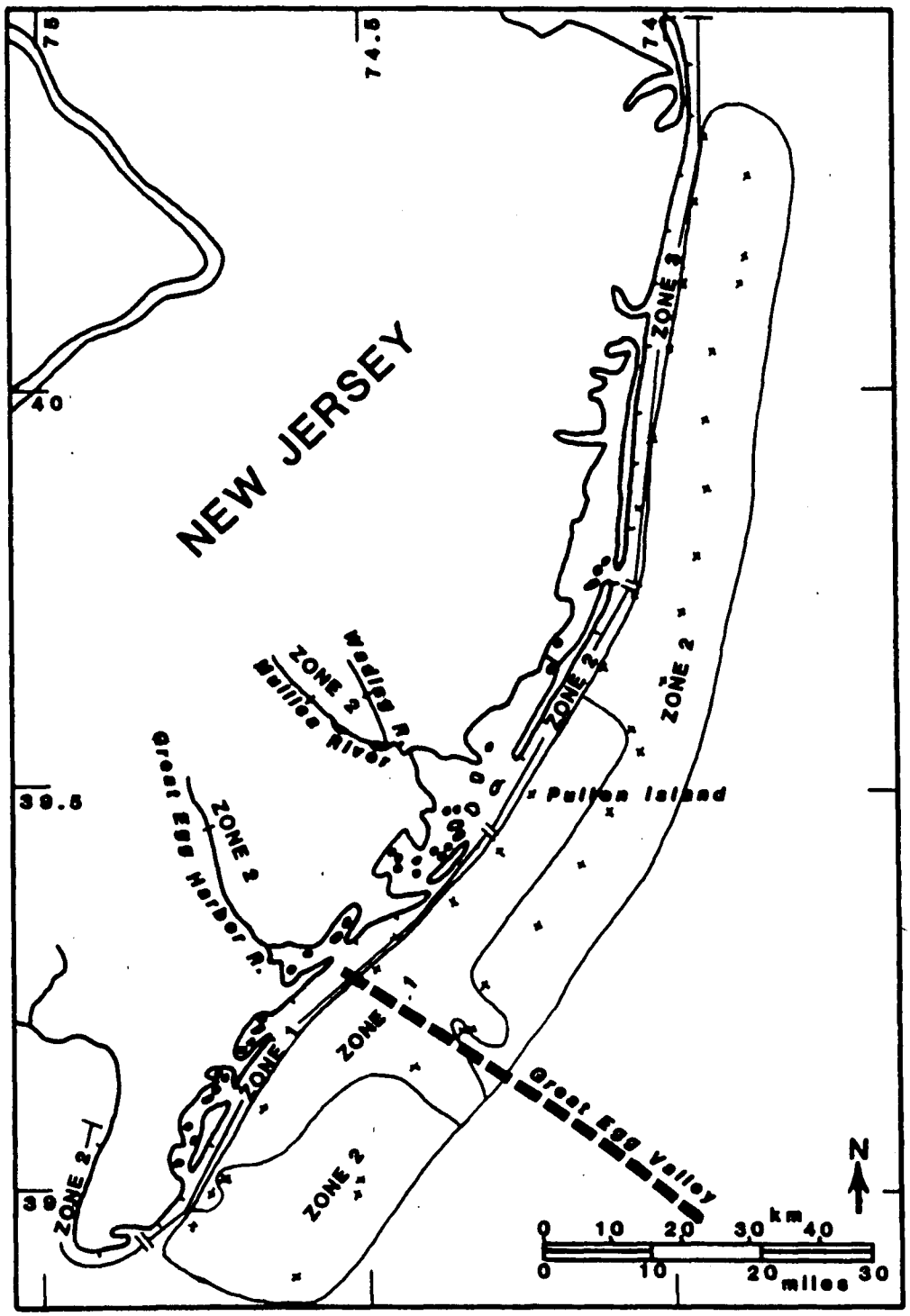

Figure 29. Mineralogical zones for beach, shelf, and river samples.

coastal formations (Cohansey, Kirkwood) north of Manasquan Inlet. This pattern implies that littoral drift is capable of transporting sand across Manasquan Inlet in large quantities, probably during large storms.

Zone 1

The hornblende-rich sands of zone 1 (figure 29) are not derived from the two major river systems in the area (Mullica River and Great Egg Harbor River). The river samples contain almost no hornblende (less than 0.5%) of the grains counted in the size fractions analyzed.

The lateral extent of the zone 1 beaches is slightly different from that defined by McMaster (1954). The southern boundary is the same (km 200), but in the north the beach sand of Pullen Island (sample B16, km 122) is now dominated (65 and 72% of the four minerals counted in the 2.25-2.75Ø and 1.75-2.25Ø fractions respectively) by black opaques. McMaster found more hornblende (50% of all heavy minerals) in this sand. It appears that the black opaque-rich sand from the north has been transported in large quantities to Pullen Island since 1954. Dredging of Little Egg Inlet could be responsible for bringing these sands (trapped in the inlet after transport from the north) to Pullen Island, but more likely the black opaque-rich sand is present because of sand transport across the inlet during large storms.

Some shelf sands from the innermost traverse are hornblende-rich (samples S40-S46 and S48; 36-74% of the 2.75-3.25Ø fraction; km 107-190; Appendix IX), and are considered to be an immediate source of the beach sands of zone 1. This immediate source is not located directly offshore however, but is displaced to the north (figure 29). Sample S40 is located 33 kilometers upcoast (northeast) of beach sample B18, which is the northernmost beach sample associated with zone 1 (figures 2 and 29). Sample S47 is located 29 kilometers upcoast (northeast) of beach sample B27, which is the closest beach sample of zone 2 sands in the south. These results indicate that sand from the shelf is transported to the beaches in a southwesterly direction.

The shelf sands sampled on the seaward transect (figure 2) are not being supplied to the beaches of zone 1. Only two of these samples (S9 and S11; km 147-157; figure 2) contain enough hornblende to be correlated with the beach sands. This pattern implies that continental shelf sands in water depths of about 18 meters are not reaching the beaches in significant proportions, while those sands at about 9 meters depth are.

The two hornblende-rich (52-64% of the 2.75-3.25Ø fraction; Appendix IX) offshore samples (S9 and S11) are located in close proximity (figure 29) to the Great Egg Harbor River channel (Veatch and Smith, 1939). The late-Pleistocene/Holocene drainage of this river apparently supplied the hornblende-rich sands to the shelf as it migrated from as far north as Little Egg Inlet to as far south

as the shelf channel position (Owens and Minard, 1979). This migration must have deposited a relatively thin blanket of hornblende-rich sands on the shelf north of the present channel. As sea level rose, reworking of the thin blanket apparently brought these sands closer to the present shoreline. The only hornblende-rich offshore (at about 18m water depth) sands that remain are those where thick deposits of the sand occur, near the shelf channel.

Zone 2

The black opaque-rich sands of northern zone 2 (between Barnegat Inlet and Little Egg Inlet; figures 2 and 29) are apparently also derived from shelf sediments. The inner and outer traverses each show mineralogies compatible with the adjacent beaches. The sediment is transported to the beaches by storm driven currents in a southwest direction as indicated at the south end of Long Beach Island (mile 74) where the beach sands are black opaque-rich, and the adjacent shelf sands are hornblende-rich. These beaches were apparently supplied with sand from the shelf adjacent to the northern end of the island.

Zone 2 beaches on the Delaware Bay shore are thought to be supplied with sand from coastal outcrops. This sand is not transported from Delaware Bay up the New Jersey coast north of Cape May Inlet.

Reevaluation of Shelf Sand Textures

The beach sand texture changes drastically (mØ = .213mm to .164mm; Appendix VIII) at Little Egg Inlet (km 118), the northern boundary between zones 1 and 2. This change is also reflected in the shelf sands, as summarized below.

The shelf sands that are mineralogically correlated with zone 1 beaches (S9, S11, S40-S46, and S48; figure 2) are all very fine or fine grained (.063-.250mm) sands (Appendix X). The zone 1 beach sands are all classified as fine sands (.125-.250mm), which is in contrast to beach deposits from the rest of the coast where the sand is of medium size (.250-.500mm), with few exceptions (B14, B15, and B26; figure 2). Shelf sediments (samples S6-S8, S10, S12-S26, and S32-S39; figure 2) that are correlated with zone 2 beach sands range from fine to very coarse sand (.125-2.000mm), but most (25%) are medium (.250-.500mm), and a large portion (20%) are coarse grained (.500-1.000mm).

This variation in texture between the immediate source sands of the zone 1 and zone 2 beaches may explain the discontinuity of sand texture at the beaches. It has been proposed that the variation in beach slope is responsible for the change in median grain size from zone 2 to zone 1 (McMaster, 1954). Actually, the reverse may be true. The fact that the source sands of zone 1 are finer grained may have resulted in a more gently sloping beach face.

GENESIS OF THE BEACH SANDS

During the Holocene transgression (18,000-7,000 years B.P.), barrier beach complexes were probably developed by the submergence of ridge-like coastal features, and/or the progradation of spits (Schwartz, 1971).

Sand was supplied to the nearshore zone by the river systems which carried sediment from the Piedmont and Highland provinces during the transgression, and by the reworking of shelf sediments. Before sea level reached the present 80m isobath, river sediment was transported directly to the shelf canyons which cut the shelf edge (figure 30). Subsequently, as sea level rose above the 80m isobath, fluvial sediment was supplied to the nearshore zone (McClennen, 1973).

As sea level continued to rise, the barrier systems may have migrated landward. This migration could be accomplished by overwash processes during storms, and may be evidenced by the presence of the ridge and swale topography on the New Jersey shelf (McClennen, 1973).

The late-Pleistocene/Holocene river drainage patterns of the coastal plain are apparently responsible for the deposition of two distinct sand types on the New Jersey shelf: the hornblende-rich zone 1 sands, and the black opaque-rich zone 2 sands.

The known river channels of the continental shelf and coastal plain of New Jersey are shown in figure 30 (Swift, 1980). The

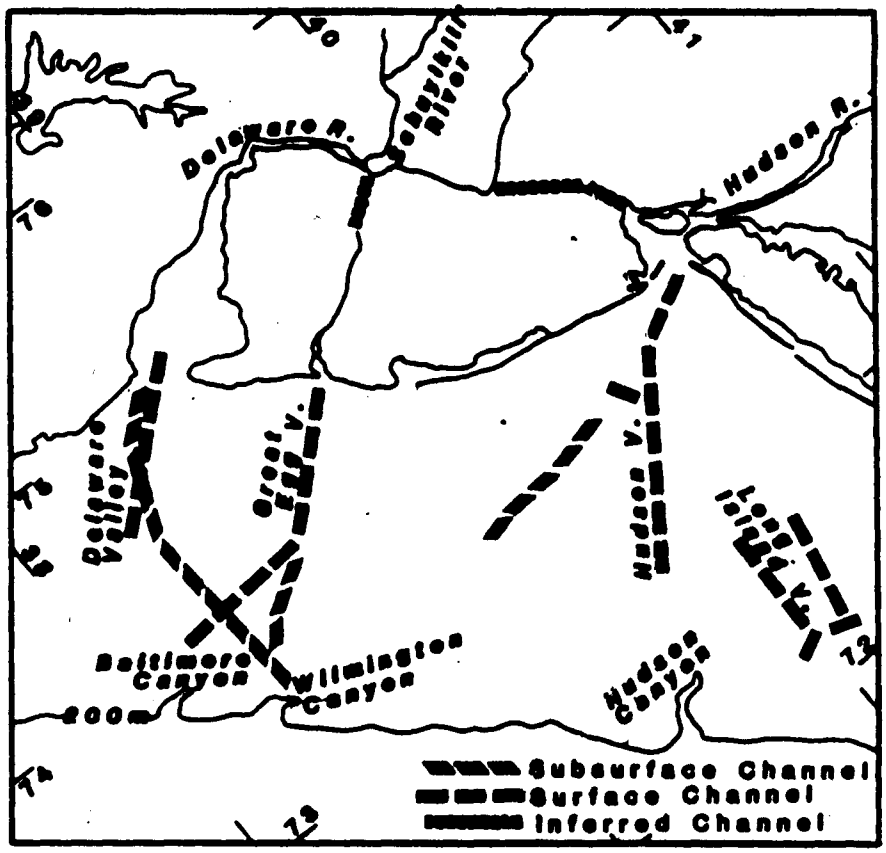

Figure 30. River channels on the New Jersey coastal plain and continental shelf (Swift, 1980).

history of these rivers is complex due to numerous migrations and piracies. However, what is known of their late-Quaternary history is summarized below.

The Hudson River migrated from the Wilmington Canyon (figure 30) north to its present position due to regional downwarping associated with glacial loading in the north (Kelling, et al, 1975). The Schuylkill River continued to the Great Egg River at the end of the Pleistocene (20,000 years B.P.), and the Delaware River did not extend inland as far as today (McClennen, 1973). At this time black opaque-rich river sands (derived from the Appalachian region) were deposited at the New Jersey nearshore zone. Headward erosion of the Delaware River subsequently captured the Schuylkill River and greatly decreased the flow of the Great Egg River.

The shelf sands were supplied by the rivers and modified by the Holocene transgression. The hornblende-rich sands of zone 1 have a derivation related to the deposition of the Pleistocene Bridgeton Formation (figure 5). This formation is rich in hornblende, and contains small scale channel deposits on the coastal plain (Owens and Minard, 1979). Owens and Minard conclude that this formation represents a period of downcutting of a major stream (ancestral Hudson River) which migrated in a southward direction from near Little Egg Inlet to Cape May. The river deposited sands in the coastal zone, and the sediments have since been reworked during the Holocene transgression.

Today the New Jersey beaches are supplied with sand derived from: (1) coastal formations exposed to marine processes, and/or (2) the continental shelf.

CONCLUSIONS

1. Three distinct beach sand types are present along the New Jersey coast; zone 1 sands are hornblende-rich fine (.125-.250 mm) sands, zone 2 sands are black opaque-rich medium (.250-.500 mm) sands with relatively large amounts of tourmaline, and zone 3 sands are glauconite-rich medium sands.

2. The major source of beach sand from Sandy Hook to Barnegat Inlet (zone 3) is the Tertiary formations occurring between Asbury Park and Monmouth. Littoral currents affect southward sand transport across Manasquan Inlet, probably during large storms.

3. The beach sands from Barnegat Inlet to Brigantine Inlet (northern zone 2) are currently derived from the inner-continental shelf. The net sediment transport direction from shelf to beach is to the southwest, not directly onshore.

4. The immediate source of beach sand from Brigantine Inlet to Cape May (zone 1) is the continental shelf sand relatively close to shore (within 7 km).

5. The Delaware Bay shore (southern zone 2) beach sands are derived from the Cape May Formation which crops out along the beaches.

6. During normal conditions sand is transported by littoral drift along the beaches, but significant sand transport may not occur across major inlets. During large storms, however, large volumes of sediment appear to have been transported across the Manasquan and Little Egg Inlets.

7. The present day sands of the Great Egg Harbor, Mullica, and Wading Rivers are not being transported in noticeable amounts to the New Jersey beaches.

8. Textural variation in nearshore (less than 18m depth) continental shelf (source) sediments accounts for the discontinuity in beach sediment median size observed at Little Egg Inlet, rather than selective sorting by longshore transport.

9. Hornblende-rich (zone 1) beach sands are apparently derived from late-Pleistocene/Holocene fluvial sediments deposited on the present continental shelf. These sediments may be related to deposits of the Bridgeton Formation and associated with Pleistocene deposition from an ancestral Hudson River.

REFERENCES

Alexander, A.E., 1934, A petrographic and petrologic study of some continental shelf sediments: Jour. Sed. Pet., V.4, p.12-22.

Berry, L.G., 1967, Powder Diffraction File, Inorganic Volume: Joint Committee on Powder Diffraction Standards.

Biederman, E., 1958, Shoreline sedimentation in New Jersey: Ph.D. dissertation, Penn State University.

Bumpus, D.F., 1965, Residual drift along the bottom on the continental shelf in the middle-Atlantic Bight area: Limnology and Oceanography, V.10, p.R50-R53.

_____, 1969, A description of the circulation on the continental shelf of the east coast of the United States in Warren, B.A. (ed), Progress in Oceanography: Pergamon Press Ltd., New York, V.6, p.111-157.

Butman, B., Folger, D., and Noble, M., 1976, Winter sediment mobility on the Atlantic outer continental shelf: Geol. Soc. Am. Abs. with Prog., V.8, p.799-800.

Carson, B., Personal communication, Lehigh University, Bethlehem, PA.

Cataldo, R.M., 1980, Sediment transport along the coast of New Jersey: Masters Thesis, Syracuse University.

Colony, R.J., 1932, Source of the sands on the south shore of Long Island and the coast of New Jersey: Jour. Sed. Pet., V.2, p.150-159.

Creager, J.S., McManus, D.A., and Collias, E.E., 1962, Electronic data processing in sedimentary size analysis: Jour. Sed. Pet., V. 32, p.833-839.

Davis, J.C., 1973, Statistics and Data Analysis in Geology: Wiley, New York, 550p.

Dietz, R.S., 1963, Wave-base, marine profile of equilibrium, and wave-built terraces: A critical appraisal: Geol. Soc. Am. Bull. 74, p.971-990.

Donahue, J.G., Allen, R.C., and Heezen, B.C., 1966, Sediment size distribution profile on the continental shelf off New Jersey: Sedimentology 7, p.155-159.

Duane, D.B., et al, 1971, Linear Shoals on the Atlantic inner continental shelf, Florida to Long Island in Swift, J.P. (ed), Shelf Sediment Transport: Process and Pattern: Dowder, Hutchinson, and Ross, Stroudsburg, PA, p.447-498.

Emery, K.O., 1968, Relict sediments of continental shelves of the world: Amer. Assoc. Petr. Geol. Bull. 52, p.445-464.

_____, 1971, Estuaries and lagoons in relation to continental shelves in Lauff, G.H. (ed), Estuaries: Amer. Assoc. for the Advan. of Sci., Washington, D.C., p.9-11.

Ewing, J., et al, 1963, Upper stratification of Hudson apron region: Jour. Geoph. Res., V.68, p.6303-6316.

Fischer, A.G., 1961, Stratigraphic record of transgressing seas in light of sedimentation of the Atlantic coast of New Jersey: Amer. Assoc. Petr. Geol. Bull. 45, p.1656-1666.

Frank, W.M. and Friedman, G.M., 1973, Continental shelf sediments off New Jersey: Jour. Sed. Pet., V.43, p.224-237.

Friedman, G.M. and Sanders, J.E., 1970, Integrated continental shelf environment research program: Sediments, organisms, and waters in New York bight and vicinity: Marit. Sed., V.6, p.26-29.

Geological Society of America, 1970, Rock Color Chart, G.S.A., Boulder Col.

Hayden, B.P. and Dolan, R., 1979, Barrier islands, lagoons, and marshes: Jour. Sed. Pet., V.49, p.1061-1072.

Hubert, J.F. and Neal, W.F., 1967, Mineral composition and dispersal patterns of deep-sea sands in the western north Atlantic petrologic province: Geol. Soc. Am. Bull. 78, p.749-772.

Hurlbut, C.S., 1971, Dana's Handbook of Mineralogy: John Wiley and Sons, 579p.

Kelley, J.T., 1981, Comment on "Quaternary Rivers on the New Jersey Shelf: Relation of Seafloor to Buried Valleys": Geology, V.9, p.98.

Kelling, G., Sheng, H., and Stanley, D.J., 1975, Mineralogic composition of sand-sized sediment on the outer margin off the mid-Atlantic states: Assessment of the influence of the ancestral Hudson and other fluvial systems: Geol. Soc. Am. Bull, 86, p.853-862.

Klovan, J.E., 1975, R- and Q-mode factor analysis in McCammon, R.B. (ed), Concepts in Geostatistics: Springer-Verlag, New York, p.21-69.

Komar, P.D., 1976, Beach Processes and Sedimentation: Prentice Hall, New Jersey, 429p.

Knebel, H.J., 1979, Hudson River: Evidence for extensive migration on the exposed continental shelf during Pleistocene time: Geol. 7, p.254-259.

Krauser, R.F. and Coch, N.K., 1978, Sediment dynamics and textural facies in the Brigantine Inlet area, New Jersey: Geol. Soc. Am. Abstr. with Prog., V.10, p.72.

Krumbein, W.C., 1934, The probable error of sampling sediments for mechanical analysis: Am. Jour. Sci., 5th Series, V.27, p.204-214.

MacGarthy, G.R., 1931, Coastal sands of the eastern United States: Am. Jour. Sci., 5th Series, V.22, p.35-50.

MacClintock, P. and Richards, H.G., 1936, Correlation of late-Pleistocene marine and glacial deposits of New Jersey and New York: Geol. Soc. Am. Bull. 47, p.289-338.

Macpherson, J.M. and Lewis, D.W., 1978, What are you sampling?: Jour. Sed. Pet., V.48, p.1341-1344.

Manson, V. and Imbrie, J., 1964, Fortran program for factor and vector analysis of geologic data using IBM 7090 or 7094/1401 computer system: Kansas Geol. Sur. Spec. Dist. Publ. 13.

Markewicz, F.J., 1969, Ilmenite deposits of the New Jersey coastal plain in Subitzky, S. (ed) Geology of Selected Areas in New Jersey and Eastern Pennsylvania and Guidebook of Excursions: Rutgers Univ. Press, New Brunswick, N.J., p.363-382.

McClennen, C.E., 1973, Nature and origin of the New Jersey continental shelf topographic ridges and depressions: Ph.D. dissertation, University of Rhode Island.

_____, 1973a, New Jersey continental shelf near bottom current meter records and recent sediment activity: Jour. Sed. Pet., V.43, No. 2, p.371-380.

McMaster, R., 1954, Petrography and genesis of New Jersey beach sands: New Jersey State Dept. of Conservation and Econ. Dev. Bull. 63, 239p.

McKinney, T.F., Stubblefield, W.L., and Swift, D.J.P., 1974, Large-scale current lineations on the central New Jersey shelf: Investigations by sidescan sonar: Marine Geol., V.17, p.79-102.

Meade, R., 1969, Landward transport of bottom sediments in estuaries of the Atlantic coastal plain: Jour. Sed. Pet., V.39, p.222-234.

Meglio, J.T., 1979, The oxidation and titanium-enrichment mechanisms of "altered ilmenite" grains in the Tertiary Kirkwood and Cohansey Formations of New Jersey: Masters Thesis, Lehigh University.

Milliman, J.D., 1972, Atlantic continental shelf and slope of the United States, Petrology of the sand fraction -- Northern New Jersey to southern Florida: U.S.G.S. Prof. Pap. 529-J.

Milliman, J.D., Pilkey, O.H., and Ross, D.A., 1972, Sediments of the continental margin off the eastern United States: G.S.A. Bull. 83, p.1315-1334.

Neiheisel, J., 1973, Source of detrital heavy minerals in estuaries of the Atlantic coastal plain: Ph.D. dissertation, Georgia Inst. Tech.

Owens, J.P. and Minard, J.P., 1979, Upper-Cenozoic sediments of the lower Delaware valley and the northern Delmarva peninsula, New Jersey, Pennsylvania, Delaware, and Maryland: U.S.G.S. Prof. Pap. 1067-D.

Owens, J.P. and Sohl, N.P., 1969, Shelf and deltaic paleoenvironments in Cretaceous-Tertiary formations of the New Jersey coastal plain in Sibitzky, S. (ed), Geology of Selected Areas in New Jersey and Eastern Pennsylvania and Guidebook of Excursions: Rutgers Univ. Press, New Brunswick, N.J., p.235-278.

Parks, J.M., 1966, Cluster analysis applied to multivariate geologic problems: Jour. Geol., V.74, p.703-715.

_____, 1970, Fortran IV program for Q-mode cluster analysis on distance function with printed dendogram: Kansas Geol. Sur. Computer Contri. 46.

Rasmussen, W.C., 1941, Local areal variation of heavy minerals in beach sand: Jour. Sed. Pet., V.11, p.68-101.

Rittenhouse, G., 1943, Transportation and deposition of heavy minerals: Geol. Soc. Am. Bull., V.54, p.1725-1780.

Schubel, J.R., 1974, Effects of tropical storm Agnes in the suspended solids of the northern Chesepeake Bay: Marine Science, V.4, p.113-132.

Schwartz, M.L., The multiple causality of barrier islands in Schwartz, M.L. (ed), Barrier Islands.

Shepard, F.P. and Cohee, G.V., 1936, Continental shelf sediments off the mid-Atlantic states: Geol. Soc. Am. Bull., V. 47, p. 441-458.

Sherif, N., Charlesworth, L.J. Jr., and Wilband, J.T., 1973, Modal analysis of heavy minerals of New Jersey beach sands by x-ray diffraction: Geol. Soc. Am. Abstr., Northeast Section, 8th Annual Meeting, V.5, p.219.

Shi, P., 1978, Interactive polynomial regression (POLYRG): Lehigh University Computer Center Software Library.

Smith, R.S. and Lawrence, M., 1975, Preliminary results of sediment transport studies on the inner continental shelf: Eos, v.56, p.60.

Stahl, L. and Koczan, J., 1974, Anatomy of a shoreface-connected sand ridge on the New Jersey shelf: Implications for the genesis of the shelf surficial sand sheet: Geol, V.2, p. 117-120.

Stanley, D.J., 1969, Atlantic continental shelf and slope of the United States - Color of marine sediments: U.S.G.S. Prof. Pap. 529-D.

Stetson, H.C., 1938, The sediments of the continental shelf off the eastern coast of the United States: Papers in Physical Oceanography and Meteorology, V.5.

_____, 1939, Summary of sedimentary conditions on the continental shelf off the east coast of the United States, in Trask, P.D. (ed), Recent Marine Sediments: A.A.P.G., Dover Publications, N.Y., p.230-244.

_____, 1949, The sediments and stratigraphy of the east coast continental margin, Georges Bank to Norfolk Canyon: Papers in Physical Oceanography and Meteorology, V.11, p.1-60.

Stubblefield, W.L., Lanelle, J.W., and Swift, D.J.P., 1975, Sediment response to the present hydraulic regime on the central New Jersey shelf: Jour. Sed. Pet., V.45, p.337-358.

Stubblefield, W.L. and Swift, D.J.P., 1976, Ridge development as revealed by sub-bottom profiles on the central New Jersey shelf: Marine Geol. 20, p.315-334.

Swift, D.J.P., 1970, Quaternary shelves and the return to grade: Marine Geol. 8, p.5-30.

_____, 1975, Barrier island genesis; evidence from the central-Atlantic shelf, eastern U.S.A.: Sediment. Geol., V.14, p.1-43.

Swift, D.J.P., et al, 1972, Holocene evolution of the shelf surface, central and southern Atlantic shelf of North America in Swift, D.J.P. (ed), Shelf Sediment Transport: Process and Pattern: Dowden, Hutchinson, and Ross, Stroudsburg, PA, p.499-574.

Swift, D.J.P., Moir, R., and Freeland, G.L., 1980, Quaternary rivers on the New Jersey shelf: Relation of seafloor to burried valleys: Geol., V.8, p.276-280.

Twitchell, D.C., et al, 1977, Delaware River: Evidence for its former extension to Wilmington submarine canyon: Science 195, p.483-484.

Uchupi, E., 1963, Sediments on the continental margin off eastern United States: U.S.G.S. Prof. Pap. 475-C, Article 94, p. C132-C137,

_____, 1968, Atlantic continental shelf and slope of the United States - Physiography: U.S.G.S. Prof. Pap. 529-C.

Veatch, A.C. and Smith, P.A., 1939, Atlantic submarine valleys of the United States and the Congo submarine valley: Geol. Soc. Am. Spec. Pap. 7.

Wolfe, P.E., 1977, The Geology and Landscapes of New Jersey: Crane, Russak, and Company, New York, 351p.

APPENDIX I. Beach, Shelf, and River Sample Locations and Descriptions.

BEACH SAMPLES

No.	Collection Date/Time	Lat./ Long.	Distance from North (km)	Observations
B1	8/25/79 1030	40°28.3' 74°00.0'	2	Sandy Hook (North Beach). Wide beach with no sand build-up at groins.
B2	8/25/79 1115	40°24.5' 73°58.7'	10	Sandy Hook. Narrow beach due to beach wall. Large sand build-up south of groins.
B3	8/25/79 1145	40°20.4' 73°58.4'	18	Galilee. Narrow beach due to beach wall. Some sand build-up south of groins.
B4	8/25/79 1215	40°15.9' 73°59.1'	26	Elberon. Very narrow, discontinuous beach due to beach wall. Large sand build-up south of groins.
B5	8/25/79 1430	40°11.7' 74° 0.5'	35	North of Shark River. Wide beach. Some sand build-up south of groins.
B6	8/25/79 1500	40° 8.2' 74° 1.6'	43	Sea Girt. Wide beach. Some sand build-up south of groins.
B7	8/25/79 1600	40° 3.5' 74° 2.7'	51	Bay Head. Wide beach. Some sand build-up south of groins.
B8	8/25/79 1630	39°58.2' 74° 4.1'	59	Lavallete. Wide beach. Some sand build-up south of groins.
B9	8/25/79 1815	39°54.2' 74° 4.8'	68	Island Beach State Park. Wide beach. No groins.
B10	8/25/79 1745	39°49.5' 74° 5.5'	76	Island Beach State Park. Wide beach. No groins.
B11	8/27/79 1645	39°45.2' 74° 6.2'	84	Barnegat Light. Wide beach. No groins. Some sand build-up south of jetty.

APPENDIX I. (Continued)

BEACH SAMPLES

No.	Collection Date/Time	Lat./ Long.	Distance from North (km)	Observations
B12	8/27/79 1730	39°41.6' 74° 8.3'	92	Harvey Cedars. Wide beach. Little sand build-up south of groins.
B13	8/27/79 1800	39°38.3' 74°10.9'	101	Ship Bottom. Wide beach. Some sand build-up south of groins.
B14	8/27/79 1815	39°35.0' 74°13.2'	109	Spray Beach. Wide beach. Some sand build-up south of groins.
B15	8/27/79 1600	39°31.4' 74°16.3'	117	South end of Long Beach Island. Wide beach. No groins.
B16	8/27/79 1100	39°28.6' 74°18.6'	122	Pullen Island. Wide beach. No groins.
B17	8/26/79 1815	39°22.9' 74°23.4'	134	Brigantine. Wide Beach. No sand build-up at groins.
B18	8/26/79 1730	39°20.8' 74°27.1'	142	Atlantic City. Very wide beach. No sand build-up at infrequent groins.
B19	8/26/79 1700	39°18.2' 74°32.1'	150	Longport. Wide beach. No sand build-up at infrequent groins.
B20	8/26/79 1615	39°14.5' 74°37.2'	158	Peck Beach. Wide beach. No groins.
B21	8/26/79 1530	39°11.6' 74°39.6'	167	Strathmere. Narrow beach with beach wall. No sand build-up on only groin.
B22	8/26/79 1445	39° 7.5' 74°42.6'	175	Sea Isle City. Very wide beach. No groins.

APPENDIX I. (Continued)

BEACH SAMPLES

No.	Collection Date/Time	Lat./ Long.	Distance from North (km)	Observations
B23	8/26/79 1415	39° 3.7' 74°44.9'	183	Stone Harbor. Wide beach. No groins.
B24	8/26/79 1330	38°59.7' 74°47.3'	191	North Wildwood. Extremely wide beach. No groins.
B25	8/26/79 1200	38°57.7' 74°50.5'	200	Wildwood Crest. Very wide beach. No groins.
B26	8/26/79 1100	38°55.7' 74°55.8'	208	Cape May. Wide beach. No sand build-up at groins.
B27	8/26/79 1030	38°59.3' 74°57.6'	216	Town Bank. Narrow beach. No sand build-up at groins. Land-fill adjacent to beach.
B28	8/26/79 1000	39° 3.8' 74°52.4'	224	Norburys Landing. Narrow beach. No sand build-up at groins.

SHELF SAMPLES

No.	Date	Time	Lat./Long.	Depth (m)	Color Code	Color Description
S6	5/23/80	1505	38°53.0'/74°37.1'	20	5Y4/4	Moderate Olive Brown
S7	6/5/80	1515	38°59.5'/74°31.2'	19	5Y5/4	Moderate Olive Brown
S8	6/5/80	1500	39° 0.4'/74°30.7'	13	10YR6/4	Moderate Yellow-ish Brown
S9	6/5/80	1400	39° 9.0'/74°25.4'	20	5Y4/2	Olive Gray
S10	6/5/80	1300	39°11.7'/74°21.0'	18	5Y5/1	Olive Gray

APPENDIX I. (Continued)

SHELF SAMPLES

No.	Date	Time	Lat./Long.	Depth (m)	Color Code	Color Description
S11	6/5/80	1250	39°12.0'/74°20.1'	19	5Y4/1	Olive Gray
S12	6/5/80	1220	39°15.2'/74°18.9'	20	5Y4/1	Olive Gray
S13	6/5/80	1030	39°19.5'/74°13.7'	20	10YR5/2	Dark Yellowish Brown
S14	6/5/80	0945	39°24.0'/74° 9.4'	17	10YR6/4	Moderate Yellowish Brown
S15	6/11/80	1530	39°28.2'/74° 7.4'	19	10YR4/2	Dark Yellowish Brown
S16	6/11/80	1500	39°32.6'/74° 4.1'	18	10YR4/3	Dark Yellowish Brown
S17	6/11/80	1425	39°35.8'/74° 4.9'	18	10YR4/2	Dark Yellowish Brown
S18	6/11/80	1355	39°37.8'/74° 1.5'	20	10YR4/3	Dark Yellowish Brown
S19	6/11/80	1330	39°43.0'/73°59.9'	20	10YR4/3	Dark Yellowish Brown
S20	6/11/80	1300	39°47.6'/73°58.4'	18	10YR4/3	Dark Yellowish Brown
S21	6/5/80	0630	39°52.4'/73°57.5'	20	10YR5/4	Moderate Yellowish Brown
S22	6/5/80	0545	39°57.9'/73°57.8'	21	10YR6/4	Moderate Yellowish Brown
S23	6/5/80	0500	40° 2.7'/73°57.2'	23	10YR4/2	Dark Yellowish Brown
S25	6/5/80	0000	40°10.0'/73°53.9'	17	5Y6/2	Light Olive Gray

APPENDIX I. (Continued)

SHELF SAMPLES

No.	Date	Time	Lat./Long.	Depth (m)	Color Code	Color Description
S26	6/4/80	2305	40°16.2'/73°53.5'	21	5YR2/1	Brownish Black
S32	6/4/80	2015	40°18.8'/73°57.6'	12	5Y4/1	Olive Gray
S33	6/4/80	1930	40°14.2'/73°58.9'	13	5Y4/1	Olive Gray
S34	6/4/80	1810	40° 8.5'/74° 0.6'	14	5Y5/1	Olive Gray
S36	6/4/80	1620	39°56.5'/74° 2.8'	15	10YR4/2	Dark Yellowish Brown
S37	6/4/80	1525	39°51.4'/74° 4.4'	11	10YR6/2	Pale Brown
S38	6/4/80	1430	39°44.8'/74° 4.8'	11	10YR6/2	Pale Brown
S39	6/4/80	1340	39°39.5'/74° 8.4'	11	5Y4/1	Olive Gray
S40	6/4/80	1245	39°35.2'/74°12.0'	10	5Y5/2	Light Olive Gray
S41	6/4/80	1155	39°29.1'/74°15.1'	9	5Y4/2	Olive Gray
S42	6/4/80	1115	39°25.3'/74°17.2'	9	5Y4/2	Olive Gray
S43	6/4/80	1035	39°21.2'/74°22.2'	7	5Y4/2	Olive Gray
S44	6/4/80	0950	39°19.2'/74°28.0'	5	5Y3/2	Olive Gray
S45	6/4/80	0930	39°16.4'/74°29.4'	10	5Y3/2	Olive Gray
S46	6/4/80	0800	39° 6.6'/74°40.9'	9	5Y3/2	Olive Gray
S47	6/4/80	0700	39° 1.0'/74°44.6'	11	5Y4/2	Olive Gray
S48	6/4/80	0640	39° 0.2'/74°46.0'	10	5Y3/2	Olive Gray

APPENDIX I. (Continued)

SHELF SAMPLES

No.	Date	Time	Lat./Long.	Depth (m)	Color Code	Color Description
S49	6/4/80	0605	38°57.5'/74°47.9'	10	5Y3/2	Olive Gray

RIVER SAMPLES

No.	Date	Lat./ Long.	Location	Color Code	Color Description
R2	6/10/80	39°27.1' 74°43.3'	Great Egg Harbor River; Route 50; Mays Landing, NJ	10YR2/2	Dusky Yellowish Brown
R3	6/10/80	39°36.7' 74°35.5'	Mullica River; Route 563; Green Bank, NJ	10YR2/4 10YR2/4	Dusky Yellowish Brown
R4	6/10/80	39°37.0' 73°29.6'	Wading River; Route 542; Wading River, NJ	5YR3/1	Brownish Black

APPENDIX II. Heavy Mineral Data of McMaster (1954). Values are number percentages except for magnetite, which is weight percent. x denotes trace (0.5% or less) amount.

1.75 - 2.25 PHI FRACTION

Minerals	Sample Location (km from north) 0	6	15	23	31	35	36	39	48	56
Andalusite	0.1	1.2	2.9	3.9	0.9	1.9	1.2	3.7	0.6	2.6
Chlorite	0.0	0.0	x	1.3	0.0	0.0	0.0	x	0.0	0.6
Diopside	0.6	0.6	0.9	0.0	0.6	2.5	1.8	2.6	2.5	4.5
Epidote	0.0	0.9	2.1	1.9	0.0	x	x	0.0	x	0.0
Garnet	0.9	16.3	2.7	3.9	3.1	2.5	3.3	2.3	2.2	2.2
Glauconite	85.3	10.8	37.9	46.0	47.1	43.8	46.6	39.7	25.0	22.4
Hornblende	0.6	4.0	6.2	1.9	5.2	3.3	2.4	6.0	6.5	6.7
Hypersthene	0.0	1.2	0.0	x	x	0.5	x	1.4	0.6	0.6
Kyanite	1.2	2.2	0.9	1.9	2.1	2.5	1.8	0.9	1.9	1.0
Muscovite	0.0	0.0	0.0	0.0	0.0	x	x	0.0	0.0	0.0
Sillimanite	0.6	x	0.6	0.0	1.6	0.8	2.4	2.6	1.9	1.0
Staurolite	3.2	29.5	12.8	17.2	10.7	5.5	5.6	7.5	9.0	7.4
Tourmaline	2.1	2.5	8.3	5.2	4.7	6.1	5.9	3.4	5.9	3.5
Tremolite	0.0	0.0	0.0	0.0	0.0	0.0	0.0	0.0	0.0	0.0
Zircon	0.0	x	0.0	x	0.0	0.0	x	0.0	0.9	0.0
Collophane	0.0	0.0	0.9	0.0	x	0.8	x	0.6	x	1.6
Black Opaques	2.1	22.5	11.3	9.7	17.5	15.0	15.7	16.4	25.0	31.7
Leucoxene	1.8	2.5	3.9	3.6	1.8	4.2	4.7	4.6	7.7	7.4

APPENDIX II. (Continued)

1.75 - 2.25 PHI FRACTION

Minerals	Sample Location (km from north) 64	72	81	89	97	106	114	119	129	137
Andalusite	2.2	2.0	1.9	2.8	1.2	1.2	x	x	1.2	2.5
Chlorite	0.0	0.6	x	x	0.0	x	1.2	1.6	0.0	0.0
Diopside	2.2	3.5	3.1	3.7	2.5	2.2	1.4	2.9	2.7	1.9
Epidote	x	x	x	0.6	0.9	x	0.0	0.6	3.4	0.0
Garnet	1.3	6.8	7.1	5.9	3.4	5.7	9.9	6.9	7.7	1.9
Glauconite	14.3	7.0	2.2	1.1	0.9	x	0.0	x	0.0	2.2
Hornblende	6.8	10.3	9.0	6.5	6.2	7.0	3.2	2.7	30.3	15.8
Hypersthene	0.8	0.6	1.2	1.7	0.9	x	0.0	0.9	3.4	1.5
Kyanite	1.6	1.8	2.8	2.3	1.8	2.2	1.4	1.5	x	0.0
Muscovite	0.0	0.0	0.0	0.0	0.6	0.0	0.0	0.0	3.1	8.1
Sillimanite	2.4	2.7	1.2	1.7	2.7	1.9	1.7	3.4	2.2	4.0
Staurolite	5.9	8.5	12.4	7.7	10.8	7.0	12.8	17.3	3.4	x
Tourmaline	5.7	7.6	5.3	11.0	9.9	5.7	2.6	6.6	4.6	3.4
Tremolite	0.0	0.0	0.0	0.0	0.0	0.0	0.0	0.0	0.6	0.6
Zircon	1.8	x	1.2	1.4	0.0	0.0	2.6	0.9	0.6	0.0
Collophane	0.0	0.0	0.0	0.0	0.0	0.0	0.0	0.0	0.0	0.0
Black Opaques	37.9	37.7	44.2	40.8	43.2	52.4	56.9	49.3	24.4	7.4
Leucoxene	8.7	4.1	3.4	5.1	8.3	6.4	3.5	0.9	2.2	5.0

APPENDIX II. (Continued)

1.75 - 2.25 PHI FRACTION

Minerals	Sample Location (km from north) 160	193	201	206	209	218	226
Andalusite	1.2	0.9	0.0	1.0	1.3	1.8	0.8
Chlorite	1.6	7.5	46.5	1.5	0.0	0.8	x
Diopside	6.9	5.3	1.3	x	0.8	0.8	x
Epidote	1.9	2.8	0.0	1.3	0.8	0.5	0.0
Garnet	2.2	10.0	0.7	4.0	5.9	3.9	2.5
Glauconite	2.2	x	0.0	0.0	0.0	0.0	0.0
Hornblende	36.3	31.2	2.9	12.8	5.2	3.1	x
Hypersthene	1.6	5.9	1.4	1.0	1.1	1.8	x
Kyanite	0.0	0.9	0.0	0.7	3.9	2.1	1.5
Muscovite	0.5	6.9	27.4	0.5	0.0	0.0	0.0
Sillimanite	4.4	2.8	0.0	4.5	2.6	1.3	2.8
Staurolite	0.9	0.6	0.0	9.8	16.3	10.4	9.3
Tourmaline	5.3	1.2	x	10.5	4.9	3.4	4.8
Tremolite	x	0.6	0.0	x	0.0	0.0	x
Zircon	0.0	1.9	0.7	0.7	1.8	1.8	6.6
Collophane	0.0	0.0	0.0	0.0	0.0	0.0	0.0
Black Opaques	7.2	12.7	5.6	32.9	48.3	62.4	63.7
Leucoxene	4.1	4.0	1.0	7.5	2.6	2.9	2.0

APPENDIX II. (Continued)

2.25 - 2.75 PHI FRACTION

Minerals	Sample Location (km from north) 0	6	15	23	31	39	48	56	64	72
Andalusite	x	1.2	x	2.1	1.8	2.1	x	0.5	0.6	x
Apatite	0.0	0.0	0.0	0.0	0.0	x	0.0	0.0	0.0	0.0
Chlorite	0.0	0.0	0.0	x	x	x	0.0	0.0	0.0	0.0
Diopside	x	0.5	x	0.0	1.8	3.6	3.1	3.0	2.0	3.8
Epidote	1.4	0.8	3.9	4.9	2.0	1.2	0.6	1.8	1.1	1.3
Garnet	2.9	7.8	7.0	7.0	6.4	6.3	6.7	11.5	4.8	6.7
Glauconite	56.0	4.8	7.3	18.8	8.7	11.0	7.3	4.4	8.0	4.8
Hornblende	2.9	2.4	2.7	1.2	5.8	11.0	10.0	4.1	6.6	10.5
Hypersthene	1.4	0.5	0.0	0.0	0.6	1.2	1.2	2.2	2.3	1.3
Kyanite	2.3	1.6	1.2	3.9	2.6	1.5	1.8	1.4	2.0	1.6
Muscovite	0.0	0.0	0.0	0.0	x	0.0	x	0.0	0.0	0.0
Rutile	0.6	1.3	1.2	0.9	1.4	0.0	0.6	1.4	0.6	x
Sillimanite	0.6	x	x	0.9	1.2	3.3	3.7	1.4	1.1	1.6
Staurolite	10.9	11.8	17.0	17.6	13.8	6.0	8.2	10.1	6.9	5.7
Titanite	0.0	0.5	0.0	0.0	0.0	0.0	x	x	x	x
Tourmaline	2.3	1.3	2.7	3.9	x	1.2	2.1	3.0	1.4	3.8
Tremolite	0.0	0.0	0.0	0.0	0.0	0.0	0.6	0.0	0.0	0.0
Zircon	x	6.5	3.9	1.5	1.2	1.5	0.6	1.9	1.1	2.4
Chloritoid	1.1	x	0.6	2.1	0.0	0.0	0.0	x	1.4	x
Black Opaques	12.9	54.8	45.7	28.6	46.6	42.4	41.2	47.6	50.4	49.3
Leucoxene	1.7	1.6	2.2	4.2	2.6	3.0	5.2	2.2	6.3	2.9

APPENDIX II. (Continued)

2.25 - 2.75 PHI FRACTION

Minerals	Sample Location (km from north) 81	89	97	106	114	119	122	129	137	145
Andalusite	2.1	1.0	0.6	1.2	0.0	x	x	0.5	1.1	0.8
Apatite	0.0	0.0	0.0	x	0.0	0.0	0.0	x	x	x
Chlorite	0.0	0.0	0.6	x	0.0	0.0	x	1.9	3.5	2.0
Diopside	0.9	2.3	1.8	2.1	x	1.1	3.8	3.0	2.9	5.9
Epidote	0.0	x	2.3	0.6	x	0.5	3.5	2.7	3.3	2.4
Garnet	7.5	9.3	6.2	5.0	8.3	6.2	2.9	3.5	2.7	2.2
Glauconite	1.5	0.0	0.6	0.6	0.0	0.0	0.0	x	0.5	0.0
Hornblende	6.9	9.9	11.1	10.4	2.1	12.4	46.8	36.3	36.1	49.2
Hypersthene	2.7	1.0	1.2	1.5	0.9	1.1	2.3	2.7	4.6	4.4
Kyanite	1.2	1.0	2.1	3.0	0.6	0.8	0.6	0.0	0.0	0.6
Muscovite	0.0	0.0	0.0	0.0	0.0	0.0	0.0	3.5	0.8	x
Rutile	x	0.0	0.0	0.0	x	0.5	x	0.0	0.0	x
Sillimanite	x	1.8	2.9	4.2	0.6	1.9	2.9	1.9	1.6	4.4
Staurolite	8.7	7.4	5.3	4.7	3.6	6.2	3.2	1.4	0.5	x
Titanite	0.0	0.8	0.6	x	x	x	0.0	0.0	0.8	x
Tourmaline	2.1	1.3	2.9	3.0	0.6	3.2	3.5	1.4	3.5	0.8
Tremolite	0.0	0.0	0.0	0.0	0.0	0.0	1.5	1.4	2.3	2.5
Zircon	0.6	1.0	0.9	x	5.7	1.6	x	0.8	0.0	0.0
Chloritoid	x	x	0.6	x	x	0.0	0.6	x	0.5	x
Black Opaques	62.2	56.4	55.5	55.3	73.5	58.8	16.9	17.5	3.3	1.7
Leucoxene	0.9	2.3	3.5	3.3	2.4	2.4	2.6	2.5	4.9	2.0

APPENDIX II. (Continued)

2.25 - 2.75 PHI FRACTION

Minerals	Sample Location (km from north) 152	160	168	176	185	193	201	206	209	218
Andalusite	0.0	0.5	0.5	0.5	0.0	0.5	x	0.5	0.0	0.9
Apatite	0.0	0.7	0.5	1.0	x	0.0	0.8	x	x	0.0
Chlorite	10.9	1.2	1.0	1.3	11.3	5.1	21.6	0.5	0.0	0.6
Diopside	3.3	6.8	6.4	5.8	2.2	4.4	1.4	3.1	2.2	1.7
Epidote	0.9	1.7	2.4	3.4	1.6	2.6	x	4.1	1.7	1.1
Garnet	4.7	1.5	6.7	3.5	1.6	3.5	1.4	7.5	7.8	5.7
Glauconite	0.9	x	0.0	x	1.3	1.0	0.8	x	0.0	0.0
Hornblende	23.7	54.3	43.6	49.4	24.7	38.0	20.2	36.2	12.4	8.9
Hypersthene	2.7	4.1	2.9	2.5	1.3	3.0	2.6	3.9	2.9	1.1
Kyanite	0.0	0.0	0.7	x	0.0	0.0	0.0	x	0.7	1.4
Muscovite	2.7	0.5	x	x	10.5	5.9	19.5	0.0	0.0	x
Rutile	0.0	0.0	0.0	0.0	0.0	0.0	0.0	0.0	x	x
Sillimanite	4.4	3.1	3.0	3.4	1.6	1.8	1.8	4.6	2.4	0.9
Staurolite	0.6	0.5	2.0	x	0.6	0.5	0.0	2.1	7.8	4.3
Titanite	0.0	x	0.5	x	0.0	0.5	x	x	0.0	0.0
Tourmaline	1.5	1.7	0.5	1.5	1.6	0.5	1.3	2.8	1.2	1.4
Tremolite	1.2	1.7	1.7	1.5	0.0	1.5	0.8	2.3	0.0	0.0
Zircon	0.0	x	0.0	0.0	0.0	0.0	x	1.8	3.9	6.6
Chloritoid	x	0.0	0.5	x	0.8	0.5	x	x	1.0	0.0
Black Opaques	6.8	5.1	12.0	2.3	1.3	7.2	3.9	15.9	49.5	58.3
Leucoxene	3.0	0.7	2.6	2.3	2.4	2.0	2.3	4.6	3.4	2.9

APPENDIX II. (Continued)

2.25 - 2.75 PHI FRACTION

Minerals	Sample Location (km from north) 226
Andalusite	x
Apatite	0.0
Chlorite	x
Diopside	0.0
Epidote	x
Garnet	x
Glauconite	0.0
Hornblende	1.6
Hypersthene	x
Kyanite	1.9
Muscovite	0.0
Rutile	1.3
Sillimanite	1.6
Staurolite	6.8
Titanite	0.0
Tourmaline	0.8
Tremolite	0.0
Zircon	5.4
Chloritoid	0.0
Black Opaques	75.4
Leucoxene	2.4

APPENDIX II. (Continued)

2.75 - 3.25 PHI FRACTION

Minerals	Sample Location (km from north) 6	15	23	31	39	64	81	89	97	106
Magnetite	1.9	x	x	6.7	0.4	2.5	x	x	x	0.0
Andalusite	0.8	1.1	0.8	1.2	0.8	x	x	x	0.0	0.0
Apatite	0.0	0.0	0.0	0.0	0.8	0.0	0.0	0.0	0.0	x
Chlorite	0.0	0.0	0.0	0.0	x	0.0	x	x	0.0	x
Diopside	1.0	0.0	x	1.2	1.5	1.2	x	0.0	0.7	0.8
Epidote	1.6	x	1.4	1.8	1.8	0.9	x	1.2	1.4	2.2
Garnet	5.6	3.1	4.2	6.2	5.7	10.7	5.4	10.4	7.2	5.3
Glauconite	1.6	3.6	1.4	2.1	2.1	1.5	x	0.0	x	x
Hornblende	2.4	x	2.5	5.9	9.8	2.4	1.2	8.4	5.7	15.6
Hypersthene	1.3	0.6	1.6	1.2	3.6	0.6	1.4	1.4	x	2.2
Kyanite	1.0	0.6	2.5	1.5	0.8	0.9	1.2	x	x	x
Muscovite	0.0	0.0	0.0	0.0	0.0	0.0	x	0.0	0.0	0.0
Rutile	1.6	1.1	1.7	1.5	0.5	0.9	1.0	0.9	1.0	1.4
Sillimanite	x	0.6	0.6	0.0	0.8	0.6	x	0.9	x	1.4
Staurolite	4.0	2.5	5.9	3.3	2.6	2.4	2.4	1.7	1.4	3.4
Titanite	1.0	0.0	0.6	1.2	x	x	0.7	x	0.0	0.0
Tourmaline	0.8	1.1	0.6	1.8	1.0	0.0	x	0.6	x	x
Tremolite	0.0	0.0	0.0	0.0	0.0	0.0	0.0	0.0	0.0	0.0
Zircon	7.2	6.4	4.0	7.7	1.8	9.4	12.9	9.6	9.9	2.2
Chloritoid	0.5	0.0	x	0.0	0.5	x	0.0	0.0	x	x
Black Opaques	65.6	74.8	65.6	57.0	57.3	65.5	71.4	62.4	65.8	59.5
Leucoxene	1.9	1.1	2.3	1.8	2.3	1.8	1.2	x	2.5	2.2

APPENDIX II. (Continued)

2.75 - 3.25 PHI FRACTION

Minerals	Sample Location (km from north) 114	119	122	129	137	145	152	160	168	176
Magnetite	x	x	x	x	0.0	x	0.0	0.0	x	x
Andalusite	0.0	x	0.6	x	0.0	0.0	0.0	x	0.0	0.0
Apatite	0.0	x	2.7	0.5	1.6	2.1	1.2	2.7	1.7	0.5
Chlorite	0.0	0.0	0.0	x	x	x	x	0.0	0.6	x
Diopside	0.5	x	2.8	4.0	3.8	3.9	3.4	4.0	3.8	3.6
Epidote	x	1.9	7.1	5.0	8.1	5.5	5.6	6.4	5.8	5.5
Garnet	6.0	10.0	6.5	9.2	2.7	2.8	2.2	5.1	11.0	3.9
Glauconite	0.0	0.0	x	0.0	0.0	0.0	x	0.0	0.6	0.0
Hornblende	3.7	14.7	48.2	52.6	56.7	60.4	57.9	55.4	39.1	60.0
Hypersthene	1.3	1.9	4.7	5.4	4.9	4.1	3.2	5.6	5.2	5.2
Kyanite	0.5	x	0.6	x	x	0.5	0.7	0.0	x	0.5
Muscovite	0.0	0.0	0.0	x	0.5	0.0	0.7	0.0	0.0	0.0
Rutile	1.6	0.0	0.0	0.0	x	0.0	0.0	x	0.0	x
Sillimanite	0.0	1.2	2.7	2.4	1.9	2.1	2.7	2.4	2.6	1.9
Staurolite	1.0	1.2	1.2	0.5	x	0.5	x	x	0.9	0.5
Titanite	1.3	x	0.6	1.0	1.1	0.5	x	1.9	0.9	0.8
Tourmaline	x	0.0	0.9	0.7	1.1	x	0.5	0.5	0.0	0.8
Tremolite	0.0	0.0	0.6	1.4	1.4	1.7	1.9	0.5	1.7	1.4
Zircon	17.7	8.4	x	1.2	0.8	x	0.5	x	1.4	0.0
Chloritoid	0.0	x	x	0.5	0.5	1.1	x	0.0	0.9	x
Black Opaques	64.1	56.4	12.4	7.1	4.9	2.1	3.7	6.1	10.4	2.5
Leucoxene	1.3	1.2	1.2	1.7	1.6	1.7	1.0	1.1	1.2	1.4

APPENDIX II. (Continued)

2.75 - 3.25 PHI FRACTION

Minerals	Sample Location (km from north) 185	193	201	206	209	218	226
Magnetite	0.0	x	0.0	x	0.1	0.0	0.0
Andalusite	x	0.0	0.0	x	0.0	1.2	0.0
Apatite	2.9	1.4	2.0	1.5	0.0	x	0.0
Chlorite	x	1.0	2.0	0.0	x	x	x
Diopside	2.6	3.6	3.3	3.7	1.8	1.8	0.0
Epidote	6.0	6.1	4.3	6.7	3.4	9.2	0.8
Garnet	3.1	5.6	3.3	10.6	20.4	9.5	1.0
Glauconite	0.0	0.5	0.0	0.0	0.0	0.0	0.0
Hornblende	56.4	57.2	57.8	46.0	12.4	24.2	1.0
Hypersthene	4.3	4.4	4.3	3.7	0.8	3.7	x
Kyanite	0.0	0.0	0.5	0.0	0.0	0.6	0.8
Muscovite	0.5	x	1.2	0.0	0.0	0.0	0.0
Rutile	0.0	0.0	0.0	0.0	0.5	x	1.3
Sillimanite	0.7	0.8	2.0	2.0	1.6	1.2	0.5
Staurolite	x	0.8	x	x	0.8	2.4	1.9
Titanite	1.4	0.5	0.5	0.6	0.5	1.5	x
Tourmaline	0.7	x	0.5	1.3	x	1.8	0.8
Tremolite	1.7	1.7	0.8	0.6	0.0	0.0	0.0
Zircon	0.0	0.5	x	1.1	x	0.6	x
Chloritoid	0.2	x	0.0	1.1	x	0.6	x
Black Opaques	1.4	5.0	1.2	16.4	48.4	29.4	69.1
Leucoxene	1.7	1.0	1.2	1.2	1.1	2.4	1.6

APPENDIX III. Methods

Preparation of Beach Samples for Size Analysis

Each of the 28 beach sand samples was slaked (to remove salt), dispersed with sodium hetametaphosphate (to disperse clays), and then wet sieved through a .062 mm sieve (to separate out all sediment finer than 4Ø). Sample B28 contained some plant debris, which was removed manually. The coarse fractions (greater than .062 mm) were dried and sieved from 2.0 mm (-1Ø) to .062 mm (4Ø) at one-half phi intervals. The size fractions were then weighed and saved.

Almost all liquid was removed from the fine (less than 0.62 mm) fractions with candle filters. After rinsing the fine sediment into a beaker, organic material was removed by adding 100 ml of sodium hypochlorite (5-6 percent solution buffered to a pH of 9.5 with hydrochloric acid). The mixtures were heated in a hot water bath at 80°C for 45 minutes. After cooling and candle filtering, the sediment samples were washed into centrifuge tubes and centrifuged at 5000 RPM for 15 minutes. The supernatant liquid was poured off and the fine (less than .062 mm) sediments were rinsed into preweighed beakers, dried, and weighed.

Preparation of Beach Samples for Mineralogical Analysis

Beach samples were selected for mineralogical analysis partially on the basis of the Q-mode factor analysis results (Appendix VII). Samples B1, B14, B18, and B28 (figure 2) were all taken in close proximity to the end member samples defined by analysis of McMaster's (1954) data. To get a more complete coverage of the coast, samples B3, B6, B8, B10, B12, B16, B21, B23, B25, and B27 (figure 2) were also analyzed.

Prepared sand samples (unsieved) were sieved to remove all sediment coarser than .297 mm (1.75Ø) and finer than .105 mm (3.25Ø). The remaining sand ranged in size from .297 - .105 mm and included the 1.75 - 2.25Ø, 2.25 - 2.75Ø, and 2.75 - 3.25Ø fractions.

Heavy mineral separations were done using a mixture of tetrabromoethane (s.g. = 2.96 Mg/m^3) and dimethyl formide (s.g. = 0.95 Mg/m^3) with a specific gravity of 2.78 Mg/m^3. This mixture had a sufficiently low specific gravity for separating the hornblende (s.g. = 3.2 Mg/m^3), black opaques (s.g. greater than 4.1 Mg/m^3), tourmaline (s.g. = 3.0 - 3.25 Mg/m^3), and a large percentage of the glauconite (s.g. greater than 2.3 Mg/m^3) (Hurlbut, 1971). McMaster (1954) used bromoform (s.g. = 2.85 Mg/m^3) as a separating

liquid, and his percentages of glauconite should therefore be lower than those resulting from this study.

After settling for 24 hours under normal gravity, the heavy fractions were washed with acetone, and then sieved into 1.75-2.25Ø, 2.25-2.75Ø, and 2.75-3.25Ø fractions. These fractions were then mounted on glass slides under cover slips with Lakeside 70 (index of refraction = 1.540).

Only the hornblende, glauconite, tourmaline, and black opaque grains were included in the point count. Three hundred grains were counted on each slide. This number was arrived at by calculating the confidence intervals on estimated mineral percentages, and then deciding if those intervals were small enough to distinquish between various mineral zones.

X-ray Diffraction Methods

A bulk heavy mineral fraction (s.g. greater than 2.78 Mg/m^3) was separated from sample B11, and a trace amount of magnetite was removed using a hand magnet. With the aid of a binocular microscope and a suction apperatus, black opaque grains were picked out mechanically. When about two hundred were collected, they were

ground with a diamonite mortar and pestle, and then the powder was suspended in a distilled water slurry and pipetted to a glass slide. After air drying overnight, the slide was x-rayed on a Norelco X-ray Diffractometer using $Cu_{k-alpha}$ radiation. The slide was scanned from zero to 70 degrees two-theta.

A bulk heavy mineral fraction (s.g. greater than 2.78 Mg/m^3) was separated from sample B23, and magnetic separations were done to increase the percentage of hornblende in the subsample. The resulting sediment was then ground with a diamonite mortar and pestle, pipetted onto a glass slide, air dried, and x-rayed.

Preparation of Source Samples for Mineralogical Analysis

Source samples were prepared for microscopic examination using the same methods as those used for the beach samples, with one exception. The river samples were heavily iron stained, as noted by a color change of the heavy liquid from yellow to red following the heavy mineral separations. Therefore the heavy mineral fractions for the three river samples were boiled in a 20% nitric acid solution prior to mounting on glass slides, to remove the iron stains.

APPENDIX IV. Preliminary Varimax Rotated Factor Measures Resulting from R-mode Factor Analysis of Data Obtained by Master (1954).

1.75 - 2.25 PHI FRACTION

Sample	Factor 1	Factor 2	Factor 3	Factor 4	Factor 5
0	.01111	0.00000	1.00000	1.00000	0.00000
6	.06860	.78468	.27941	.85747	.75519
15	.15132	.45061	.74716	.74977	.43208
23	.03679	.37281	.72040	.88471	.38998
31	.07896	.40898	.69220	.74035	.36573
35	.13125	.39894	.75943	.66306	.40883
36	.11199	.39431	.75582	.65563	.37192
39	.19800	.44440	.73936	.64956	.44929
48	.18269	.61885	.60536	.45477	.58844
56	.19920	.64676	.58657	.40753	.67583
64	.19319	.76023	.50357	.23818	.72272
72	.25350	.85276	.42187	.32996	.77720
81	.18647	.92148	.29274	.32245	.85886
89	.21632	.91271	.39091	.23204	.84885
97	.18569	.91123	.38514	.17617	.85684
106	.17366	.94643	.28080	.12999	.90058
114	.06088	.99570	.11705	.21794	.92013
119	.07775	.96764	.19099	.28656	.87143
129	.76695	.82107	.44950	.44390	.75967
137	.76726	.50740	.49457	.31644	.73923
160	.90788	.72658	.71898	.45791	.63662
193	.96645	.71809	.45947	.49707	.77769
201	1.00000	.08318	0.00000	.12480	1.00000
206	.33855	.87807	.44405	.24402	.78039
209	.08401	.95965	.20234	.29285	.87391
218	.05774	.99012	.14149	.11161	.93458
226	0.00000	1.00000	.09487	0.00000	.90150

APPENDIX IV. (Continued)

2.25 - 2.75 PHI FRACTION

Sample	Factor 1	Factor 2	Factor 3
0	.22089	1.00000	1.00000
6	.04703	.24115	.19403
15	.08078	.44993	.32878
23	.13007	.79179	.58291
31	.13836	.44653	.31305
39	.28384	.49517	.30993
48	.28075	.50681	.29730
56	.15779	.41577	.21503
64	.19001	.43069	.28250
72	.24446	.40210	.21439
81	.11472	.23473	.12182
89	.18848	.28043	.11070
97	.22848	.36009	.15886
106	.23682	.34615	.15477
114	.01726	.00934	0.00000
119	.20156	.26902	.12039
122	.80097	.83089	.36818
129	.74375	.62258	.41806
137	.85266	.82922	.51875
145	.98845	.87719	.44898
152	.76329	.51992	.57266
160	1.00000	.84910	.42177
168	.83126	.80365	.36046
176	.96268	.88503	.44577
185	.80601	.42013	.74870
193	.85909	.63500	.54127
201	.84294	.08383	.90866
206	.73678	.80710	.33954
209	.25781	.36284	.16277
218	.17247	.18720	.11179
226	0.00000	0.00000	.05893

APPENDIX IV. (Continued)

2.75 - 3.25 PHI FRACTION

Sample	Factor 1	Factor 2	Factor 3
6	.07538	.34055	.40937
15	0.00000	.23676	.48020
23	.07745	.40205	.49003
31	.13602	.52645	.46590
39	.23905	.48169	.46385
64	.06946	.15732	.26375
81	.01366	.04714	.40006
89	.14713	.08659	.28279
97	.09914	.10436	.34933
106	.25180	.36485	.48172
114	.05989	0.00000	.38473
119	.24542	.17649	.32326
122	.85560	.89979	.69620
129	.90902	.85876	.64169
137	.97309	1.00000	.86282
145	1.00000	.98421	.90124
152	.96546	.92831	.94790
160	.95885	.94999	.77934
168	.81233	.76632	.52158
176	.98618	.98007	.87218
185	.97725	.98572	.90727
193	.95095	.89991	.83958
201	.98260	.92497	1.00000
206	.80929	.77593	.50965
209	.30325	.16153	0.00000
218	.54508	.71952	.37804
226	.00176	.02282	.51425

APPENDIX V. Varimax Rotated Factor Loading Matrices Resulting from R-mode Factor Analysis of Data Obtained by McMaster (1954).

1.75 - 2.25 PHI FRACTION

Variable	Factor 1	Factor 2	Factor 3
Andalusite	.020	.422	.464
Chlorite	.093	-.879	.097
Diopside	.680	.165	.181
Epidote	.656	.037	-.080
Garnet	.122	.100	-.654
Glauconite	-.445	-.001	.656
Hornblende	.950	-.018	.015
Hypersthene	.793	-.229	-.218
Kyanite	-.555	.443	-.357
Muscovite	.154	-.891	.079
Sillimanite	.599	.297	-.177
Staurolite	-.514	.350	-.438
Tourmaline	.026	.723	.032
Tremolite	.790	-.264	-.081
Zircon	-.076	-.067	-.638
Collophane	-.120	.200	.611
Black Opaques	-.219	.388	-.711
Leucoxene	.183	.555	.321

APPENDIX V. (Continued)

2.25 - 2.75 PHI FRACTION

Variable	Factor 1
Andalusite	-.284
Apatite	.623
Chlorite	.489
Diopside	.787
Epidote	.219
Garnet	-.523
Glauconite	-.385
Hornblende	.926
Hypersthene	.817
Kyanite	-.778
Muscovite	.402
Rutile	-.686
Sillimanite	.627
Staurolite	-.880
Titanite	.160
Tourmaline	-.168
Tremolite	.851
Zircon	-.591
Chloritoid	-.247
Black Opaques	-.804
Leucoxene	-.088

2.75- 3.25 PHI FRACTION

Variable	Factor 1
Magnetite	-.395
Andalusite	-.452
Apatite	.824
Chlorite	.392
Diopside	.931
Epidote	.857
Garnet	-.079
Glauconite	-.537
Hornblende	.972
Hypersthene	.895
Kyanite	-.568
Muscovite	.467
Rutile	-.898
Sillimanite	.825
Staurolite	-.797
Titanite	.328
Tourmaline	-.032
Tremolite	.847
Zircon	-.763
Chloritoid	.402
Black Opaques	-.976
Leucoxene	-.284

APPENDIX VI. Final R-mode Factor Measures Resulting from Factor Analysis on Data Presented by McMaster (1954).

1.75 - 2.25 PHI FRACTION (number of factors set at 3)

Sample	Factor 1	Factor 2	Factor 3
0	0.00000	.69437	1.00000
6	.29815	.88677	.21194
15	.29838	.85693	.62988
23	.16022	.81740	.65659
31	.20377	.81846	.62378
35	.25606	.83102	.66395
36	.23831	.83090	.66422
39	.32545	.83643	.63069
48	.37990	.89953	.46771
56	.40299	.90601	.44344
64	.44247	.94811	.33959
72	.51696	.95847	.24969
81	.47084	.96127	.14612
89	.51761	.99596	.20031
97	.49301	1.00000	.19746
106	.47332	.97665	.12610
114	.37165	.96016	.01495
119	.38965	.97229	.06745
129	.87286	.81569	.29433
137	.69393	.61199	.48977
160	1.00000	.84481	.48348
193	.95502	.69450	.36134
201	.44326	0.00000	.48539
206	.60028	.96558	.24892
209	.39277	.97054	.07764
218	.37365	.96909	.03003
226	.32384	.96808	0.00000

APPENDIX VI. (Continued)

2.25 - 2.75 PHI FRACTION (number of factors set at 1)

Sample	Factor 1
0	.22089
6	.04903
15	.08078
23	.13007
31	.13836
39	.28384
48	.28075
56	.15779
64	.19001
72	.24446
81	.11472
89	.18848
97	.22848
106	.23682
114	.01726
119	.20156
122	.80097
129	.74375
137	.85266
145	.98845
152	.76329
160	1.00000
168	.83126
176	.96268
185	.80601
193	.85909
201	.84294
206	.73678
209	.25781
218	.17247
226	0.00000

APPENDIX VI. (Continued)

2.75 - 3.25 PHI FRACTION (number of factors set at 1)

Sample	Factor 1
6	.07538
15	0.00000
23	.07745
31	.13602
39	.23905
64	.06946
81	.01366
89	.14713
97	.09914
106	.25180
114	.05989
119	.24542
122	.85560
129	.90902
137	.97309
145	1.00000
152	.96546
160	.95885
168	.81233
176	.98618
185	.97725
193	.95095
201	.98260
206	.80929
209	.30325
218	.54508
226	.00176

APPENDIX VII. Oblique Projection Matrices Resulting from Q-mode Factor Analysis on Four Variables Obtained by McMaster (1954) (glauconite, hornblende, tourmaline, and black opaques).

1.75 - 2.25 PHI FRACTION

	End Member Samples		
Sample	226	0	160
0	.000	1.000	.000
6	.848	.417	.159
15	.239	.929	.163
23	.182	.975	.041
31	.308	.926	.102
35	.293	.938	.073
36	.293	.943	.049
39	.757	.557	.169
48	.644	.681	.185
56	.757	.557	.169
64	.880	.338	.169
72	.889	.164	.268
81	.937	.038	.204
89	.942	.028	.171
97	.953	.021	.154
106	.964	-.005	.136
114	.986	-.005	.053
119	.987	.003	.059
129	.470	-.048	.795
137	.242	.073	.913
160	.000	.000	1.000
193	.185	-.060	.945
201	.790	-.035	.464
206	.844	-.009	.374
209	.973	-.005	.110
218	.989	-.004	.047
226	1.000	.000	.000

APPENDIX VII. (Continued)

2.25 - 2.75 PHI FRACTION

	End Member Samples		
Sample	226	145	0
0	.000	.000	1.000
6	.975	.019	.091
15	.948	.032	.165
23	.706	-.005	.566
31	.931	.092	.187
39	.876	.213	.251
48	.912	.206	.176
56	.968	.062	.097
64	.941	.101	.161
72	.944	.185	.101
81	.985	.089	.026
89	.980	.153	.001
97	.972	.177	.014
106	.974	.165	.014
114	1.000	.008	.000
119	.972	.188	.003
122	.308	.935	.004
129	.403	.893	.004
137	.055	.993	.019
145	.000	1.000	.000
152	.235	.955	.040
160	.059	.995	.003
168	.233	.960	-.000
176	.012	1.000	.003
185	.007	.995	.057
193	.147	.979	.027
201	.147	.977	.043
206	.370	.908	.006
209	.963	.223	.001
218	.985	.131	.001
226	1.000	.000	.000

APPENDIX VII. (Continued)

2.75 - 3.25 PHI FRACTION

Sample	End Member Samples 226	201
6	.999	.022
15	1.000	-.013
23	.999	.024
31	.993	.089
39	.983	.155
64	.999	.022
81	1.000	.003
89	.989	.119
97	.995	.072
106	.963	.240
114	.998	.043
119	.963	.239
122	.230	.966
129	.114	.990
137	.066	.996
145	.014	1.000
152	.043	.998
160	.089	.993
168	.238	.963
176	.021	.999
185	.004	1.000
193	.067	.996
201	.000	1.000
206	.317	.938
209	.964	.235
218	.759	.625
226	1.000	.000

APPENDIX VIII. Size Analysis Results. All values have been converted to millimeters.

Sample	Location (km from north)	Median (Ø50)mm	Trask Sorting Ø25/Ø75	Trask Skewness $Ø75Ø25/(Ø50)^2$
B1	0	.460	1.189	1.000
B2	10	.339	1.206	1.028
B3	18	.321	1.164	1.000
B4	26	.423	1.176	1.007
B5	35	.301	1.218	.927
B6	43	.460	1.222	.986
B7	51	.418	1.117	1.000
B8	59	.304	1.091	.993
B9	68	.291	1.106	1.021
B10	76	.306	1.148	1.000
B11	84	.297	1.218	1.021
B12	92	.268	1.144	.966
B13	101	.304	1.168	.993
B14	109	.245	1.152	.966
B15	117	.213	1.202	.993
B16	122	.164	1.164	1.014
B17	134	.150	1.172	1.028
B18	142	.130	1.129	1.021
B19	150	.154	1.202	1.094
B20	158	.163	1.172	1.057
B21	167	.135	1.129	1.007
B22	175	.160	1.176	1.035
B23	183	.152	1.164	1.042
B24	191	.168	1.164	1.042
B25	200	.138	1.106	1.021
B26	208	.156	1.152	1.035
B27	216	.289	1.114	.993
B28	224	.304	1.435	1.338

APPENDIX IX. Point Count Results. Values are number percentages.

Sample	Location (km from north)	Size Fraction	Glauconite	Hornblende	Tourmaline	Black Opaques
B1	2	1.75-2.25Ø	62.0	2.3	4.0	31.7
		2.25-2.75Ø	9.7	3.7	1.7	85.0
B3	18	1.75-2.25Ø	88.3	2.0	3.7	6.0
		2.25-2.75Ø	52.0	3.0	12.7	32.3
		2.75-3.25Ø	3.3	0.7	4.0	92.0
B6	43	1.75-2.25Ø	73.0	2.0	4.7	20.3
		2.25-2.75Ø	42.0	4.5	4.5	48.9
B8	59	1.75-2.25Ø	38.7	10.7	10.3	40.3
		2.25-2.75Ø	17.3	11.0	7.7	64.0
		2.75-3.25Ø	0.3	12.7	5.0	82.0
B10	76	1.75-2.25Ø	54.2	2.5	14.2	29.2
		2.25-2.75Ø	27.3	9.3	11.3	52.0
B12	92	1.75-2.25Ø	0.3	4.0	11.0	28.0
		2.25-2.75Ø	2.0	22.0	11.7	64.3
		2.75-3.25Ø	0.0	35.7	6.0	58.3
B14	109	2.25-2.75Ø	6.7	20.0	25.3	48.0
		2.75-3.25Ø	1.7	25.7	14.0	58.7
B16	122	1.75-2.25Ø	0.3	13.0	15.0	71.7
		2.25-2.75Ø	0.3	22.3	12.7	64.7
		2.75-3.25Ø	0.0	50.3	13.0	36.7
B18	142	2.25-2.75Ø	0.3	65.3	18.7	15.7
		2.75-3.25Ø	1.0	74.7	15.0	9.3
B21	167	2.25-2.75Ø	0.7	42.7	15.0	41.7
		2.75-3.25Ø	0.0	68.3	19.3	15.7
B23	183	2.25-2.75Ø	1.0	60.7	27.7	10.7
		2.75-3.25Ø	0.0	69.3	21.7	9.0
B25	200	2.25-2.75Ø	0.3	59.3	9.0	31.3
		2.75-3.25Ø	0.0	78.0	8.0	14.0

APPENDIX IX. (Continued)

Sample	Location (km from north)	Size Fraction	Glauconite	Hornblende	Tourmaline	Black Opaques
B27	216	1.75-2.25Ø	0.0	1.3	7.3	91.3
		2.25-2.75Ø	0.0	1.7	2.7	95.7
		2.75-3.25Ø	0.0	2.0	1.7	96.3
B28	224	1.75-2.25Ø	0.0	4.2	8.3	87.5
		2.25-2.75Ø	0.0	6.0	5.0	89.0
		2.75-3.25Ø	0.0	3.7	1.3	95.0
S6	193	1.75-2.25Ø	0.0	12.3	6.7	81.0
		2.25-2.75Ø	0.0	13.7	3.7	82.7
		2.75-3.25Ø	0.0	18.3	2.3	79.3
S7	180	1.75-2.25Ø	0.7	21.3	15.3	62.7
		2.25-2.75Ø	0.0	10.3	7.0	82.7
		2.75-3.25Ø	0.0	8.3	2.3	89.3
S8	178	1.75-2.25Ø	0.0	24.0	10.0	66.0
		2.25-2.75Ø	0.0	13.7	4.0	82.3
		2.75-3.25Ø	0.0	5.3	1.3	93.3
S9	157	1.75-2.25Ø	0.3	48.3	7.7	43.7
		2.25-2.75Ø	1.0	30.7	9.0	59.3
		2.75-3.25Ø	0.0	64.0	8.7	27.3
S10	147	1.75-2.25Ø	4.7	15.0	10.3	70.0
		2.25-2.75Ø	0.3	28.0	7.3	64.3
		2.75-3.25Ø	0.0	18.0	3.7	78.3
S11	147	2.25-2.75Ø	0.3	40.7	11.0	48.0
		2.75-3.25Ø	0.0	51.7	15.3	33.0
S12	142	1.75-2.25Ø	0.3	19.7	18.0	62.0
		2.25-2.75Ø	0.0	24.7	18.7	56.7
		2.75-3.25Ø	0.0	34.0	6.0	60.0
S13	132	1.75-2.25Ø	0.0	11.7	7.0	81.3
		2.25-2.75Ø	0.0	12.7	4.0	83.3
		2.75-3.25Ø	0.0	27.0	4.7	68.3
S14	122	1.75-2.25Ø	1.7	24.7	5.7	68.0
		2.25-2.75Ø	0.0	10.0	4.3	85.7
		2.75-3.25Ø	0.0	6.7	0.7	92.7

APPENDIX IX. (Continued)

Sample	Location (km from north)	Size Fraction	Glauconite	Hornblende	Tourmaline	Black Opaques
S15	117	1.75-2.25Ø	2.7	20.0	6.0	71.3
		2.25-2.75Ø	2.3	12.0	5.3	80.3
		2.75-3.25Ø	0.7	12.7	4.0	82.7
S16	106	1.75-2.25Ø	2.0	19.0	7.3	71.7
		2.25-2.75Ø	0.3	11.3	4.0	84.3
		2.75-3.25Ø	0.3	20.0	3.0	76.7
S17	104	1.75-2.25Ø	3.0	17.0	5.7	74.3
		2.25-2.75Ø	0.0	9.7	2.0	88.3
		2.75-3.25Ø	0.3	15.7	1.7	82.3
S18	94	1.75-2.25Ø	0.0	15.3	7.7	77.0
		2.25-2.75Ø	0.3	11.7	6.3	81.7
		2.75-3.25Ø	0.0	15.7	2.7	81.7
S19	86	1.75-2.25Ø	0.3	17.0	7.3	75.3
		2.25-2.75Ø	0.0	7.7	3.3	89.0
		2.75-3.25Ø	0.7	9.3	1.3	88.7
S20	81	1.75-2.25Ø	0.0	8.0	3.3	88.7
		2.25-2.75Ø	0.0	2.0	1.7	96.3
		2.75-3.25Ø	0.3	7.3	3.7	88.7
S21	69	1.75-2.25Ø	1.0	14.0	2.3	82.7
		2.25-2.75Ø	0.0	10.3	3.3	86.3
		2.75-3.25Ø	0.0	12.0	1.7	86.3
S22	59	1.75-2.25Ø	6.7	10.0	1.3	82.0
		2.25-2.75Ø	0.3	7.0	1.3	91.3
		2.75-3.25Ø	0.0	13.7	1.3	85.0
S23	51	1.75-2.25Ø	22.7	27.3	5.7	44.3
		2.25-2.75Ø	1.3	15.0	3.3	80.3
		2.75-3.25Ø	0.3	11.3	1.7	86.7
S25	36	1.75-2.25Ø	2.7	34.0	8.0	55.3
		2.25-2.75Ø	0.7	20.3	5.3	73.7
		2.75-3.25Ø	0.0	7.0	2.0	91.0

APPENDIX IX. (Continued)

Sample	Location (km from north)	Size Fraction	Glauconite	Hornblende	Tourmaline	Black Opaques
S26	25	1.75-2.25Ø	33.0	9.0	3.7	54.3
		2.25-2.75Ø	6.7	19.3	4.3	69.7
		2.75-3.25Ø	1.0	21.3	1.3	76.3
S32	21	1.75-2.25Ø	36.7	9.7	14.7	39.0
		2.25-2.75Ø	15.0	12.3	7.3	65.3
		2.75-3.25Ø	2.7	22.0	2.0	73.3
S33	30	1.75-2.25Ø	21.3	0.7	1.3	76.7
		2.25-2.75Ø	5.9	0.8	0.8	92.4
S34	41	1.75-2.25Ø	2.2	2.2	3.5	91.7
		2.25-2.75Ø	0.3	4.7	4.0	91.0
		2.75-3.25Ø	0.3	18.7	3.3	77.7
S36	63	1.75-2.25Ø	5.0	8.3	10.3	76.3
		2.25-2.75Ø	0.7	5.0	5.3	89.0
		2.75-3.25Ø	0.0	5.7	0.7	93.7
S37	72	1.75-2.25Ø	0.0	6.0	8.7	85.3
		2.25-2.75Ø	0.0	7.3	7.3	85.3
		2.75-3.25Ø	0.3	7.0	4.0	88.7
S38	86	1.75-2.25Ø	0.0	3.0	6.3	90.7
S39	96	2.25-2.75Ø	0.0	23.7	8.7	67.7
		2.75-3.25Ø	0.0	31.0	10.3	58.7
S40	107	2.25-2.75Ø	0.0	42.3	7.7	50.0
		2.75-3.25Ø	0.0	69.3	5.7	25.0
S41	119	2.25-2.75Ø	0.0	41.3	6.0	52.7
		2.75-3.25Ø	0.0	61.7	7.3	31.0
S42	125	2.25-2.75Ø	0.0	31.0	10.7	58.3
		2.75-3.25Ø	0.0	47.0	12.7	40.3
S43	135	1.75-2.25Ø	0.3	44.3	14.3	41.0
		2.25-2.75Ø	0.0	47.0	15.0	38.0
		2.75-3.25Ø	0.0	63.7	8.7	27.7

APPENDIX IX. (Continued)

Sample	Location (km from north)	Size Fraction	Glauconite	Hornblende	Tourmaline	Black Opaques
S44	145	2.25-2.75Ø	3.3	44.7	8.0	44.0
		2.75-3.25Ø	0.0	69.3	12.0	18.7
S45	150	1.75-2.25Ø	0.0	45.7	4.7	49.7
		2.25-2.75Ø	0.0	60.3	6.3	33.3
		2.75-3.25Ø	0.7	74.0	3.3	22.0
S46	175	1.75-2.25Ø	3.4	41.1	8.0	47.5
		2.25-2.75Ø	3.3	40.7	7.3	48.7
		2.75-3.25Ø	0.0	70.0	9.0	21.0
S47	186	1.75-2.25Ø	0.0	9.3	6.3	84.3
		2.25-2.75Ø	0.0	9.3	1.7	89.0
		2.75-3.25Ø	0.0	13.3	3.0	83.7
S48	190	2.25-2.75Ø	0.3	36.7	6.3	56.7
		2.75-3.25Ø	0.0	35.7	4.3	60.0
S49	195	1.75-2.25Ø	0.0	5.3	3.0	91.7
		2.25-2.75Ø	0.0	26.0	5.0	69.0
		2.75-3.25Ø	0.0	35.7	4.3	60.0
R2	152	1.75-2.25Ø	0.0	0.3	0.7	99.0
		2.25-2.75Ø	0.0	0.0	0.7	99.3
		2.75-3.25Ø	0.0	0.3	1.3	98.3
R3	122	1.75-2.25Ø	0.0	0.0	2.3	97.7
		2.25-2.75Ø	0.0	0.0	2.3	97.7
		2.75-3.25Ø	0.0	0.0	0.3	99.7
R4	122	1.75-2.25Ø	0.0	0.3	0.7	99.0
		2.25-2.75Ø	0.0	0,0	0.0	100.0
		2.75-3.25Ø	0.0	0.3	0.3	99.3

APPENDIX X. Textures of Shelf and River Samples.

SHELF SAMPLES

No.	Texture
S6	Medium sand with shell fragments.
S7	Medium sand with shell fragments.
S8	Medium sand.
S9	Fine sand with shell fragments and worm tubes.
S10	Fine to medium sand with shell fragments.
S11	Fine sand with shell fragments.
S12	Fine sand with shell fragments.
S13	Medium sand with shell fragments and worms.
S14	Medium to coarse sand with worms, shell fragments, and pebbles.
S15	Coarse to very coarse pebbly sand with shell fragments.
S16	Very coarse pebbly sand with shell fragments and cobbles.
S17	Medium pebbly sand with shell fragments.
S18	Coarse pebbly sand with sand dollars, shell fragments, and orange-colored fragments.
S19	Medium pebbly sand with shell fragments, clams, and sand dollars.
S20	Coarse pebbly sand with shell fragments and worms.
S21	Very coarse sand with pebbles.
S22	Coarse pebbly sand with worms.
S23	Very coarse sand.

APPENDIX X. (Continued)

SHELF SAMPLES

No.	Texture
S24	Mud with shell fragments and worms.
S25	Medium to coarse sand with shell fragments and worms.
S26	Medium to fine pebbly sand with shell fragments and cobbles.
S32	Medium sand with shell fragments.
S33	Coarse pebbly sand with worms.
S34	Coarse muddy sand with abundant shell fragments, and worms.
S35	Mud with large shells, pebbles, and worms.
S36	Medium sand with worms.
S37	Medium sand with worms.
S38	Coarse pebbly sand with worms.
S39	Fine muddy sand with shell fragments.
S40	Fine muddy sand.
S41	Fine sand with shell fragments and worms.
S42	Fine muddy sand with shell fragments and worms.
S43	Fine sand with abundant worms, and shell fragments.
S44	Very fine muddy sand with plant debris, worms, and shell fragments.
S45	Very fine muddy sand with plant debris, worms, shell fragments, and snails.
S46	Fine sand with shell fragments.
S47	Coarse sand with shell fragments.

APPENDIX X. (Continued)

SHELF SAMPLES

No.	Texture
S48	Fine muddy sand with worms and shell fragments.
S49	Fine muddy sand with mussels and shell fragments.

RIVER SAMPLES

No.	Texture
R2	Medium to coarse muddy sand with plant debris.
R3	Medium to coarse muddy sand with plant debris.
R4	Sandy and pebbly mud.

APPENDIX XI. Oblique Projection Matrices Resulting from Q-Mode Factor Analysis on Point Count Data.

1.75 - 2.25 PHI FRACTION

Sample	Location (km from north)	End Member Sample R3	B3	S9
B1	2	.382	.893	.020
B3	18	.000	1.000	.000
B6	43	.197	.966	.010
B8	59	.488	.680	.257
B10	76	.369	.875	.069
B12	92	.772	.036	.254
B16	122	.791	.016	.274
B27	216	.979	.005	.032
B28	224	.946	.005	.080
S6	193	.847	.003	.212
S7	180	.624	.022	.463
S8	178	.618	.004	.477
S9	157	.000	.000	1.000
S10	147	.768	.071	.300
S12	142	.635	.020	.444
S13	132	.854	.003	.203
S14	122	.628	.022	.464
S15	117	.713	.037	.369
S16	106	.727	.029	.355
S17	104	.767	.040	.306
S18	94	.797	.003	.275
S19	86	.769	.006	.308
S20	81	.915	-.000	.123
S21	69	.837	.010	.222
S22	59	.880	.079	.155
S23	51	.325	.397	.638
S25	36	.371	.041	.711
S26	25	.694	.515	.175
S32	21	.487	.669	.260
S33	30	.945	.267	.000
S34	41	.976	.025	.035
S36	63	.875	.072	.165
S37	72	.923	.006	.111
S38	86	.964	.004	.055
S43	135	.004	.010	.997
S45	150	.128	-.007	.908
S46	175	.159	.052	.883

APPENDIX XI. (Continued)

1.75 - 2.25 PHI FRACTION

Sample	Location (km from north)	End Member Samples R3	B3	S9
S47	186	.890	.003	.157
S49	195	.946	.000	.079
R2	152	1.000	-.001	.001
R3	122	1.000	.000	.000
R4	122	1.000	-.001	.001

2.25 - 2.75 PHI FRACTION

Sample	Location (km from north)	End Member Samples R4	B18	B3
B1	2	.917	.035	.132
B3	18	.000	.000	1.000
B6	43	.361	.011	.756
B8	59	.751	.160	.310
B10	76	.542	.146	.553
B12	92	.827	.356	.051
B14	109	.621	.434	.214
B16	122	.836	.364	.026
B18	142	.000	1.000	.000
B21	167	.499	.751	.021
B23	183	-.089	.994	.051
B25	200	.272	.908	-.028
B27	216	.992	.025	.006
B28	224	.974	.081	.009
S6	193	.948	.174	-.001
S7	180	.952	.143	.012
S8	178	.947	.176	-.000
S9	157	.763	.486	.016
S10	147	.817	.422	.001
S11	147	.599	.678	-.000
S12	142	.757	.451	.043
S13	132	.951	.162	.001
S14	122	.962	.128	.004
S15	117	.932	.160	.038
S16	106	.955	.144	.006

MICROMEX CORRECTION GUIDE (M-6)

CORRECTION

The preceding document has been re-photographed to assure legibility and its image appears immediately hereafter.

APPENDIX XI. (Continued)

1.75 - 2.25 PHI FRACTION

Sample	Location (km from north)	End Member Samples R3	B3	S9
S47	186	.890	.003	.157
S49	195	.946	.000	.079
R2	152	1.000	-.001	.001
R3	122	1.000	.000	.000
R4	122	1.000	-.001	.001

2.25 - 2.75 PHI FRACTION

Sample	Location (km from north)	End Member Samples R4	B18	B3
B1	2	.917	.035	.132
B3	18	.000	.000	1.000
B6	43	.361	.011	.756
B8	59	.751	.160	.310
B10	76	.542	.146	.553
B12	92	.827	.356	.051
B14	109	.621	.434	.214
B16	122	.836	.364	.026
B18	142	.000	1.000	.000
B21	167	.499	.751	.021
B23	183	-.089	.994	.051
B25	200	.272	.908	-.028
B27	216	.992	.025	.006
B28	224	.974	.081	.009
S6	193	.948	.174	-.001
S7	180	.952	.143	.012
S8	178	.947	.176	-.000
S9	157	.763	.486	.016
S10	147	.817	.422	.001
S11	147	.599	.678	-.000
S12	142	.757	.451	.043
S13	132	.951	.162	.001
S14	122	.962	.128	.004
S15	117	.932	.160	.038
S16	106	.955	.144	.006

APPENDIX XI. (Continued)

2.25 - 2.75 PHI FRACTION

Sample	Location (km from north)	End Member Samples R4	B18	B3
S17	104	.970	.115	-.002
S18	94	.946	.159	.013
S19	86	.973	.095	.003
S20	81	.993	.025	.003
S21	69	.964	.128	.001
S22	59	.979	.080	.002
S23	51	.932	.192	.015
S25	36	.895	.281	.008
S26	25	.846	.269	.100
S32	21	.777	.180	.264
S33	30	.959	.004	.075
S34	41	.979	.062	.011
S36	63	.972	.070	.020
S37	72	.963	.106	.015
S39	96	.855	.357	.005
S40	107	.617	.670	-.020
S41	119	.653	.636	-.024
S42	125	.757	.502	.005
S43	135	.427	.812	.003
S44	145	.510	.731	.038
S45	150	.301	.894	-.044
S46	175	.592	.658	.039
S47	186	.972	.109	-.003
S48	190	.715	.563	-.013
S49	195	.856	.368	-.010
R2	152	.999	.002	.002
R3	122	.996	.006	.006
R4	122	1.000	.000	.000

2.75 - 3.25 PHI FRACTION

Sample	Location (km from north)	End Member Samples R3	B18
B3	18	.998	.015
B8	59	.967	.162
B12	92	.785	.532

APPENDIX XI. (Continued)

2.75 - 3.25 PHI FRACTION

Sample	Location (km from north)	End Member Samples R3	B18
B14	109	.845	.426
B16	122	.478	.821
B18	142	.000	1.000
B21	167	.098	.979
B23	183	.004	.992
B25	200	.055	.990
B27	216	.997	.024
B28	224	.995	.041
S6	193	.947	.228
S7	180	.984	.096
S8	178	.992	.059
S9	157	.277	.928
S10	147	.946	.230
S11	147	.420	.854
S12	142	.806	.503
S13	132	.883	.375
S14	122	.989	.073
S15	117	.969	.159
S16	106	.936	.257
S17	104	.959	.189
S18	94	.959	.193
S19	86	.982	.106
S20	81	.986	.088
S21	69	.974	.140
S22	59	.968	.160
S23	51	.976	.132
S25	36	.988	.080
S26	25	.930	.270
S32	21	.922	.290
S34	41	.943	.239
S36	63	.991	.061
S37	72	.986	.086
S39	96	.816	.485
S40	107	.223	.945
S41	119	.337	.901
S42	125	.545	.773
S43	135	.283	.925

APPENDIX XI. (Continued)

2.75 - 3.25 PHI FRACTION

Sample	Location (km from north)	End Member Samples R3	B18
S44	145	.139	.974
S45	150	.168	.958
S46	175	.168	.965
S47	186	.968	.162
S48	190	.338	.902
S49	195	.795	.517
R2	152	1.000	.005
R3	122	1.000	.000
R4	122	1.000	.003

VITA

Tom Scot Schroeder was born July 25, 1956 in Paterson, New Jersey to Mr. and Mrs. Arthur H. Schroeder. The author graduated from Paramus High School (New Jersey) in May, 1974. He received a B.S. in Environmental Science and Resource Management in May, 1978 from Lehigh University, and attended Lehigh University as a graduate student in Geology from August, 1978 to September, 1980, where he is working towards an M.S. degree. The author worked as a teaching assistant in physics while in graduate school at Lehigh, and is presently employed as a geological engineer by Tenneco Oil Company's Central Gulf Division in Lafayette, Louisiana. He is married to Monica Schroeder.